

UNDERSTANDING FLUCTUATIONS IN NON-EQUILIBRIUM
SYSTEMS

ARNAB PAL



A thesis submitted to the Jawaharlal Nehru University
for the degree of Doctor of Philosophy

October 2015

Dedicated to my parents.

DECLARATION

I, hereby, declare that this thesis is composed independently by me at Raman Research Institute, Bangalore, India, under the supervision of Dr. Sanjib Sabhapandit. The subject matter presented in this thesis has not previously formed the basis of the award of any degree, diploma, associateship, fellowship or any other similar title in any other University. I also declare that I have run it through the **Turnitin** plagiarism software.

Dr. Sanjib Sabhapandit

Arnab Pal

Theoretical Physics Group
Raman Research Institute
Bangalore 560 080
India

CERTIFICATE

This is to certify that the thesis entitled “**Understanding Fluctuations in Non-equilibrium Systems**” submitted by Arnab Pal for the award of the degree of Doctor of Philosophy of Jawaharlal Nehru University is his original work. This has not been published or submitted to any other University for any other Degree or Diploma.

Prof. Ravi Subrahmanyam
(Centre Chairperson)
Director
Raman Research Institute
Bangalore 560 080
India

Dr. Sanjib Sabhapandit
(Thesis Supervisor)

ACKNOWLEDGEMENTS

...How come it is so difficult to start....

Though only my name pops out on the cover of this dissertation, a great many people have contributed to its creation. I am indebted to all of them who have made this possible and because of whom I will cherish my graduate experience throughout my life.

I owe my deepest gratitude to my advisor, Dr. Sanjib Sabhapandit. I am grateful to him that he gave me the freedom to explore on my own, and at the same time the guidance to recover when my steps faltered. His patience and constant support helped me overcome many crisis situations and finish this dissertation. My co-advisor, Prof. Abhishek Dhar, has been always there to make insightful comments and constructive criticisms at different stages of my research. His passion and discipline have been indispensable to my growth as a scientist over these past five and a half years. I was fortunate to have the opportunities to discuss the experimental aspects with Dr. Pramod Pullarkat during the course of several projects which added new facets to my understanding. Discussions with Prof. Joseph Samuel and Dr. Supurna Sinha have been always very intriguing being academic or non academic. I had the privilege to attend Prof. Satya Majumdar's lectures and his teaching has taught and inspired me a lot. I am also grateful to him for his encouragement and motivating me to nourish my own ideas. I would also like to thank Dr. Hugo Touchette with whom I had a chance to interact and his critical comments regarding my work have helped me a lot to envisage a better understanding. I also thank him for discussing and sharing few fundamental ideas in large deviation theory with me which has helped me to build up a part of my thesis. I am grateful to him for this remarkable

assistance. Our group secretary Manjunath has been always there to assist me by all means and I thank him from the bottom of my heart. I am especially grateful to the library associates who have been tremendously generous in all sorts of matter. It is my pleasure to express my gratitude to them.

Many friends have helped me stay sane through these many years. I greatly value their friendship and care which have helped me to overcome the setbacks and stay focused. Though this list is way far from complete, it is my pleasure name a few : Prasad, Suman, Chaitra, Anjan, Alok, Chandra, Miguel, Sandipan and Amrita. I can not forget acknowledging Jagdish, Mahavir, Avinash, Swamynathan, Jyothi, Samim, Rajib, Debasish, Mriganko, Safi, Rahul, Santanu, Raj, Rajsekhar, Rituparno, Debadrita, Abir, Amit, Rajarshi, Aswath, Deepak, Meera, Varun, Sanjay, JK, RK, MK, Arijit, Arif, Antara, Wasim and Abhijit whose company I had enjoyed throughout my RRI days. I thank Anupam Kundu for his support and affection towards me throughout my doctoral days.

Away from RRI, my college buddies were always cheerful and stood by me at every instant. I will take the opportunity to thank these guys: Nirmalya, Suvo, Devagnik, Manik, Trina and Monk. I would also like to take the pleasure of recalling few of my oldest school buddies Partha, Sandip, Siddhartha, Subhrosankha. You chaps rock.

Finally, and most importantly, I would like to thank my wife Ishita. Her unconditional support, encouragement, perseverance and unwavering love were undoubtedly the pathway upon which the past thirteen years of my life have been built. I thank my parents for their astounding belief in me. At every footstep, they have allowed me to be as ambitious as I wanted. From them I have gained so much drive and ability to tackle challenges head on. I am grateful to my brother and my grandmothers whose unconditional support and love has led me to this stage. Also, I thank Ishita's parents who provided me with unending encouragement and support.

SYNOPSIS

The formalism of equilibrium statistical mechanics is established in an elegant way where the probabilities are a priori given by the Boltzmann-Gibbs measure with the normalization constant known as the partition function (summation over all possible energy configurations). In principle, one can then compute the thermodynamic observables within an established framework. On the other hand, though non-equilibrium phenomena are ubiquitous in nature, there exists no such unified approach. They are usually described by the dynamics and no such Boltzmann alike formulae for the probabilities are a priori known. One has to solve the evolution equation corresponding to the dynamics, named as the master equation, to have information about these probabilities, which is a daunting task most of the time. As a consequence, thermodynamic observables are not also quantified generically. Nevertheless, in the last decade, a tremendous progress has been made in this field which aims at making a general statement about the fluctuations of physical observables during a non-equilibrium process. This goes under the nomenclature *fluctuation theorem*. Within this framework, the notion of stochasticity among the thermodynamic observables such as performed work, dissipated heat, power flux, entropy production (unlike the standard thermodynamics where every observable is defined as an average quantity) has been introduced. One can now talk about the probabilities, cumulants etc. for these observables. Moreover it allows one to apply the theorems arbitrarily far from equilibrium and to finite size system (extremely relevant for biomolecular, single molecular experiments, colloidal systems, nanotubes, precision measurement etc.). It has also been found that these results are also very useful to express symmetries (reminiscent of microscopic dynamics) of the so-called *large*

deviation functions associated to the different observables (for instance work, dissipated heat, injected power, entropy production etc.).

Non-equilibrium situation generically arises due to thermodynamic affinities or forces such as temperature, density gradients or external perturbations viz. time modulated dragging, oscillations, anisotropic shear flow, applied fields etc. and they are usually considered to be deterministic in nature. There have been rigorous theoretical developments in the measurement of these observables for such *deterministic protocols*. High precision experiments have been able to validate these theories. On the contrary, there have been not much anticipation on the effects of *stochastic control protocols* in this observable statistics. In principle, microscopic driving is always accompanied by random fluctuations from the surrounding and one needs to put this fact into consideration. The conceptual barrier lies on the very nature of the stochastic driving: *What kind of driving is feasible? Whether the stochasticity is reversible or irreversible by nature? How much entropy production is then associated with the driving?* Furthermore, from an experimental point of view, a deterministic driving is never perfect and will always be followed by uncontrolled random fluctuations (e.g. the experiments done with the optical tweezers, probing AFM-s, zipping-unzipping biomoleculars through optical trap etc.) making this issue crucial for current research interests.

While the *fluctuation theorem* deals only with the symmetry properties of the probability distributions, it does not offer a detailed description of the full probability distributions. Therefore, one may be interested in going beyond *fluctuation theorem* and characterize the stochastic properties of these observables in details. This thesis has probed to such investigations of the statistical properties of these kind of systems both analytically and by numerical simulations. In general, the fluctuations (Gaussian or non-Gaussian) are encoded in the *large deviation functions* associated with the probability distributions

asymptotically. The *large deviation functions* are said to play the role of free energy in the equilibrium processes for the processes which are away from equilibrium. They not only encode the typical fluctuations, they also do contain the rare, giant or the atypical fluctuations. Moreover, the typical *large deviation function* is quadratic around the average (where it is maximum), a reflection of the central limit theorem for small fluctuations. Computing *large deviation functions* for correlated systems is a difficult task, in general which has been successfully accomplished only for a handful of oversimplified systems. This thesis cites few such examples where such functions can be measured.

In this thesis, we have computed the *large deviation functions* as well as the probability distributions for the stochastic observables of interest in the asymptotic time limit for a large class of systems. It is shown that this method also allows to provide the largest eigenvalue and the corresponding eigenfunctions of the Fokker-Planck operator. The *large deviation functions* computed here possess certain symmetry properties namely Gallavotti-Cohen symmetry, Spohn-Lebowitz symmetry and they might be non generic. At asymptotic time limit, the validation of this symmetry is known as the steady state fluctuation theorems. To be specific, for various systems, the observable entropy production invariably satisfies this theorem. However, this is not the case for the other observables like work, heat, power flux etc. Various parts of the thesis will discuss a variety microscopic models which are affected due to the thermal fluctuations. These are not only hypothetical models, rather quite experimentally accessible. As a matter of fact, one of these model systems have been investigated in a table top experiment in Lyon, France. Moreover, in this kind of systems, a lot analytical progress can be made and the *fluctuation theorem* can be examined. The aim is not restricted to the computation of the *large deviation functions* and to verify the symmetry properties. The analysis extends to characterizing the full probability distribution functions

of these observables with respect to the system parameters with an insight that they can be verified in laboratories. The thesis consists of two parts. The first part discusses the paradigm model of a colloidal particle in an optical trap. We investigate the observable statistics using our formalism in details. The second part contains another microscopic model, where the methodology has been revised in order to characterize the fluctuations in such an out of equilibrium system.

A colloidal particle in a harmonic trap with fluctuating locations:

A colloidal particle in a harmonic trap is a paradigm set up to study microscopic systems since the thermal fluctuations play a major role in the dynamics of the systems. Motivated by experiments based on atomic force microscopy or the optical tweezers, this part of the thesis is focused to study the work fluctuations for such a Brownian particle in a harmonic trap with fluctuating locations. Consider the particle diffusing in a harmonic trap where the location of the trap is modulated according to an Ornstein-Uhlenbeck process. Earlier studies were made on similar systems where the drive was deterministic like a constant velocity or a given time dependent modulation. Nevertheless, in reality deterministic drives are ideal situations while there will be always tiny random fluctuations associated with it. One should therefore look at the systems of practical importance where the driving is stochastic. The fluctuations of the mechanical work done by the trap on the Brownian particle were computed in terms of the *large deviation functions* using the method sketched out in this thesis. Moreover, it was realized that a complete asymptotic form of the probability density function of the work done can be obtained. In the next part of the thesis, we studied the dissipated heat and the total entropy production suitably defined in the context of the problem. A general formulation was provided using the concept of *boundary terms*. It was found that these terms have a crucial role while interplaying between the observables. Full computation for all the observables was provided in terms of the relevant parameters of the system. At the end,

the validity of the steady state fluctuation theorem in this system was examined for all these observables. The effects of stochasticity in such validation was also discussed. Interestingly, we find that the validation of the *fluctuation theorem* is not generic. We found that the theorem for the heat dissipation is restricted in the parameter space so as the mechanical work and the Jarzynski work. On the contrary, these theorems were found to be robust for the total entropy production. This leads one to predict that the unboundedness of the phase space or rise in energy allows the system to attain massive but rare fluctuations and this perhaps results in the failure. Despite these being rare events, we have managed to quantify them systematically by using the principles of large deviation.

An underdamped colloidal particle driven by a stochastic field:

The later part of the thesis extends to the earlier studies to the underdamped regime where one can no more neglect the inertia terms. Consider an *underdamped Brownian particle* dragged through a viscous medium. We investigate the work statistics due to the external force field on this system. Deploying the same technique, that was introduced earlier, properties of the work done were studied. The work distribution is accompanied by non-Gaussian fluctuations so enforces one to ply the large deviation principle. As before, statistics for the work was derived in terms of the *large deviation functions*. We also obtain the validation of the *fluctuation theorem* in a restricted parameter space with a different characteristic to that of the earlier. It turns out that in certain limit this model mimics the system of a Brownian particle connected to two heat baths where the observable of interest is the heat flown from one bath to the other. We have been able to compute the heat distribution and the currents analytically in details. These are very important theoretical models in the context of biological transport and experiments based on matter, charge or energy conduction. Results such as ours can therefore be easily verified in the table top

experiments.

To summarize, using an extensive framework, we have studied the effects of stochastic driving in the linear diffusive models. We have derived the conditions that the stochastic driving should hold in order to verify the *fluctuation theorem* for the total entropy production. This method moreover allows one to compute the observables in general and verify the fluctuation theorems making a connection with *large deviation functions*. This method is found to be quite general and thus will be applicable to a plenty of equivalent models being at an equilibrium or a non-equilibrium steady state .

Dr. Sanjib Sabhapandit

Arnab Pal

Theoretical Physics Group
Raman Research Institute
Bangalore 560 080
India

PUBLICATIONS

- Arnab Pal and Sanjib Sabhapandit.
Work fluctuations for a Brownian particle in a harmonic trap with fluctuating locations.
Phys. Rev. E, **87**, 022138, 2013.
- Arnab Pal and Sanjib Sabhapandit.
Work fluctuations for a Brownian particle driven by a correlated external random force.
Phys. Rev. E, **90**, 052116, 2014.
- Arnab Pal and Sanjib Sabhapandit.
Heat and Entropy fluctuations of a generalized Langevin system
Manuscript in preparation.
- Arnab Pal.
Diffusion in a potential landscape with stochastic resetting
Phys. Rev. E, **91**, 012113, 2015.

CONTENTS

1	INTRODUCTION	1
1.1	The principle of statistical mechanics	2
1.2	Equilibrium Statistical Mechanics	3
1.2.1	Microcanonical, Canonical and Grand Canonical Ensemble	3
1.3	Non-equilibrium statistical mechanics (NESM)	5
1.3.1	Rudiments of NESM	6
1.4	Fluctuations in Equilibrium and Non-Equilibrium systems	10
1.4.1	Why and When Fluctuations are Important?	12
1.4.2	Stochastic Thermodynamics	13
1.4.3	Theoretical Investigations	14
1.4.4	Experimental Investigations	22
1.4.5	How to measure the Fluctuations	24
1.5	Prologue of the thesis	28
1.6	Outline of the thesis	30
2	WORK FLUCTUATIONS OF A BROWNIAN PARTICLE IN A MOVING HARMONIC TRAP	33
2.1	Abstract	33
2.2	Introduction	33
2.3	The model	37
2.4	Moment Generating Function	39
2.5	Complete Derivation of the Moment Generating Function	40
2.6	Explicit results for $\mu(\lambda)$ and $g(\lambda)$	46
2.7	Analysis of $g(\lambda)$	47
2.7.1	The case: $\delta < 1$	50
2.7.2	The case: $\delta > 1$	50

2.7.3	The case: $\delta = 1$	51
2.8	Probability Density Function	51
2.8.1	The case of no singularities	54
2.8.2	The case of one singularity	55
2.8.3	The case of three singularities	58
2.8.4	The case of four singularities	62
2.9	Large Deviation Function and Fluctuation Theorem	66
2.10	Conclusion	69
3	HEAT AND ENTROPY FLUCTUATIONS OF A GENERAL LANGEVIN SYSTEM	73
3.1	Abstract	73
3.2	Introduction	74
3.3	A general formalism	75
3.4	Model	80
3.5	Characterizing the Heat dissipation: A systematic study	82
3.5.1	Definition of the heat dissipation	82
3.5.2	Probability distribution	84
3.5.3	Symmetry properties and the Fluctuation theorem	91
3.6	Characterizing the total Entropy production: A systematic study	92
3.6.1	Definition of the total entropy production	92
3.6.2	Probability distribution	95
3.6.3	Symmetry properties and the Fluctuation theorem	96
3.7	A simple description of the heat and the total entropy fluctuations	97
3.8	Summary	104
4	WORK FLUCTUATIONS OF A BROWNIAN PARTICLE DRAGGED THROUGH A MEDIUM	107
4.1	Abstract	107
4.2	Introduction	107
4.3	Model	110

4.4	Moment generating function	111
4.5	Detailed calculation of the MGF	112
4.6	Explicit results for $\mu(\lambda)$ and $g(\lambda)$	118
4.7	Probability Distribution function	120
4.7.1	Case of no singularities	124
4.7.2	Case of a singularity	124
4.8	The case of a Brownian particle connected to two thermostats	127
4.9	Large deviation function and the fluctuation theorems	129
4.10	Summary	131
A	ASYMPTOTIC EXPANSIONS OF THE INTEGRALS AROUND THE BRANCH POINT	133
A.1	Steepest descent method with a branch point	133
A.1.1	The branch point is not between the origin and the saddle point: $\lambda_a \notin (0, \lambda^*)$	133
A.1.2	The branch point is between the origin and the saddle point: $\lambda_a \in (0, \lambda^*)$	135
	BIBLIOGRAPHY	141

ACRONYMS

NESM	Non-Equilibrium Statistical Mechanics
NESS	Non-Equilibrium Steady (Stationary) State
PDF	Probability Density Function
LDF	Large Deviation Function
MGF	Moment Generating Function
FT	Fluctuation Theorem
TFT	Transient Fluctuation Theorem
SSFT	Steady State Fluctuation Theorem
FDT	Fluctuation Dissipation Theorem
JE	Jarzynski Equality
CI	Crooks Identity
AFM	Atomic Force Microscope
i.c.	Initial Condition
sd	Stochastic Driving

**All we have to decide is what to do with the time that is given to
us - Gandalf the Grey.**

INTRODUCTION

An extended system at mechanical and thermal equilibrium obeys the principles of thermodynamics [1, 2, 3, 4] that are embodied in the laws of equilibrium statistical mechanics [5, 6, 7, 8, 9, 10, 11, 12]. The fundamental property is that such a system, consisting of a huge number of microscopic degrees of freedom, can be described in equilibrium by only a few macroscopic parameters, called the state variables. The values of these parameters can be determined by optimizing a potential function (such as the entropy, the Free energy, the Gibbs free energy) chosen according to the external constraints imposed upon the system. Based on these, founding principles of equilibrium statistical mechanics were laid by Boltzmann and Gibbs. On the other hand, non-equilibrium systems are simply the systems which are not in equilibrium. These are complex systems consisting of a large number of degrees of freedom and evolve according to rules that violate *detailed balance*. Examples include - living organisms, transport in mechanical and biological systems, as well as epidemic spreading, pedestrian/vehicular traffic, stock markets, and social networks. Surprisingly, we still do not hold a general conceptual framework to characterize such systems contrary to the systems in equilibrium. Nor there are specific answers to questions like these (i) What are the macroscopic observables should we include to have a fair description of the system? (ii) Do universal laws exist? Can one define universality classes for systems out of equilibrium? Are there some general equations of state? (iii) Can the stationary state be derived by optimizing a potential? (iv) Can one postulate a general form for the microscopic measure that would generalize the Gibbs-Boltzmann canonical law? (vi) How the to quantify the statistical properties of the observ-

ables under the effects of external perturbations? These are the open questions of non-equilibrium statistical mechanics and achieving the answers perhaps has been one very important quest in the second half of the last century.

1.1 THE PRINCIPLE OF STATISTICAL MECHANICS

Statistical mechanics is concerned about the study of the special laws which govern the behavior and the properties of macroscopic bodies. Macroscopic bodies are formed of a large number of individual particles, such as atoms or molecules. Considerably the general character of these laws does not rely upon the dynamics (classical or quantum) which describes the motion of the individual particles in a body. At first sight it might then seem that, as the number of particles increases, so also must the complexity and intricacy of the properties of the mechanical system, and that no trace of regularity can be found in the behavior of a macroscopic body. This is not true since, new types of regularities emerge as the number of particles increases.

In principle, we can obtain complete information concerning the motion of a mechanical system by constructing and integrating the equations of motion of the system, which are equal in number to its degrees of freedom. But if we are concerned with a system which, though it obeys the laws of classical mechanics, has a very large number of degrees of freedom, the actual application of the methods of mechanics involves the necessity of setting up and solving the same number of differential equations, which in general is impracticable. Since the microscopic picture is not viable we adopt a macroscopic picture where we are more interested in the coarse grained variables. This however waives a lot of microscopic details and thus one needs a statistical description.

The laws of the statistical mechanics, emerging because of a *large number of particles* forming the body, cannot in any way be receded

to purely mechanical laws. One of their unique features is that they cease to have meaning when applied to systems with a small number of constituents. Thus, although the motion of systems with a very large number of degrees of freedom obeys the same laws of mechanics as that of systems consisting of a small number of particles, the existence of many degrees of freedom results in laws of a different kind. Consequently, the most elementary symmetries of the motion of the individual particles are broken by the large assemblies made of them.

1.2 EQUILIBRIUM STATISTICAL MECHANICS

Equilibrium statistical mechanics has a very elegant and well defined structure and is applicable for systems which are not subjected to any perturbations like thermodynamic affinities or external driving.

1.2.1 *Microcanonical, Canonical and Grand Canonical Ensemble*

Microcanonical ensemble characterizes isolated systems those cannot exchange energy, matter with its surroundings and thus keeping the total energy, number of molecules to be conserved. This is a collection of system for which the configurational probability is defined consistent with the total energy. Moreover, any given member of the ensemble is *equally likely* to be found in one of these configurations. On the other hand, isolated systems are hard to realize rather they are mostly found to interact with the environment.

For most purposes, the precise nature of the surrounding is not very relevant; all one needs is that it should maintain its equilibrium property all along. In addition, a natural alternative appears to quantify equilibrium property in terms of certain intensive parameters of the system such as temperature T , pressure P , chemical potential μ .

Therefore in this case, whenever the system of interest interacts with the surroundings or environment, they exchange energy in the form of heat. This is called the thermal interaction. In this case equilibrium is defined when the system and the surrounding maintain an identical temperature though energy is allowed to fluctuate. This is the *thermal equilibrium*. In certain cases, though the systems are thermally insulated, they are capable of interacting with each other mechanically. The systems are then said to exchange energy by doing macroscopic work on each other. In this case, the intensive parameter is pressure and the volume of the system fluctuates. This is the notion of *mechanical equilibrium*. Such an ensemble of systems in which macrostates are defined through the parameters N, V, T , is characterized as the *canonical ensemble*. Under this ensemble, since the exchanges take place through the energy or the volume, these observables can fluctuate.

On the other hand, in many physical and chemical situations, a given system immersed in a large reservoir can exchange both energy and particles with each other. Here, the set of intensive parameters contains both temperature and chemical potential while E, N are allowed to vary. This is the *grand canonical ensemble* picture, which consists of the given system and a large number of mental copies thereof, the members of the ensemble carry out a mutual exchange of both energy and particles. These systems preserve such kind of *chemical equilibrium* in each cases by maintaining constant values for the intensive variables. In other words, the system and the surroundings interact till the intensive variables reach a constant value respectively. Here the fluctuating quantities of interests are the energy and the number of particles. Henceforth this ensemble picture characterizes these fluctuations within a suitable framework.

These possibilities were explored by *J. W. Gibbs* in 1901. He first gave the explicit formulas for the probability distribution of these fluctuating quantities when the system of interest is at thermal, mechanical or chemical equilibrium. These distributions are known as the *Gibbs distributions*. The distribution for the translational motion of

molecules (e.g. a polyatomic gas) in terms of the momenta was first derived by *J.C. Maxwell* in 1860. This gives the measurement of the mean kinetic energy of the molecules which is valid quite independently of the nature of the motion of the atoms within the molecule and the rotation of the molecule. A similar formula was derived by *L. Boltzmann* earlier in 1877 to study ideal gas in the classical statistical physics. Boltzmann derived the distribution of molecules of an ideal gas among the various states and the mean occupancy of molecules in a given energy state. These probabilities are usually constructed from the Hamiltonian of the system which contains the entire microscopic details. Following the footsteps of Boltzmann and Gibbs, these time independent distributions take the form such as $P_{\text{eq}}(\mathcal{C}) \propto e^{-H(\mathcal{C})}$, where $H(\mathcal{C})$ is the total energy in a particular configuration \mathcal{C} derived from the Hamiltonian of the system as a function of the extensive variables. The proportionality constant is fixed through the normalization and known as the *partition function (sum over configurations)*. The thermodynamical observables like average energy, specific heat, entropy, magnetic moment, susceptibility, conductance etc. are then easy to determine from this function. These results are the cornerstone of the equilibrium statistical mechanics and successfully used to determine the fundamental statistical properties of macroscopic systems at equilibrium.

1.3 NON-EQUILIBRIUM STATISTICAL MECHANICS (NESM)

Consider a metal rod which is thermally isolated along its length but connected to two different heat reservoirs only at the two ends. If the temperature remains identical for both of them, then the rod is in thermal equilibrium with the two reservoirs and observables can be computed by the laws of equilibrium statistical mechanics. On the other hand, if there is a temperature gradient present between the reservoirs, then there will be a flow of heat energy between the

reservoirs even in stationary states. This is the simplest example of a non-equilibrium situation. The laws of equilibrium physics ceases to exist here. Such systems are defined by the dynamics and depends on every details present (unlike equilibrium cases) like the nature of interaction of the system with the surroundings etc.. A major difficulty is that, even if such a system is presumably known (or assumed) to adjust in a time-independent state in due course, the appropriate stationary weights are not generally known.

1.3.1 Rudiments of NESM

Unlike equilibrium statistical mechanics, with its well-established foundations, a similar overarching framework for NESM remains elusive. They are usually tackled by the language of stochastic Markov processes, general concepts of the configurational probabilities and their evolution in time, as described by *master equations* (discrete cases) or the *Fokker Planck equations* (continuous cases) [13, 14, 15, 16, 17, 18, 19, 20].

Given a set of rules of stochastic evolution determined by the external perturbations, it is possible to write down equations which govern the time-dependent weights $P(\mathcal{C}, t)$, which yields the probability of the system being in configuration \mathcal{C} (a configuration of the microstates) at time t . The evolution for the configuration probability $P(\mathcal{C}, t)$ can be simply realized using the *master equations*. Let us consider a set of configurations $\{\mathcal{C}_1, \mathcal{C}_2, \dots\}$ which system accesses during a given interval of time. At a given time t , the system can be found in one this configuration. The evolution of the system is specified by the following rule: Between t and $t + dt$, the system can jump from a configuration \mathcal{C} to a configuration \mathcal{C}' . It is assumed that the transition rate from \mathcal{C} to \mathcal{C}' does not depend on the previous history of the system (*Markov hypothesis*). The rate of transition per unit time will be denoted by the Markov matrix $M(\mathcal{C}', \mathcal{C})$ (or equivalently, by

$M(\mathcal{C} \rightarrow \mathcal{C}')$). For simplicity, we are considering the rates to be time independent. For a complex system ruled by the Markovian dynamics, the master equation dictates

$$\frac{d}{dt} P(\mathcal{C}, t) = \sum_{\mathcal{C}' \neq \mathcal{C}} M(\mathcal{C}, \mathcal{C}') P(\mathcal{C}', t) - \sum_{\mathcal{C}' \neq \mathcal{C}} M(\mathcal{C}', \mathcal{C}) P(\mathcal{C}, t), \quad (1)$$

where the first term is the inward probability flux from $\mathcal{C}' \rightarrow \mathcal{C}$ and the second term is the outward probability flux from \mathcal{C} to \mathcal{C}' . The Markov matrix complies the following properties

- The diagonal terms $M(\mathcal{C}, \mathcal{C})$ is a negative number: it represents the rate of leaving the configuration \mathcal{C} . However, the off diagonal terms represent inwards/static flux and thus they are non-negative.
- The sum of each column in $M(\mathcal{C}, \mathcal{C}')$ identically vanishes. This is a consequence of the conservation of the total probability.

Since our interest is in the full dynamical behavior of such a statistical system, we must imagine (a) repeating the same experiment many times, (b) forming an ensemble of trajectories through configuration space, and (c) computing time dependent averages of macroscopic observables from this ensemble. The results can then easily be compared with the averages obtained separately from $P(\mathcal{C}, t)$.

It is important to realize that a complex system will have a Markov matrix of very large order that can not be diagonalized generically. This is just the starting point of NESM.

The first characterization between the equilibrium and the non-equilibrium principles was first investigated by *L. Onsager*. Let us rewrite the master equation Eq. (1) in the following manner

$$\frac{d}{dt} P(\mathcal{C}, t) = \sum_{\mathcal{C}'} \{M(\mathcal{C}, \mathcal{C}') P(\mathcal{C}', t) - M(\mathcal{C}', \mathcal{C}) P(\mathcal{C}, t)\} = \sum_{\mathcal{C}'} J(\mathcal{C}, \mathcal{C}'), \quad (2)$$

where $J(\mathcal{C}, \mathcal{C}')$ is the local probability current between the configurations

$$J(\mathcal{C}, \mathcal{C}') = M(\mathcal{C}, \mathcal{C}') P(\mathcal{C}', t) - M(\mathcal{C}', \mathcal{C}) P(\mathcal{C}, t) \quad (3)$$

Now, there can be two classes of stationary state for which the left hand side in Eq. (2) vanishes. If it so happens, that each term of Eq. (2) within the summation vanishes, then the stationary state will be called an *equilibrium state*

$$M(\mathcal{C}, \mathcal{C}') P_{\text{eqm}}(\mathcal{C}') = M(\mathcal{C}', \mathcal{C}) P_{\text{eqm}}(\mathcal{C}), \quad (4)$$

where $P_{\text{eqm}}(\mathcal{C}, t) \equiv P_{\text{eqm}}(\mathcal{C})$ is the *equilibrium configuration*. In other words, the local currents $J(\mathcal{C}, \mathcal{C}')$ vanish for all the configurations $\mathcal{C}, \mathcal{C}'$ at thermodynamic equilibrium

$$J(\mathcal{C}, \mathcal{C}') = 0, \quad \forall \mathcal{C}, \mathcal{C}'. \quad (5)$$

These two conditions Eq. (4) and Eq. (5) are identical and constitute the principle of *detailed balance* which is a fingerprint of equilibrium. This is nothing but a consequence of the time reversal symmetry of the microscopic dynamics of the system realized by Onsager. On the other hand, there are situations when the systems inherently break the principle of detailed balance and thus there exists a steady flux both at finite and infinite time as well. This is due to the coarse graining procedure, when non-relevant degrees of freedom are integrated out and the resulting effective dynamics appears to be irreversible for the effective degrees of freedom we are interested in, within some limited space and time scales. These configurational states are broadly called *non-equilibrium steady (stationary) states* (NESS). In this case, the left hand side of Eq. (2) vanishes due to the collective dynamics of the configurations however each term in the right hand side is not necessarily zero. It is the dynamics which makes the right hand side to be zero cumulatively. This is equivalent to show the presence of local currents $J(\mathcal{C}, \mathcal{C}') \neq 0$ in the system. We will refer to such stationary states as $P_{\text{NESS}}(\mathcal{C})$ or the NESS.

The following example gives us an idea about the Markovian dynamics and its evolution rules. Consider a three site random walk with periodic boundary conditions. Let us denote the sites as $\{x - 1, x, x + 1\}$ so that the configuration matrix is $\mathcal{C} = \{(1, 0, 0), (0, 1, 0), (0, 0, 1)\}$. The dynamics is simply given according to the rule that the walker jumps to the right and to the left with rates u and v respectively. The evolution equation for $P(x, t)$, the probability to be in the site x at time t is given by Eq. (1) where the Markov matrix is given by

$$M = \begin{pmatrix} -u - v & v & u \\ u & -u - v & v \\ v & u & -u - v \end{pmatrix}. \quad (6)$$

It is easy to verify the properties of the Markov matrix (like negative diagonal terms, terms in each column adding to zero, zero eigenvalue corresponding to the stationary state) easily. It is easy to compute the time dependent measures $P(\mathcal{C}, t)$ for this problem

$$P(\mathcal{C}, t) = e^{\lambda_1 t} \psi_1 + e^{\lambda_2 t} \psi_2 + e^{\lambda_3 t} \psi_3, \quad (7)$$

where ψ_i -s are the respective eigenvectors for λ_i -s

$$\begin{aligned} \lambda_1 &= 0 \\ \lambda_2 &= \frac{1}{2}(-3u - 3v - \sqrt{3}\sqrt{2uv - u^2 - v^2}) \\ \lambda_3 &= \frac{1}{2}(-3u - 3v + \sqrt{3}\sqrt{2uv - u^2 - v^2}) \end{aligned} \quad (8)$$

It is important to note that this system does not have an equilibrium state because of the presence of the local currents. The large time stationary solution is a NESS given in the following

$$j = \frac{1}{3}(u - v) \quad (9)$$

$$P(\mathcal{C})_{\text{NESS}} = \frac{1}{3} (1 \ 1 \ 1)^T \quad (10)$$

However, it should be emphasized that, only if the dynamics is Markovian, then these weights can be constructed formally from the rules of evolution Eq. (1), Eq. (2). For generic complex systems, when the Markov hypothesis is relaxed, such kind of evolution is far too intractable.

1.4 FLUCTUATIONS IN EQUILIBRIUM AND NON-EQUILIBRIUM SYSTEMS

In the equilibrium statistical physics, we are mostly concerned with the evaluation of statistical averages of the various macroscopic observables at equilibrium. These equilibrium averages are identical to the results expected from relevant measurements through experiments within a high degree of accuracy. The mean square fluctuations of extensive quantities (volume, energies etc.) are found to be directly proportional to the size of the system while that of an intensive quantity (pressure, chemical potential etc.) is inversely proportional to the same. In either case, the relative fluctuations are inversely proportionate to the square root of the size of the system. Thus, except for the situations encountered in a critical region, normal fluctuations are typically thermodynamically negligible. Nevertheless, this does not imply that the fluctuations are altogether irrelevant to any physical phenomena occurring around us. In fact, the very presence of fluctuations at the microscopic level is of fundamental importance to characterize several properties of the system displayed at the macroscopic level. In the following, we will state few examples where fluctuations play a very crucial role.

Firstly, in a homogeneous, isotropic systems such as liquid or gas, density fluctuations are related to the spatial correlations of the system. Unlike in a single phase system where the fluctuations are thermodynamically negligible, they can assume considerable importance in multiphase systems, especially in the neighbourhood of a critical point. In the latter case, we obtain a rather high degree of density fluctuations or spatial correlation among the molecules of the system. The spatial correlations among the molecules of a fluid extend over macroscopic distances (order of system size) typifying the inception of long range order in the system. Consequently, the intensity of the

scattered waves also becomes abnormally large, which gives rise to the spectacular phenomena of *critical opalescence*.

Secondly, the study of fluctuations in time, leads to the concept of *correlation functions*. The *correlation functions* play a vital role in relating the dissipative properties of a system, such as the viscous drag force a fluid or the electrical resistance of a conductor, with the microscopic properties (such as position or velocity fluctuations) of the system in a state of equilibrium. This relationship manifests itself in the so-called *fluctuation dissipation theorem* (FDT) [21, 22, 23, 24]. The most striking feature of the FDT is that it relates, in a fundamental manner, the fluctuations of a physical quantity pertaining to the equilibrium state of the given system to a dissipative property which, in practice, is realized only when the system is away from equilibrium due to an external force. For instance, fluctuations in the motions of electrons in an electric resistor give rise to a spontaneous thermal e.m.f. which is shown to be connected to the resistance via the FDT. Another example of the FDT is the theorem of Wiener and Khintchine that relates the time dependent correlation functions to the frequency spectrum of fluctuations [24]. This theorem serves a considerable value in assessing the noise in circuits as well as in the transmission of electromagnetic signals.

Thirdly, fluctuations provide a natural framework for understanding a class of problems known in the literatures as *random walk* [25, 26, 27] and *Brownian motion* [28]. Brownian motion is ubiquitous in nature and one of the most stepping stone in the NESM. When mobile particles are immersed in an ambient medium, the particles undergo an incessant and irregular motion. This is known as the Brownian motion. The most common case of Brownian motion is the one originally observed by R. Brown, particles suspended in a fluid. However, less commonly more exotic situations are also encountered like an electron immersed in a black body radiation field (a gas of photon in equilibrium). Also, the motion of the particles need not be translational; rotational motion can also partake of the irregular character.

However, there is no hope to compute this irregularity of in detail, but it may be true that certain averaged features vary in a regular way, which can be described by simple laws. It is then important to suitably reformulate these irregularities via the principles of stochastic processes. The averaging processes are manifold but finally gives a correct measure of the average quantities. We note that the Brownian motion is the simplest non-equilibrium process that we encounter in physics. Henceforth the role of fluctuations, that lead to the non-equilibrium behavior in these processes, is of extreme importance for a better grasping of the subject.

1.4.1 *Why and When Fluctuations are Important?*

System trajectories in non-equilibrium states are characterized by the external driving source acting on the system and also due to the thermal force (due to the coupling with the surrounding). The thermodynamic quantities defined along these trajectories like injected and dissipated energies, applied work etc. therefore are affected due to the fluctuations [29]. For example, let us consider the motion of a Brownian particle suspended in a fluid and subjected to a constant external force. Because of thermal fluctuations, the work performed on the particle by this force per unit time, i.e., the injected power, fluctuates. The power fluctuations gradually become more and more important as the external force gets reduced. Equivalently, smaller the system size becomes, the larger the importance of thermal fluctuations becomes profound; though, they do not play much role in macroscopic systems or in thermodynamic limit. Nevertheless, the injected and dissipated energies may fluctuate in macroscopic systems if the dynamics is chaotic. For instance, think of a motor that stirs a fluid strongly. The motor can be driven by imposing a constant velocity. Because of the turbulent motion of the fluid, the power fluctuates in order to keep a constant velocity profile. These simple examples show that fluctu-

ations of the energies may be important not only in microscopic but also in macroscopic systems such as hydrodynamic flows, granular media, and opto-mechanical systems [30, 31, 32]. While dealing with fluctuations in out-of-equilibrium systems, we usually consider two classes: one where thermal fluctuations play a significant role (thermal systems) and another where the fluctuations are athermal and mostly due to the chaotic motion.

In this thesis I will mainly focus on the former case and briefly discuss few perspectives of the same. We emphasize again that the fluctuations play a major role in thermal systems since the system energy being injected or dissipated are smaller/same order of $k_B T$ (k_B being the Boltzmann constant and T is the ambient temperature). This limit is relevant to biological, nano, and micro systems.

1.4.2 Stochastic Thermodynamics

The viewpoint of equilibrium thermodynamics concerns with the study of the flow of energy or the conversion of energy in equilibrium. Linear irreversible thermodynamics extends the nineteenth-century concepts of equilibrium thermodynamics to systems that are close to or away from equilibrium. First out of equilibrium exact results were developed by Green and R. Kubo known as the *Green-Kubo formula* [21, 22] and the *linear response theory* [23]. Linear response theory allows to express transport properties caused by small external fields through equilibrium correlation functions provided that the system resides in a small (or linear order) deviation from equilibrium. Beyond this linear response regime, for a long time, no universal exact results were available.

Over the last twenty years new approaches have revealed general laws applicable to non-equilibrium systems. Systematically, the realm of linear response now has been extended into genuine non-equilibrium region along with the validity of exact thermodynamics statements

has been revisited. These exact results, which become particularly relevant for small systems, generically describe the statistics of thermodynamic observables such as exchanged heat, applied work, power flux or entropy production taken from ensembles with well-specified initial conditions. Unlike classical thermodynamical theory where fluctuations are small and neglected, *stochastic thermodynamics* gives a detailed description to measure the fluctuations which become immensely important in the small scale systems such as colloidal particles, biopolymers (DNA, RNA, proteins), enzymes and molecular motors [33, 34, 35]. Moreover, they systematically derive how the macroscopic irreversibility emerges from the microscopic reversibility. These are concisely known as the *fluctuation theorems* (FT) [36, 37, 38, 39, 19].

1.4.3 *Theoretical Investigations*

Non-equilibrium situations can be realized in diverse ways. First, the system can be prepared initially in equilibrium state and then genuine driving, that can be caused by the action of external force fields, flows or unbalanced chemical reactions, will lead to a non-equilibrium state. Secondly, if the system is subjected to thermodynamical forces or affinities such as multiple thermal or chemical reservoirs, it will eventually reach a NESS at large times. It has been found that the very presence of time dependent drivings also can lead to non-equilibrium situations asymptotically. The first case is clearly distinguished by the finite time dynamics and the FT valid at this regime are known as the *Transient Fluctuation Theorems* (TFT). On the other hand, the later cases take place in NESS at asymptotic times and the results valid in that realm are known as *Steady State Fluctuation Theorems* (SSFT).

1.4.3.1 Evans-Searles Transient Fluctuation Theorems

FT due to Evans-Searles [40] shows how irreversibility naturally emerges in macroscopic systems from reversible microscopic dynamics. These theorems are given in terms of the the dissipation function Ω_t which is a quantitative measurement of irreversibility. Considering the dynamics to be ergodic and be consistent with the initial condition, the relations are given by

$$\frac{p(\Omega_t = \mathcal{A})}{p(\Omega_t = -\mathcal{A})} = \exp[\mathcal{A}] \quad (11)$$

where $p(\Omega_t) = \mathcal{A}$ is the probability density of those trajectories which span in the phase space upto finite time t for the functional Ω_t to take values between \mathcal{A} and $\mathcal{A} + d\mathcal{A}$ starting from suitable initial conditions.

The limit $\langle \Omega_t \rangle = 0$ for all trajectories initiated anywhere in phase space, is the manifestation of *microscopic reversibility*. In other words, this condition implies that the system is in equilibrium, and the probabilities of observing any trajectory and its corresponding time reversal trajectory are equal (*detailed balance*). On the other hand, when $\langle \Omega_t \rangle > 0$, we have macroscopic dynamics moving in the forward direction while the reversed direction indicates $\langle \Omega_t \rangle < 0$. Therefore, $\langle \Omega_t \rangle \neq 0$ is the condition for *macroscopic irreversibility*. This belongs to the TFT class.

This was first observed in simulations of two dimensional sheared fluids by Evans and Morris [41]. Explicit expressions for the work distribution have been calculated by Mazonka *et al* [42] and Van Zon *et al* [43, 44, 45] independently in the case of uniformly moving harmonic traps in an ambient medium. The work distributions are found to be accompanied by Gaussian fluctuations and they validate Eq. (11). In contrast, the dissipated heat, generated due to the interaction of the system with its surroundings, turned out to be non-Gaussian with exponential tails and satisfy the transient FT with significant modification [43, 44, 45].

1.4.3.2 Work-Fluctuation Theorems-Jarzynski Equality

There exists a remarkable result particularly for the observable *applied work* due to Jarzynski [46, 47]. He showed that the work applied to driving the system from an initial equilibrium state, characterized by an initial value λ_0 of the driving protocol, to a final state, characterized by λ_t , via a time dependent Hamiltonian $\mathcal{H}(x, \lambda)$ for a *finite time* $\tau: 0 \leq \tau \leq t$, obeys the Jarzynski Equality (JE)

$$\langle e^{-\beta W} \rangle = e^{-\beta \Delta \mathcal{F}} \quad (12)$$

where the work W is given by

$$W = \int_0^t \dot{\lambda} \frac{\partial \mathcal{H}(x, \lambda)}{\partial \lambda} d\tau. \quad (13)$$

β is the inverse temperature and $\Delta \mathcal{F} = \mathcal{F}(\lambda_t) - \mathcal{F}(\lambda_0)$ is the free energy difference between the equilibrium states corresponding to the final value λ_t and the initial value λ_0 of the control parameter. This definition of work rather seems to be non-identical to the one that appears in mechanics, known as the *mechanical work*. This definition (which we will name as the *thermodynamical work* or *Jarzynski work*) has been used in less familiar context compared to the former one, used frequently in standard thermodynamics or the classical mechanics. The following example will demonstrate the fundamental differences between these two definitions.

Consider a schematic depiction of a single-molecule pulling experiment Fig. 1, that represents schematically a simpler version of experiments carried out Liphardt *et al* [49] and later by Collin, Ritort *et al* [50]. DNA handles tether a strand of RNA between two beads. One of them is held by a micropipette and kept fixed, while the other one is confined in a harmonic trap such that it is allowed to fluctuate or be driven due to the external perturbation. The entire system is immersed in a solution at room temperature. This plays the role of an *ambient medium*. The *work parameter* λ is defined as the distance between the end of the pipette and the center (or the minimum) of the

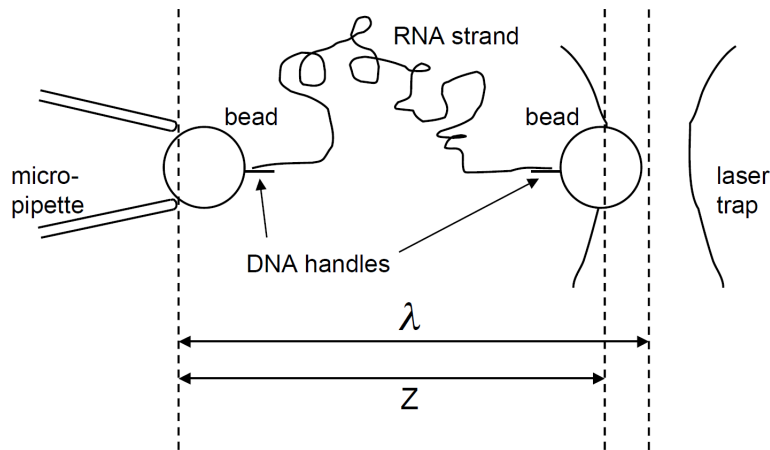


Figure 1: A single strand of RNA, tethered between two beads (micro-spheres). This diagram has been taken from [48].

trap. The work parameter can be externally manipulated, by varying the position of the trap Fig. 1. To make a connection between generic thermodynamic processes, let us view the RNA strand, DNA handles, and the two beads as the *system of interest*. The position of the fluctuating bead is denoted by z . When λ is held fixed, the system relaxes to a state of thermal equilibrium, characterized by the same. Let us now perform the following sequence of steps: (i) prepare the system by fixing the work parameter at $\lambda = A$, allowing the system to relax to equilibrium, (ii) perturb the system by varying the work parameter from its initial value $\lambda_0 = A$ to some final value $\lambda_t = B$ according to a given protocol. While changing the work parameter, we perform external work on it. The notation λ_τ specifies the value of the work parameter at a time τ during this interval, from $\tau = 0$ to $\tau = t$. Finally, (iii) fixing λ at the new value B , we allow the system to relax to a new state of equilibrium. No work is done during this last step since the work parameter is kept fixed. Thus we have performed an irreversible thermodynamic process, in which the system begins and

ends in equilibrium states but passes through non-equilibrium states at intermediate times. The amount of work W performed during a single realization of this process depends on the protocol and on the initial condition where the system was prepared. Since the system is continually jostled by the solution, its response to the perturbation will be accompanied by randomness. Upon repetition of the process many times, W typically will vary from one realization to the next. Thus we obtain statistical fluctuations in the amount of work performed. Secondly, we have to mention the nature of the modulation according to which we change the protocol which is stated below. Let us imagine that we stretch the molecule by varying λ at a uniform rate. The time-dependence of the work parameter is then described by: $\lambda_\tau = A + (B - A)\tau/t$. If F_τ denotes the force that the trap exerts on the bead at time τ , then there are two natural ways to define the work performed during this process [48]:

$$\begin{aligned} W_{\text{mech}} &= \int F \, dz = \int F_\tau \, z_\tau \, d\tau \\ W_{\text{therm}} &= \int F \, d\lambda = \int F_\tau \, \dot{\lambda}_\tau \, d\tau \end{aligned} \quad (14)$$

In both cases we integrate force versus displacement. The difference is that in the first case the displacement refers to the position of the bead, dz , while in the second case, the displacement of the trap, $d\lambda$ appears. In some sense, the first one is the work on the bead due to the trap and it is referred as the *mechanical work*. On the other hand, the later is the work performed by the experimentalist who moves the trap and usually known as the *thermodynamic work* or the *Jarzynski work*. It is worth pointing out that the *Jarzynski work* satisfies Eq. (12), not the *mechanical work*.

The relation given by Eq. (12) was originally derived for a isolated system governed by Hamiltonian dynamics (averaging over the *initial condition*). But it was shown later to hold for the stochastic dynamics as well when the system is kept in contact with a reservoir (averaging over the *initial condition* and the *noisy variables* produced due to the bath). Its validity requires that one has to start from an

equilibrium distribution but not that the system must relax at time t into new equilibrium. The relation has a paramount relevance of itself since it allows to measure the free energy difference (equilibrium property) from a non-equilibrium nonlinear measurement of the observable *Jarzynski work*. The maximum work theorem can be recovered simply using the Jensen's inequality $\langle W \rangle \geq \Delta\mathcal{F}$. As mentioned earlier, this relation holds true for any time so belongs to the TFT class.

For a charged particle in a harmonic trap, work fluctuations and the Jarzynski equality have been studied theoretically in the presence of a time independent and dependent magnetic [51] and an electric field [52, 53, 54, 55, 56].

1.4.3.3 Work-Fluctuation Theorems-Crooks Identity

Crooks later provided a significant generalization to the Jarzynski equality by considering the probability distribution of work $p(W)$ spent in the forward (F) process and the reversed (R) process within a *finite time* window [57, 58]. Here forward process means that the external protocol $\lambda(\tau)$ acts on the initial equilibrium state at time $\tau = 0$ and it ends at the final non-equilibrium state at time $\tau = t$. In the reversed process, the system evolves with the reversed protocol $\tilde{\lambda}(\tau) = \lambda(t - \tau)$ and one prepares the system in the equilibrium distribution corresponding to λ_t . This can be categorized into the TFT class. As a consequence of the time-reversal symmetry of the microscopic evolution Crooks Identity (CI) yields

$$\frac{p_F(W)}{p_R(-W)} = e^{\beta(W - \Delta\mathcal{F})} \quad (15)$$

where $p_F(W)$ and $p_R(W)$ indicate the distribution of work (*thermodynamic work* or the *Jarzynski work* defined in the last section) in the *forward* (F) and the *backward/reversed* (R) process respectively. Here $\Delta\mathcal{F}$ can be obtained by locating the crossover of the two distributions for

biomolecular applications. Jarzynski equality appears to be a straight forward corollary to this identity.

1.4.3.4 Entropy Production Theorems-Seifert Relation

Seifert extended the idea of Clausius inequality in microscopic systems. He derived an identity for the total entropy production along a trajectory in *finite time* [59]. This is given by

$$\langle e^{-\Delta s_{\text{tot}}} \rangle = 1 \quad (16)$$

where

$$\Delta s_{\text{tot}} = \Delta s_{\text{m}} + \Delta s_{\text{sys}}. \quad (17)$$

is the *total entropy production* The stochastic or trajectory dependent *system* entropy is defined as in the similar genre as Shannon,

$$\Delta s_{\text{sys}} = -\ln p(x_t, \lambda_t) + \ln p(x_0, \lambda_0) \quad (18)$$

and the *medium* entropy change Δs_{m} can be identified with the heat dissipated $q[x(\tau)]$ into the environment in the thermodynamic sense

$$\Delta s_{\text{m}}[x(\tau)] = q[x(\tau)]/T. \quad (19)$$

This relation holds for arbitrary initial distribution $p(x, 0)$, arbitrary time dependent driving λ_τ for a finite length of time t (TFT class). Using Jensen's inequality, we find $\langle \Delta s_{\text{tot}} \rangle \geq 0$, which is as same as the *Clausius inequality* or the *entropy maximum theorem*.

This relation has been proven for a bound particle trapped in a harmonic potential in the presence of a time-dependent force or a magnetic field, when the system was prepared in non-equilibrated conditions [60].

1.4.3.5 Gallavotti-Cohen Steady State Fluctuation Relation

In a NESS at an *infinite time* with fixed λ , the stochastic functionals obey the stronger *steady state fluctuation theorem* (SSFT)

$$\lim_{\tau \rightarrow \infty} \frac{1}{\tau} \ln \frac{p(\Omega_\tau = \omega\tau)}{p(\Omega_\tau = -\omega\tau)} = \omega \quad (20)$$

This relation was first proven by Gallavotti and Cohen in 1995 by assuming the dynamics to be chaotic [61]. This was later proved by Lebowitz, Spohn [62] and Kurchan [63] for stochastic diffusive dynamics. Later, this result has been proven valid for the *total entropy production* even in finite times [64, 65]

$$\frac{p(\Delta s_{\text{tot}})}{p(-\Delta s_{\text{tot}})} = e^{\Delta s_{\text{tot}}/k_B}. \quad (21)$$

But still there were questions about the validity for this theorem for other thermodynamic observables of interests such as work, heat or power flux. This is the main result for the SSFT class.

Using path integral techniques, Farago determined the statistics of the power injected by the thermal forces into an underdamped particle and examined the validation of the SSFT in 2002 [66]. Van Zon *et al* computed the probability distribution function (PDF) for work and the heat in great details in a system comprising a Brownian particle diffusing in a moving optical trap [43, 44, 45, 67, 68].

Average heat current and the distribution of exchanged heat with the corresponding FT were studied in few models of heat transport using the Langevin formalism. Examples include a single particle attached to two heat baths, two coupled particles attached to two different baths [69, 70, 71], heat flow through harmonic chain [72, 73, 74] and an anharmonic crystal [75]. Using the Onsager-Machlup path integral representation in NESS, Taniguchi and Cohen investigated PDFs and the SSFT for work and heat on a number of systems, including a Brownian particle in an electric field, a driven torsion pendulum, electric circuits etc. [76, 77, 78, 79].

1.4.3.6 Hatano-Sasa Equality for NESS

Hatano Sasa relation is a phenomenological derivation of *steady-state thermodynamics* organized around non-equilibrium steady states [80, 81] (SSFT class). This yields fluctuation theorems for transitions between steady states from the microscopic point of view. It relates the entropy change between the NESSs due to the transition to the excess heat flowing into the system

$$\langle e^{-(\Delta\phi + q_{\text{ex}}/T)} \rangle = 1 \quad (22)$$

where the steady states $p_s(x, \lambda)$ are represented in terms of the non-equilibrium potential $\phi(x, \lambda)$

$$p_s(x, \lambda) = \exp[-\phi(x, \lambda)]. \quad (23)$$

The excess heat q_{ex} is the heat associated with changing the external control parameter and differs from the total heat dissipation $q[x(\tau)]$ by the heat inevitably dissipated to maintain the corresponding NESSs.

We note that these relations mentioned so forth more or less fall into two categories: one is the exponential average over the observable and second is the ratio between two conjugate probability distribution functions. The first class is named as the *integral fluctuation theorem* e.g. Eq. (12), Eq. (16), Eq. (22). The second class, which deals with the full distributions, is known as the *detailed fluctuation theorem* e.g. Eq. (11), Eq. (15), Eq. (20). The *integral fluctuation theorems* can be derived straightway from the *detailed fluctuation theorems*.

1.4.4 Experimental Investigations

In this thesis, I have mostly looked into the problems addressed from the theoretical point of view. However, these problems are either motivated by experiments or leaves a scope for experimental verification in future days. Hence, it is important to present a brief overview of

the experimental advancements which has lead new discoveries and better understanding in this field till date. The simplest models systems which were studied at the early stage are moving harmonic traps [82, 83]. They studied Eq. (11) for finite time and the Eq. (20) in NESS. Trepagnier *et al* in [84] studied experimentally the transition from one NESS to another by changing the speed of the moving trap verifying Eq. (22). Mapping electric circuits into the dragged colloidal particle, Ciliberto and co-workers investigated corresponding FTs and PDFs [85]. Later Ciliberto *et al* verified Eq. (16) in an experimental analysis of the energy exchanged between two conductors kept at different temperature and coupled by the electric thermal noise which can be mapped to a model of two Brownian particles kept at different temperatures and coupled by elastic force [86]. Carberry *et al* investigated the fluctuations of a colloidal particle in a stiffness varying harmonic trap [87]. Their results verified Eq. (11). For strongly localized initial conditions, Eq. (11) has also been verified experimentally by Khan and Sood [88]. Blicke *et al* measured the work fluctuations for a colloidal particle between two equilibrium states and subjected to a time dependent non-harmonic potential. They found the work distribution to be non-Gaussian nevertheless the PDF satisfied the Jarzynski equality and Crooks identity [89]. In a series of experiments, Ciliberto *et al* reported various energy fluctuations (heat, work, entropy) in a harmonic oscillator driven out of equilibrium by an external force. The oscillator is modelled as an underdamped driven torsional pendulum and they aimed to check the *Jarzynski equality* and the *Crooks identity*. They also determined the free energy difference using this model in case of a linear (equilibrium) and sinusoidal (NESS) forcing [90, 91, 92]. Speck *et al* analyzed the entropy production fluctuations and Eq. (21) in a NESS originated in a system of a single particle driven by a constant force in a periodic potential [93].

1.4.5 How to measure the Fluctuations

It is well understood from the preceding sections that symmetry properties emerge in non-equilibrium systems through the given configurational probability distribution. But the more fundamental question is how to compute these distributions. In the absence of a general rule, one uses various schemes to solve the stationary states far from equilibrium. Gaussian fluctuations are amenable and easy to measure. But in certain scenarios the stationary states generate nontrivial non-Gaussian fluctuations, thus can not be framed using general methods of stochastic processes. In the following, we will present a simple example of non-equilibrium system which generate non-Gaussian fluctuations inherently.

1D Biased Random Walk:

Consider a biased random walk on 1D N -site infinite lattice of unity lattice basis Fig. 2, where the walker takes a right step with a probability p and takes a left step with probability $q = 1 - p$. We ask the question: what is the probability $P(m, N)$ that the walker is at site m after N steps. The dynamics is simple to describe

$$x_n = x_{n-1} + \zeta_n \quad (24)$$

where

$$\zeta_n = \begin{cases} -1 & \text{with probability } q, \\ 1 & \text{with probability } p \end{cases} \quad (25)$$

The answer is given by the binomial distribution

$$P(m, N) = p^{\frac{N+m}{2}} q^{\frac{N-m}{2}} \frac{N!}{\left(\frac{N+m}{2}\right)! \left(\frac{N-m}{2}\right)!} \quad (26)$$

The mean displacement or the drift term is simple to compute and given by $\langle m \rangle = N(p - q)$. The mean square displacement of the walker is $\sigma^2 = \langle m^2 \rangle - \langle m \rangle^2 = 4Npq$. Even though the expression

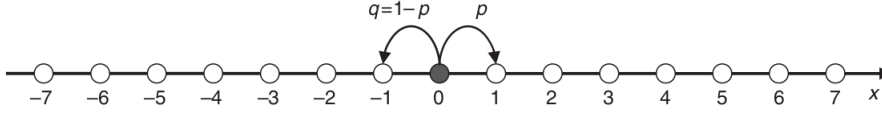


Figure 2: A schematic diagram of a 1D N-site biased random walk. We ask: what is the probability $P(m, N)$ that the walker is at m-th site after N-steps ?

Eq. (26) is complete and we know perfectly well how to calculate each term in it, we will make use of Stirling’s formula for the factorial to produce an expression more amenable especially when N (the number of steps) is large. Stirling’s formula is given by

$$N! \approx \sqrt{2\pi N} \exp[N(\ln N - 1)] \tag{27}$$

Using this and making a very crucial assumption that m fluctuates within \sqrt{N} , we find that the combinatorial factor has the form

$$P(m, N) \sim e^{-\frac{[m-N(p-q)]^2}{8Npq}} \tag{28}$$

So, in other words, the walker more or less stays within the span of \sqrt{N} . This is the *typical* behavior of the walker. This result can also be proved from the so called *central limit theorem* [27, 26]. But what happens, when we have to consider beyond the *typical Gaussian fluctuations* i.e. we ask the following: what is the probability that the walker does not stay within the square root distance, rather explores beyond it. In other words, how do we quantify the probability when $m \sim O(N)$? This answer can be addressed within the framework of *large deviation principles* and the probabilities are usually represented by the *large deviation functions* (LDF) These functions encode the *non-Gaussian, atypical or rare fluctuations* which are beyond the Gaussian regime. For instance, in the above example one can show that

$$P(m, N) \sim \exp[N \Phi(\frac{m}{N})] \tag{29}$$

where $\Phi(\frac{m}{N})$ is known as the large deviation function and given by

$$\Phi(z) = -\frac{1+z}{2} \log\left(\frac{1+z}{2p}\right) - \frac{1-z}{2} \log\left(\frac{1-z}{2q}\right), \quad (30)$$

where $z = m/N$. This is the most general large- N result and valid for any range of m . It is easy to reproduce the Gaussian fluctuations from the large deviation functional form if one expands it around the *mean value* upto $\mathcal{O}(\sqrt{N})$ and exactly at the mean $\bar{z} = p - q$, the LDF vanishes (See Fig. 3). Gaussian fluctuations are generically denoted as typical fluctuations and the atypical or rare or large fluctuations are characterized by non-universal and non-Gaussian fluctuations. This envisages one to investigate this complex nature of the randomness beyond the law of large numbers or the central limit theorem in different systems.

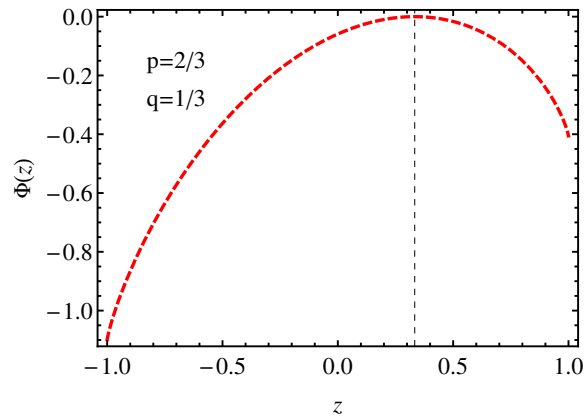


Figure 3: The large deviation function Eq. (30) corresponding to the biased random walk with $p = 2/3$, $q = 1/3$. The LDF vanishes at $\bar{z} = p - q$, as indicated by the dashed line in the figure.

The theory of *large deviations* [94, 95, 96, 97] is concerned with the exponential decay of probabilities of rare but nonzero fluctuations in stochastic systems. The large deviation theory generally appears as an extension of *Cramer's theorem* in the context of sample means of random variables. One can say that this theory is a refinement of the *law of large numbers* and *central limit theorem*, which is majorly applicable to small fluctuations. There are several correspondences between statistical mechanics and large deviation theory. As a matter

of fact, in every sense the mathematics of statistical mechanics can be elegantly explained within the framework of *large deviation principle*.

The equilibrium properties of many-particle systems are described at a probabilistic level by statistical mechanical ensembles, such as the microcanonical, canonical or the grand canonical ensembles. By defining these ensembles explicitly focusing on large deviation theory, the study of equilibrium states and their fluctuations in a given ensemble can eventually be reduced to the study of properly defined large deviation functions. Naturally, connections between equilibrium statistical mechanics and large deviation theory become tremendously overlapped. For example, the entropy function and the free energy function become equivalent to the LDFs on the basis of microcanonical and canonical ensemble respectively. *Variational principles*, such as the entropy maximization or the minimum free energy principle, follow straight-way from the *contraction principle* in the large deviation theory [94]. The analogy with the extremum principle often motivates one to consider the large deviation functions as the non-equilibrium free energy [95, 98]. In fact, large deviation theory not only justifies these principles, but also provides a prescription for generalizing them to arbitrary macrostates and arbitrary many-particle systems. So, it appears to be intuitive to extend these principles in the realm of non-equilibrium physics. So it appears that the study of large deviations arising in out-of-equilibrium physical systems has been the most successful venture in the field of Non-equilibrium statistical mechanics in recent times.

The dynamical nature of non-equilibrium systems follows a framework similar to the equilibrium one. At equilibrium, thermodynamic limits are considered in terms of the *extensive* variables such as the *number of particles* or the *volume element*. To extend the idea in non-equilibrium case including the large deviation analysis, one would generically require such *extensive* variable. Being out of equilibrium, one naturally includes *time* possibly as the *extensive* parameter controlling a large deviation principle. The idea is to define the system

precisely, calculate the states from the first principles (microscopic or coarse-grained), and proceed from there to derive large deviation principles for observables that are functions of the system's state associating the concept of *large* to the control variable such as time or the system size.

The knowledge of the rate function usually provides a complete description of the fluctuations present in the system. It is often found that most of the non-equilibrium systems are characterized by atypical fluctuations taking place either with an exponentially decaying probability or at an infinite time scale. Thus, the large deviation principle systematically can behold these certain features and characterizing these states no longer remain elusive. The 1D random walk, described above is a typical example of non-equilibrium system where the steady states are characterized completely using the large deviation functions. In this thesis, we will discuss stochastic diffusive models where the systems will be driven away from equilibrium by applying time constrained driving. The steady states and the useful observables such as the entropy production, work flux, dissipated heat can generate non Gaussian fluctuations and the measurement of these fluctuations will be quantified via the large deviation functions. It is important to clarify that the computation of LDFs is a daunting task generically with a countable number of examples existing. Yet, it will turn out that we can compute them exactly for the systems of our interests which is certainly a great endeavour *per se*.

1.5 PROLOGUE OF THE THESIS

Over the last two decades or so, several attempts are made to understand out of equilibrium systems and measure the observable fluctuations and their distributions in details by probing various class of external but *deterministic driving*. This includes constant dragging, linear and nonlinear time dependent forcing, sinusoidal oscillations,

non-conserving driving, anisotropic shear flow and etc. The realm of deterministic driving thus is well understood and poses no further conceptual challenge. Surprisingly, though there are plenty of examples of *deterministic driving* which triggers the system out of equilibrium, only a few attempts have been made on the issue of *stochastic driving*.

This thesis is aimed at the thorough investigation of the fluctuations of the relevant thermodynamic observables under *stochastic driving*. Stochastic driving is an issue of both conceptual as well as practical interest. The conceptual barrier lies on the nature of the stochastic driving: whether it is a reversible or an irreversible process? One may then wonder whether the energy transferred to the system can be treated as work, otherwise one has to incorporate the work source of the driving in addition. Furthermore, the question is how much entropy exchange is involved in this process? On the other hand, from the experimental point of view, a deterministic driving/protocol is never perfect and always accompanied by uncontrollable small random fluctuations. The following experiment performed in Lyon is the first of this league to raise this issue. The authors have studied the work fluctuations in a system of a colloidal particle in a harmonic trap where the trap is being modulated by stochastic force in a table top experiment [99]. This group has also studied the dynamics of the tip of an AFM (Atomic Force Microscope) subjected to random Gaussian driving and measured the work fluctuations in NESS [99]. This problem was analytically tackled in [100] where the author has computed the full probability distributions of the work and then verified the SSFT Eq. (20) at large time. Recently, Gatién *et al* considered a stationary Markovian dynamics on a bipartite joint system made of a system with two states and an independent energy source which is also modelled as a two level Markov process. They measured the the work statistics of the system driven by a stochastic (reversible) energy source in terms of the large deviation functions [101, 102]. Furthermore, they showed that the work statistics satisfy the Crooks

Identity Eq. (15). This has put the condition that a system subjected to a stochastic driving can be seen thermodynamically as a system subjected to a work source, only when the stochastic driving protocol is statistically reversible. Under this assumption, the authors found that the total entropy production indeed satisfies the Eq. (15) or Eq. (20).

In this thesis, I will try to address the questions regarding the *stochastic driving* by looking into diffusive Langevin models which have not been anticipated before. The models studied here are paradigm examples of non-equilibrium systems where the large deviation functions can be estimated exactly and verified through *computer simulations* and perhaps from the *table top experiments* [103, 104].

1.6 OUTLINE OF THE THESIS

In this section, we briefly outline the main contents of the thesis. Our aim is primarily two fold. Firstly, we are interested in computing the full probability distribution functions of these observables, represented by the LDFs. It is important to analyze the role of driving parameter in the dynamics and the distributions will reflect this issue. Secondly, we intend to study the symmetry properties of the PDFs in the context of the FT in the steady state. We will try to see whether there lies any common feature which emerges due to the stochastic driving.

In the preceding chapter, we study the paradigm problem of an overdamped Brownian particle inside a harmonic trap. In the earlier studies, the source of non-equilibrium was induced by the modulation of the trap by a constant velocity or a linear and sinusoidal time dependent dragging. Instead, we drive the trap with stochastic modulation. This investigation thus indeed gives a more realistic way to treat the dragged Brownian particle confined in a potential. To be specific, the dynamics of the trap is modelled as the Ornstein-Uhlenbeck process, which is a linear process. We study the work fluctuations

on the particle due to the driving for a finite time in the NESS. We derive the full distribution of the applied work in terms of the system parameters. We then study the validation of the FT in the case of stochastic driving by looking into the *symmetry properties* of the PDFs [103].

The third chapter presents a brief summary of the stochastic driving on the other observables such as the heat dissipation, the total entropy production in the NESS for the paradigm model introduced in the previous chapter. We derive the corresponding PDFs in terms of the system parameters and discuss the symmetry properties of the PDFs. Subsequently, we briefly chalk out the *boundary effects* on the various observables which lead to a non universal domain of the validation of the FT in the parameter space. At the end, we present a simple probabilistic model and explain the typical and atypical (due to the *boundary terms*) behavior of the observables reproducing a qualitative behavior of the work, heat and entropy fluctuations found already in the Langevin systems [45, 68, 105].

In the final chapter, we incorporate the *inertial effects* on the system. We consider an underdamped Brownian particle which is being dragged through the medium by a stochastic force. This mimics the situation of a colloidal particle which is in a bath consisting of many particles where they have equilibrated faster than the mesoscopic heavy Brownian particle. The bath, maintained at a constant temperature, serves as a source of the friction and the noise. Relating them via the fluctuation-dissipation theorem, the stochastic motion of the Brownian particle can be framed suitably in a Langevin setup. In the absence of any external drive, the system reaches a stationary state. However any non-zero external drive will lead the system away from equilibrium and we have studied the effects of this drive to the system. Later, we have analyzed the observable statistics in great details. This model can be of very importance from the viewpoint of transport phenomena as, in suitable limits, it mimics the system of a Brownian particle connected with two different thermal baths at the two ends.

The difference in the temperature leads to a non-equilibrium situation and it is important to characterize the heat current or the work on the particle due to the thermal baths. Though in reality, measuring the mean or the fluctuations of these observables are quite complicated, nevertheless, we have derived few exact results which can be tested in the conduction experiments. At the very end of this chapter, we investigate the symmetry properties of the corresponding distribution functions and make a comment on the FT suited in the current context [104]. We add general comments and a brief overview in the conclusion.

WORK FLUCTUATIONS OF A BROWNIAN PARTICLE IN A MOVING HARMONIC TRAP

2.1 ABSTRACT

In this chapter, we have studied the motion of a Brownian particle in a harmonic trap. The location of the trap is modulated according to an Ornstein-Uhlenbeck process. We investigate the fluctuation of the work done by the modulated trap on the Brownian particle in a given time interval in the steady state. We compute the large deviation as well as the complete asymptotic form of the probability density function of the work done. The theoretical asymptotic forms of the probability density function are in very good agreement with the numerics. We also discuss the validity of the fluctuation theorem for this system.

2.2 INTRODUCTION

A Brownian particle confined in a harmonic trap in one spatial dimension serves as the paradigm problem to introduce the basic concepts of stochastic thermodynamics and compute the average observables systematically. Let us first consider a situation when the trap is kept static. In that case, the particle will diffuse around the minimum of the trap and will eventually reach to an equilibrium distribution, peaked at the minimum of the potential and given by Boltzmann distribution. But a generic non-equilibrium situation arises if the trap is not static, rather it acquires motion. The simplest way to perturb the system would be to drag the trap with a constant velocity. In that case,

the system will certainly be out of equilibrium, however at long times it will reach an effective equilibrium state provided that the motion is observed in a co-moving frame (i.e. in the reference frame of the moving well). Let us illustrate this model in the following. Consider the Brownian particle in a harmonic trap, in contact with a thermal bath at temperature $T = \beta^{-1}$, is pulled through the medium by a constant velocity. Considering the overdamped motion, let x denote the location of the particle, and let

$$U(x, t) = \frac{k}{2}(x - y)^2 \quad (31)$$

where $U(x, t)$ is the moving potential well and y is the minimum of the trap. Let v be the velocity at which the trap is being pulled. Assume furthermore that the thermal forces can be modeled as the sum of linear friction and white noise, then the equation of motion is simply given by

$$\dot{x} = -\frac{1}{\gamma} \frac{\partial U}{\partial x} + \eta \quad (32)$$

$$\dot{y} = v$$

where γ is the viscosity and η is the thermal noise with the correlations $\langle \eta(\tau) \rangle = 0$, $\langle \eta(\tau) \eta(\tau') \rangle = 2D\delta(\tau - \tau')$. The diffusion constant is denoted by D and satisfies the Stokes-Einstein relation $D\gamma = k_B T$. The observables of interests are (i) the work done due to the modulation of the trap

$$W_\tau = \int_0^\tau \frac{\partial U}{\partial y} \dot{y} dt = - \int_0^\tau k(x - vt)v dt \quad (33)$$

and (ii) the entropy production of the medium given by $\Delta s^{\text{med}} = -\beta Q$ where the heat part is defined as

$$Q_\tau = \int_0^\tau [-\gamma \dot{x} + \eta] \dot{x} dt \quad (34)$$

*Brownian particle in
a harmonic trap
driven with a
constant velocity*

In a series of paper, this problem has been studied extensively both theoretically [43, 44, 45, 42, 106, 68] and experimentally [82, 83]. The authors have computed the work and the heat distributions in finite time and in the NESS. The results have also been verified through

the experiments. Moreover, it has been shown that though the work distribution always satisfies the TFT and SSFT, indeed that is not true for the heat distributions. They provided an extended fluctuation theorem that differs from the typical SSFT. It was found that the ratio of the probability for absorption of heat (by the particle from the fluid) to the probability to supply heat (by the particle to the fluid) is much larger here than in the conventional fluctuation theorem. Later, the authors extended the theory in the case of small electrical circuits. They measured the power and the heat fluctuations in the following set ups. This was initially done for a parallel resistor and capacitor with a constant current source and the analogy with a Brownian particle dragged through a fluid was referred. The connection was made under the name *Brownian-Nyquist* analogy [85, 86]. In the following, we provide the analogy for a quick reference. Consider an electric circuit in which a resistor with resistance R and a capacitor with capacitance C are arranged in parallel. The circuit is subject to a constant, nonfluctuating current source I . Energy is being dissipated in the resistor as the form of heat. The fluctuations are controlled by a voltage generator and can be modelled as Gaussian white noise δV_t , often known as the Nyquist noise. In addition, let's define q_t as the charge that has gone through the resistor, i_t as the current that is going through it (so $i_t = dq_t/dt$). Therefore standard calculations yield

$$R \frac{dq_t}{dt} = -\frac{q_t - I t}{C} - \delta V_t \quad (35)$$

The heat developed in the resistor is given by

$$Q_\tau = \int_0^\tau [i_t R + \delta V_t] \dot{q}_t dt, \quad (36)$$

which is nothing but the time integrated voltage times the current. Using a suitable analogy, it can be shown that the heat fluctuations in the parallel RC circuit behaves completely analogous to the heat for the Brownian particle, and thus satisfies the extended FT. On the

Brownian-Nyquist

Analogy with an

Electric Circuit

other hand, the work fluctuations in this circuit is the time integrated power flux and given by

$$W_\tau = - \int_0^\tau [q_t - I t] \frac{I}{C} dt \quad (37)$$

This happens to be precisely the same form of work as for a Brownian particle and satisfies the TFT and the SSFT at large times. A similar behavior can also be observed in the case of a serial RC circuit with Nyquist noise and imposed voltage. But all this class of problems are treated with a family of deterministic driving. Alternatively, we want to model similar systems with experimentally more feasible driving protocols like the stochastic driving.

Recently, in reference [99] reported experiments on the fluctuations of the work done by an external Gaussian random force on two different stochastic systems coupled to a thermal bath: (i) a colloidal particle in an optical trap and (ii) an atomic-force microscopy cantilever. Analytical results have been obtained for the second system in [100]. In the first experiment, a colloidal particle immersed in water (which acts as thermal bath) is confined in an optical trap. The position of the trap is modulated according to a Gaussian Ornstein-Uhlenbeck process. The authors have experimentally determined the probability density function of the work done on the colloidal particle by the random force exerted by the modulating trap. I will present here the analytical treatment of this problem in details which is the first most attempt of this paradigm problem under stochastic driving [103].

In Sec. 2.3, we define the model. Sec. 2.4 contains the derivation of the moment generating function of work done W_τ in a given time τ , which has the form $\langle e^{-\lambda W_\tau} \rangle \approx g(\lambda) e^{\tau \mu(\lambda)}$ for large τ . In this chapter, the focus will be on the mechanical work Eq. (40) and its distribution functions. Sec. 2.5 contains the details of the method to evaluate the moment generating function. The results are explicitly given in Section 2.6. In Sec. 2.7, we analyze the function $g(\lambda)$ in terms of θ and δ . We invert the moment generating function to obtain the asymptotic form (for large τ) of the PDF of W_τ in Sec. 2.8. We have found in

Sec. 2.7 that $g(\lambda)$ can either be analytic, or can have either one branch point or three or four branch points, depending on the values of the tuning parameters of the problem. The case when $g(\lambda)$ is analytic, is simpler and the asymptotic PDF can be obtained by the usual saddle point approximation, which is given by Eq. (118) in Sec. 2.8.1. In Sec. 2.8.2, we deal with case when $g(\lambda)$ has one branch point. The cases when $g(\lambda)$ has three and four branch points are discussed in Secs. 2.8.3 and 2.8.4, respectively. The analytical results obtained in each section are supported by numerical simulation performed on the system. Sec. 2.9 contains a discussion on large deviation function and validity of the fluctuation theorem in the context of the problem at hand. Finally, we summarize the chapter in Sec. 2.10.

2.3 THE MODEL

Consider a Brownian particle suspended in a fluid at temperature T , with the viscous drag coefficient γ . The particle is confined in a quadratic potential (harmonic trap) around the position y and having a stiffness k . The position $x(t)$ of the particle is described by the overdamped Langevin equation

$$\frac{dx}{dt} = -\frac{x-y}{\tau_\gamma} + \xi(t), \quad (38)$$

where $\tau_\gamma = \gamma/k$ is the relaxation time of the harmonic trap. The thermal noise $\xi(t)$ is taken to be Gaussian with mean $\langle \xi(t) \rangle = 0$ and covariance $\langle \xi(t)\xi(s) \rangle = 2D\delta(t-s)$, where the diffusion coefficient $D = \gamma^{-1}k_B T$ with k_B being the Boltzmann constant. An external time-varying random force is exerted by the trap on the Brownian particle by externally modulating the position of the trap according to an Ornstein-Uhlenbeck process

$$\frac{dy}{dt} = -\frac{y}{\tau_0} + \zeta(t), \quad (39)$$

where $\zeta(t)$ is an externally generated Gaussian white (non-thermal) noise with mean $\langle \zeta(t) \rangle = 0$ and covariance $\langle \zeta(t)\zeta(s) \rangle = 2A\delta(t-s)$.

There is no correlation between the externally applied noise and the thermal noise, $\langle \zeta(t)\xi(s) \rangle = 0$. The system eventually reaches steady state, and in the steady state the trap exerts a correlated random force $k y(t)$ on the Brownian particle with mean $\langle y(t) \rangle = 0$ and covariance $\langle y(t)y(s) \rangle = A\tau_0 \exp(-|t-s|/\tau_0)$. The quantity of our interest is the work done in the steady state, by the random force exerted by the trap on the Brownian particle in a given time duration τ . This is given (in units of $k_B T$) by

$$W_\tau^{\text{mech}} = \frac{1}{k_B T} \int_0^\tau k y(t) \dot{x} dt, \quad (40)$$

with the initial condition (at $\tau = 0$) drawn from the steady state distribution. We notice that this is the definition of the *mechanical work* (i.e force times displacement of the particle) and clearly different from that due to Jarzynski, which can be given in this context as

$$W_\tau^J = \frac{1}{k_B T} \int_0^\tau dt k(y-x) \dot{y}. \quad (41)$$

We will denote W_τ^{mech} as W_τ throughout this chapter and any other usage of same notation, if any, will be explained in the context.

It will prove convenient to use the following dimensionless parameters (which characterizes the *stochastic modulation*) for future context

$$\theta = A/D, \quad \text{and} \quad \delta = \tau_0/\tau_\gamma. \quad (42)$$

Here, θ characterizes the ratio between the thermal and the external probed noise respectively. The time scale separation between the system's own relaxation and the external driving has been denoted by δ . From an experimental perspective [99], it is natural to use another parameter that measures the deviation of the system from equilibrium:

$$\alpha = \frac{\langle x^2 \rangle}{\langle x^2 \rangle_{\text{eq}}} - 1, \quad (43)$$

where $\langle x^2 \rangle$ is the variance of x in the steady state in the presence of trap modulation, whereas $\langle x^2 \rangle_{\text{eq}} = D\tau_\gamma$ is the corresponding variance

at equilibrium, i.e., without the presence of the trap modulation ($y = 0$). It should be noted that, the three parameters introduced above are not independent of each others and are related by

$$\alpha = \theta\delta^2(1 + \delta)^{-1}. \quad (44)$$

The mean work can be computed easily using the above equations and one finds $\langle W_\tau \rangle \approx \alpha\tau/\tau_0$ for large τ . Although the mean work is positive (and large for large τ), there can be negative fluctuations (with small probabilities) and the fluctuation theorem quantifies the ratio of the probabilities of the positive and the negative fluctuations.

2.4 MOMENT GENERATING FUNCTION

To compute the distribution of W_τ , we first consider the moment generating function restricting to fixed initial and final configurations (x_0, y_0) and (x, y) respectively:

$$Z(\lambda, x, y, \tau|x_0, y_0) = \langle e^{-\lambda W_\tau} \delta[x - x(\tau)]\delta[y - y(\tau)] \rangle_{(x_0, y_0)}, \quad (45)$$

where $\langle \dots \rangle_{(x_0, y_0)}$ denotes an average over the histories of the thermal noises starting from the initial condition (x_0, y_0) . It can be shown that $Z(\lambda, x, y, \tau|x_0, y_0)$ satisfies the Fokker-Planck equation

$$\frac{\partial Z}{\partial \tau} = \mathcal{L}_\lambda Z \quad (46)$$

with the initial condition $Z(\lambda, x, y, 0|x_0, y_0) = \delta(x - x_0) \delta(y - y_0)$, and the Fokker-Planck operator is given by

$$\begin{aligned} \mathcal{L}_\lambda = D \frac{\partial^2}{\partial x^2} + \theta D \frac{\partial^2}{\partial y^2} + \frac{\delta}{\tau_0} \frac{\partial}{\partial x} (x - y) + \frac{1}{\tau_0} \frac{\partial}{\partial y} y \\ + \frac{2\lambda\delta}{\tau_0} y \frac{\partial}{\partial x} + \frac{\lambda\delta^2}{\tau_0^2 D} y(x - y) + \frac{\lambda^2\delta^2}{\tau_0^2 D} y^2. \end{aligned} \quad (47)$$

We do not know whether the above partial differential equation can be solved to obtain Z . Fortunately, however, one does not require the complete solution of the above equation to determine the large- τ behavior of the distribution of W_τ .

The solution of the Fokker-Planck equation can be formally expressed in the eigenbases of the operator \mathcal{L}_λ and the large τ behavior is dominated by the term having the largest eigenvalue. Thus, for large- τ ,

$$Z(\lambda, x, y, \tau | x_0, y_0) = \chi(x_0, y_0, \lambda) \Psi(x, y, \lambda) e^{\tau \mu(\lambda)} + \dots, \quad (48)$$

where $\Psi(x, y, \lambda)$ is the eigenfunction corresponding to the largest eigenvalue $\mu(\lambda)$ and $\chi(x_0, y_0, \lambda)$ is the projection of the initial state onto the eigenstate corresponding to the eigenvalue $\mu(\lambda)$. While we cannot solve the Fokker-Planck equation, the functions in Eq. (48) can be obtained using a method sketched in the following.

2.5 COMPLETE DERIVATION OF THE MOMENT GENERATING FUNCTION

The evolution equations (38) and (39) can be presented in the matrix form

$$\frac{d\mathbf{U}}{dt} = -\frac{1}{\tau_0} \mathbf{A} \mathbf{U} + \boldsymbol{\eta}(t), \quad (49)$$

where $\mathbf{U} = (x, y)^\top$ and $\boldsymbol{\eta} = (\xi, \zeta)^\top$ are column vectors and \mathbf{A} is a 2×2 matrix given by

$$\mathbf{A} = \begin{pmatrix} \delta & -\delta \\ 0 & 1 \end{pmatrix}. \quad (50)$$

Using the integral representation of δ -function such as

$$\delta(\mathbf{U} - \mathbf{U}(\tau)) = \int \frac{d^{2N} \boldsymbol{\sigma}}{(2\pi)^{2N}} e^{i \boldsymbol{\sigma}^\top (\mathbf{U} - \mathbf{U}(\tau))}, \quad (51)$$

where $\boldsymbol{\sigma}^\top = (\sigma_1, \sigma_2, \dots, \sigma_{2N})$, we find the *restricted* moment generating function, defined by Eq. (45), to be

$$Z(\lambda, \mathbf{U}, \tau | \mathbf{U}_0) = \int \frac{d^2 \boldsymbol{\sigma}}{(2\pi)^2} e^{i \boldsymbol{\sigma}^\top \mathbf{U}} \langle e^{-\lambda W_\tau - i \boldsymbol{\sigma}^\top \mathbf{U}(\tau)} \rangle_{\mathbf{U}_0}, \quad (52)$$

where $\boldsymbol{\sigma}^\top = (\sigma_1, \sigma_2)$.

Substituting dx/dt from Eq. (38) in Eq. (40) we get

$$W_\tau = \int_0^\tau dt \left[-\frac{\delta^2}{\tau_0^2 D} y(x-y) + \frac{\delta}{\tau_0 D} y\xi \right], \quad (53)$$

which is useful to rewrite as

$$W_\tau = \frac{1}{2} \int_0^\tau dt \left[\frac{1}{\tau_0^2} \mathbf{U}^\top \mathbf{A}_1 \mathbf{U} + \frac{1}{\tau_0} (\mathbf{U}^\top \mathbf{A}_2^\top \boldsymbol{\eta} + \boldsymbol{\eta}^\top \mathbf{A}_2 \mathbf{U}) \right], \quad (54)$$

where

$$\mathbf{A}_1 = \frac{\delta^2}{D} \begin{pmatrix} 0 & -1 \\ -1 & 2 \end{pmatrix} \quad \text{and} \quad \mathbf{A}_2 = \frac{\delta}{D} \begin{pmatrix} 0 & 1 \\ 0 & 0 \end{pmatrix}. \quad (55)$$

Now, we proceed by defining the finite-time Fourier transforms and their inverses as follows:

$$[\tilde{\mathbf{U}}(\omega_n), \tilde{\boldsymbol{\eta}}(\omega_n)] = \frac{1}{\tau} \int_0^\tau dt [\mathbf{U}(t), \boldsymbol{\eta}(t)] \exp(-i\omega_n t), \quad (56)$$

$$[\mathbf{U}(t), \boldsymbol{\eta}(t)] = \sum_{n=-\infty}^{\infty} [\tilde{\mathbf{U}}(\omega_n), \tilde{\boldsymbol{\eta}}(\omega_n)] \exp(i\omega_n t), \quad (57)$$

with $\omega_n = 2\pi n/\tau$. In the frequency domain, the Gaussian noise configurations denoted by $[\boldsymbol{\eta}(t) : 0 < t < \tau]$ is described by the infinite sequence $[\tilde{\boldsymbol{\eta}}(\omega_n) : n = -\infty, \dots, -1, 0, +1, \dots, \infty]$ of Gaussian random variables with the correlation

$$\langle \tilde{\boldsymbol{\eta}}(\omega) \tilde{\boldsymbol{\eta}}^\top(\omega') \rangle = \frac{2D}{\tau} \delta(\omega + \omega') \text{diag}(1, \theta). \quad (58)$$

In terms of the Fourier transform Eq. (54) can be written as

$$W_\tau = \frac{\tau}{2} \sum_{n=-\infty}^{\infty} \left[\frac{1}{\tau_0^2} \tilde{\mathbf{U}}^\top(\omega_n) \mathbf{A}_1 \tilde{\mathbf{U}}(-\omega_n) + \frac{1}{\tau_0} \left\{ \tilde{\mathbf{U}}^\top(\omega_n) \mathbf{A}_2^\top \tilde{\boldsymbol{\eta}}(-\omega_n) + \tilde{\boldsymbol{\eta}}^\top(\omega_n) \mathbf{A}_2 \tilde{\mathbf{U}}(-\omega_n) \right\} \right]. \quad (59)$$

Equation (49) gives

$$\tilde{\mathbf{U}}(\omega_n) = \tau_0 \mathbf{G} \tilde{\boldsymbol{\eta}}(\omega_n) - \frac{\tau_0}{\tau} \mathbf{G} \Delta \mathbf{U}, \quad (60)$$

where $\mathbf{G} = [i\omega \mathbf{I} + \mathbf{A}]^{-1}$ with $\mathbf{u} = \omega_n \tau_0$, $\Delta \mathbf{U} = \mathbf{U}(\tau) - \mathbf{U}(0)$, and \mathbf{I} being the identity matrix. The elements of \mathbf{G} are: $G_{11} = (\delta + i\mathbf{u})^{-1}$, $G_{22} = (1 + i\mathbf{u})^{-1}$, $G_{12} = \delta G_{11} G_{22}$, and $G_{21} = 0$. Note that $\mathbf{G}(-\mathbf{u}) =$

$G^*(u)$, $\tilde{\eta}(-\omega) = \tilde{\eta}^*(\omega)$, and $\tilde{U}(-\omega) = \tilde{U}^*(\omega)$. Substituting \tilde{U} in Eq. (54), and grouping the negative n indices together with their positive counterparts in the summation, we get

$$\begin{aligned} W_\tau = & \left[\frac{1}{2} \tilde{\tau} \tilde{\eta}_0^T (G_0^T A_1 G_0 + A_2 G_0 + G_0^T A_2^T) \tilde{\eta}_0 - \Delta U^T (G_0^T A_1 G_0 + G_0^T A_2^T) \tilde{\eta}_0 \right. \\ & \left. + \frac{1}{2\tau} \Delta U^T (G_0^T A_1 G_0) \Delta U \right] \\ & + \sum_{n=1}^{\infty} \left[\tilde{\tau} \tilde{\eta}^T (G^T A_1 G^* + A_2 G^* + G^T A_2^T) \tilde{\eta}^* - \tilde{\eta}^T (G^T A_1 G^* + A_2 G^*) \Delta U \right. \\ & \left. - \Delta U^T (G^T A_1 G^* + G^T A_2^T) \tilde{\eta}^* + \frac{1}{\tau} \Delta U^T (G^T A_1 G^*) \Delta U \right], \end{aligned}$$

in which $G_0 = G(u=0) = A^{-1}$ and $\tilde{\eta}_0 = \tilde{\eta}(0)$.

Next, we we express $U(\tau)$ in terms of the Fourier series

$$U(\tau) = \lim_{\epsilon \rightarrow 0} \sum_{n=-\infty}^{\infty} \tilde{U}(\omega_n) e^{-i\omega_n \epsilon}. \quad (61)$$

While inserting \tilde{U} from Eq. (60) into the above equation, we observe that $(1/\tau) \sum_n G e^{-i\omega_n \epsilon} \rightarrow 0$ as $\tau \rightarrow \infty$. This is because in the large- τ limit, the summation can be converted to an integral which can be closed via the lower half plane, and the G is analytic there. Thus, using only the first term of Eq. (60), we get

$$\begin{aligned} \sigma^T U(\tau) = & \tau_0 \sigma^T G_0 \tilde{\eta}_0 \\ & + \tau_0 \sum_{n=1}^{\infty} [e^{-i\omega_n \epsilon} \tilde{\eta}^T G^T \sigma + e^{i\omega_n \epsilon} \sigma^T G^* \tilde{\eta}^*]. \end{aligned} \quad (62)$$

Using this expression as well as W_τ from above in Eq. (52), we get

$$Z(\lambda, U, \tau | U_0) = \int \frac{d^2 \sigma}{(2\pi)^2} e^{i\sigma^T U} \prod_{n=0}^{\infty} \langle e^{s_n} \rangle, \quad (63)$$

where s_n is quadratic in $\tilde{\eta}$, given by

$$s_0 = -\frac{\lambda \tau}{2} \tilde{\eta}_0^T B_0 \tilde{\eta}_0 + \alpha_0^T \tilde{\eta}_0 - \frac{\lambda}{2\tau} \Delta U^T G_0^T A_1 G_0 \Delta U, \quad (64)$$

and

$$\begin{aligned} s_n = & -\lambda \tau \tilde{\eta}^T B_n \tilde{\eta}^* + \tilde{\eta}^T \alpha_n + \alpha_{-n}^T \tilde{\eta}^* \\ & - \frac{\lambda}{\tau} \Delta U^T G^T A_1 G^* \Delta U \quad \text{for } n \geq 1, \end{aligned} \quad (65)$$

in which we have used the following definitions:

$$B_n = G^T A_1 G^* + A_2 G^* + G^T A_2^T, \quad (66)$$

$$B_0 = G_0^T A_1 G_0 + A_2 G_0 + G_0^T A_2^T, \quad (67)$$

$$\alpha_n = \lambda [G^T A_1 G^* + A_2 G^*] \Delta U - i\tau_0 e^{-i\omega_n \epsilon} G^T \sigma, \quad (68)$$

$$\alpha_{-n}^T = \lambda \Delta U^T [G^T A_1 G^* + G^T A_2^T] - i\tau_0 e^{i\omega_n \epsilon} \sigma^T G^*. \quad (69)$$

Therefore, calculating the average $\langle e^{s_n} \rangle$ independently for each $n \geq 1$ with respect to the Gaussian PDF $P(\tilde{\eta}) = \pi^{-2} (\det \Lambda)^{-1} \exp(-\tilde{\eta}^T \Lambda^{-1} \tilde{\eta}^*)$ with $\Lambda = (2D/\tau) \text{diag}(1, \theta)$ we get

$$\langle e^{s_n} \rangle = \frac{\exp(\alpha_{-n}^T \Omega_n^{-1} \alpha_n - \frac{\lambda}{\tau} \Delta U^T G^T A_1 G^* \Delta U)}{\det(\Lambda \Omega_n)}, \quad (70)$$

where $\Omega_n = \tau(\lambda B_n + \tau^{-1} \Lambda^{-1})$. For the $n = 0$ term, calculating the average $\langle e^{s_0} \rangle$ with respect to the Gaussian PDF $P(\tilde{\eta}_0) = (2\pi)^{-1} (\det \Lambda)^{-1/2} \exp(-\frac{1}{2} \tilde{\eta}_0^T \Lambda^{-1} \tilde{\eta}_0)$, we get

$$\langle e^{s_0} \rangle = \frac{\exp(\frac{1}{2} \alpha_0^T \Omega_0^{-1} \alpha_0 - \frac{\lambda}{2\tau} \Delta U^T G_0^T A_1 G_0 \Delta U)}{\sqrt{\det(\Lambda \Omega_0)}}. \quad (71)$$

Since, $\langle e^{s_n} \rangle = \langle e^{s_{-n}} \rangle$, the product in Eq. (63) yields

$$\begin{aligned} \prod_{n=0}^{\infty} \langle e^{s_n} \rangle &= \exp\left(-\frac{1}{2} \sum_{n=-\infty}^{\infty} \ln[\det(\Lambda \Omega_n)]\right) \\ &\times \exp\left(\frac{1}{2\tau} \sum_{n=-\infty}^{\infty} [\alpha_{-n}^T \tau \Omega_n^{-1} \alpha_n - \lambda \Delta U^T G^T A_1 G^* \Delta U]\right). \end{aligned} \quad (72)$$

The determinant in the above expression is found to be

$$\det(\Lambda \Omega_n) = [1 + 4\theta\lambda(1 - \lambda)\delta^2 u^2 |G_{11}|^2 |G_{22}|^2]. \quad (73)$$

Now, taking the large τ limit, we replace the summations over n by integrals over ω , i.e., $\sum_n \rightarrow \tau \int \frac{d\omega}{2\pi}$. After, evaluating the integral, the argument of the exponential in first line of Eq. (72) yields

$$-\frac{\tau/\tau_0}{4\pi} \int_{-\infty}^{\infty} du \ln[\det(\Lambda \Omega_n)] = \tau\mu(\lambda), \quad (74)$$

where $\mu(\lambda)$ will be given by Eq. (86). Similarly, converting the argument of the exponential in the second line of Eq. (72) in the integral forms, after some manipulation we get

$$\prod_{n=0}^{\infty} \langle e^{s_n} \rangle \approx e^{\tau\mu(\lambda)} \exp\left[-\frac{1}{2} \sigma^T H_1 \sigma + i\Delta U^T H_2 \sigma + \frac{1}{2} \Delta U^T H_3 \Delta U\right], \quad (75)$$

in which H_1 , H_2 , and H_3 are given by

$$H_1 = \frac{D\tau_0}{2\pi} \int_{-\infty}^{\infty} du G^* \tilde{\Omega}^{-1} G^T, \quad (76)$$

$$H_2 = -\lim_{\epsilon \rightarrow 0} \frac{\lambda}{2\pi} \int_{-\infty}^{\infty} du e^{iu\epsilon/\tau_0} (G^\dagger \tilde{A}_1 G + G^\dagger \tilde{A}_2^T) (\tilde{\Omega}^{-1})^* G^\dagger, \quad (77)$$

$$H_3 = \frac{\lambda^2}{2\pi D\tau_0} \int_{-\infty}^{\infty} du (G^T \tilde{A}_1 G^* + G^T \tilde{A}_2^T) \tilde{\Omega}^{-1} \times (G^T \tilde{A}_1 G^* + \tilde{A}_2 G^*) - \frac{\lambda}{2\pi D\tau_0} \int_{-\infty}^{\infty} du [G^T \tilde{A}_1 G^*], \quad (78)$$

where we have used where $\tilde{\Omega}_n = \tau^{-1} D\Omega_n$ and $\tilde{A}_{1,2} = DA_{1,2}$ so that the integrands remain dimensionless and dimensions are carried outside to the integrals. We then evaluate the integrals performing the method of contours in the complex u plane, and using $G^*(u) + G(u) = 2GAG^*$ and $G^*(u) - G(u) = 2iuGG^*$, which yields

$$H_1(\lambda) = \frac{D\tau_0}{\delta(1+\delta)\nu(\lambda)} \begin{pmatrix} 1 + \delta + \theta\delta^2 & \theta\delta^2 \\ \theta\delta^2 & \theta\delta + \theta\delta^2 \end{pmatrix}, \quad (79)$$

$$H_2(\lambda) = -\frac{\nu(\lambda) - 1}{2\nu(\lambda)} \begin{pmatrix} 1 & 0 \\ 0 & 1 \end{pmatrix} - \frac{\lambda\delta}{(1+\delta)\nu(\lambda)} \begin{pmatrix} \theta\delta & \theta\delta \\ 1 & 0 \end{pmatrix}, \quad (80)$$

$$H_3(\lambda) = \frac{\lambda\delta^2}{D\tau_0(1+\delta)\nu(\lambda)} \begin{pmatrix} \lambda\theta\delta & 1 \\ 1 & \lambda - 1 \end{pmatrix}. \quad (81)$$

Finally, inserting Eq. (75) in Eq. (63), and performing the Gaussian integral over σ while using the facts that H_1 and H_3 are symmetric and $H_3 = H_1^{-1} H_2^T + H_2 H_1^{-1} H_2^T$ we get

$$Z(\lambda, \mathbf{u}, \tau | \mathbf{u}_0) \approx e^{\tau\mu(\lambda)} \exp\left(-\frac{1}{2} \mathbf{u}_0^T L_2(\lambda) \mathbf{u}_0\right) \times \frac{1}{2\pi\sqrt{\det H_1(\lambda)}} \exp\left(-\frac{1}{2} \mathbf{u}^T L_1(\lambda) \mathbf{u}\right), \quad (82)$$

with $L_1(\lambda) = H_1^{-1} + H_1^{-1} H_2^T$ and $L_2(\lambda) = -H_1^{-1} H_2^T$. From the above equation, it is trivial to identify $\chi(\mathbf{u}_0, \lambda)$ and $\Psi(\mathbf{u}, \lambda)$ used in Eq. (48). Since, $L_1 + L_2 = H_1^{-1}$, it is evident that $\int \chi(\mathbf{u}, \lambda) \Psi(\mathbf{u}, \lambda) d\mathbf{u} = 1$.

Application of the Langevin operator given by Eq. (47) on $\Psi(\mathbf{U}, \lambda)$ yields

$$\begin{aligned}
 \mathcal{L}_\lambda \Psi(\mathbf{U}, \lambda) = & \left[D(L_1^{1,1})^2 + \alpha D(L_1^{1,2})^2 - \frac{\delta}{\tau_0} L_1^{1,1} \right] x^2 \Psi(\mathbf{U}, \lambda) \\
 & + \left[D(L_1^{1,2})^2 + \alpha D(L_1^{2,2})^2 + \frac{\delta}{\tau_0} (1 - 2\lambda) L_1^{1,2} \right. \\
 & \quad \left. - \frac{1}{\tau_0} L_1^{2,2} - \frac{\delta^2}{D\tau_0^2} \lambda(1 - \lambda) \right] y^2 \Psi(\mathbf{U}, \lambda) \\
 & + \left[2DL_1^{1,1}L_1^{1,2} + 2D\alpha L_1^{1,2}L_1^{2,2} + \frac{\delta}{\tau_0} (1 - 2\lambda) L_1^{1,1} \right. \\
 & \quad \left. - \frac{1 + \delta}{\tau_0} L_1^{1,2} + \frac{\delta^2}{D\tau_0^2} \lambda \right] xy \Psi(\mathbf{U}, \lambda) \\
 & + \left[-DL_1^{1,1} - \alpha DL_1^{2,2} + \frac{1 + \delta}{\tau_0} \right] \Psi(\mathbf{U}, \lambda), \tag{83}
 \end{aligned}$$

where $L_1^{i,j}$ denotes the (i, j) -th element of the matrix L_1 . Using the explicit expressions on the right-hand side of the above equation, after simplification, we find the coefficients of $x^2\Psi(\mathbf{U}, \lambda)$, $y^2\Psi(\mathbf{U}, \lambda)$, and $xy\Psi(\mathbf{U}, \lambda)$ to be zero. The last term in square brackets in front of $\Psi(\mathbf{U}, \lambda)$ yields $\mu(\lambda)$ given by Eq. (86). This verifies the eigenvalue equation $\mathcal{L}_\lambda \Psi(\mathbf{U}, \lambda) = \mu(\lambda)\Psi(\mathbf{U}, \lambda)$.

The steady-state of the system is given by

$$P_{SS}(\mathbf{U}) = \Psi(\mathbf{U}, 0) = \frac{\exp\left(-\frac{1}{2}\mathbf{U}^T H_1^{-1}(0)\mathbf{U}\right)}{2\pi\sqrt{\det H_1(0)}}. \tag{84}$$

Integrating Eq. (52) over \mathbf{U} and then averaging over the initial condition \mathbf{U}_0 with respect to the steady state distribution $P_{SS}(\mathbf{U}_0)$, we obtain $Z(\lambda)$, given by Eq. (91), with

$$\begin{aligned}
 g(\lambda) &= (\det H_1(\lambda) \det H_1(0) \det L_1(\lambda) \det[H_1^{-1}(0) + L_2(\lambda)])^{-1/2} \\
 &= (\det[1 - \nu(\lambda)H_2^T(\lambda)] \det[1 + H_2^T(\lambda)])^{-1/2}, \tag{85}
 \end{aligned}$$

where to obtain the second expression, we have substituted the expressions of L_1 , L_2 and $H_1(0) = \nu(\lambda)H_1(\lambda)$. To evaluate $g(\lambda)$, we then need to insert the matrix H_2 and evaluate the determinants. The detailed results are given in the following section.

2.6 EXPLICIT RESULTS FOR $\mu(\lambda)$ AND $g(\lambda)$

Using the method developed in the last section, we obtain

$$\mu(\lambda) = \frac{1}{2\tau_c} [1 - \nu(\lambda)], \quad \tau_c = \tau_0(1 + \delta)^{-1}, \quad (86)$$

in which $\nu(\lambda)$ is given by,

$$\nu(\lambda) = \sqrt{1 + 4\alpha\lambda(1 - \lambda)}, \quad \alpha = \alpha(1 + \delta)^{-1}. \quad (87)$$

We observe that the eigenvalue satisfies the Gallavotti-Cohen symmetry $\mu(\lambda) = \mu(1 - \lambda)$. In terms of the column vector $\mathbf{u} = (x, y)^T$, the eigenfunctions are

$$\Psi(x, y, \lambda) = \frac{1}{2\pi\sqrt{\det H_1(\lambda)}} \exp\left[-\frac{1}{2}\mathbf{u}^T L_1(\lambda)\mathbf{u}\right], \quad (88)$$

$$\chi(x_0, y_0, \lambda) = \exp\left[-\frac{1}{2}\mathbf{u}_0^T L_2(\lambda)\mathbf{u}_0\right], \quad (89)$$

where the matrices H_1 , L_1 , and L_2 are given in Section 2.5.

Using the explicit forms one can verify the eigenvalue equation

$$\begin{aligned} \mathcal{L}_\lambda \Psi(x, y, \lambda) &= \mu(\lambda)\Psi(x, y, \lambda) \\ \int_{-\infty}^{\infty} \int_{-\infty}^{\infty} \chi(x, y, \lambda)\Psi(x, y, \lambda) dx dy &= 1 \end{aligned} \quad (90)$$

From the above expressions, we also find that $\mu(0) = 0$ and $\chi(x_0, y_0, 0) = 1$. Since the $\lambda = 0$ case of Eq. (45) gives the PDF of the variables (x, y) and $\mu(0)$ is the largest eigenvalue, it follows from Eq. (48) that $\Psi(x, y, 0)$ is the steady-state PDF of (x, y) . Therefore, averaging over the initial variables (x_0, y_0) with respect to the steady-state PDF $\Psi(x_0, y_0, 0)$ and integrating over the final variables (x, y) , we find the moment generating function of the work in the steady state as

$$Z(\lambda, \tau) = \langle e^{-\lambda W_\tau} \rangle = g(\lambda) e^{\tau\mu(\lambda)} + \dots, \quad (91)$$

where

$$\begin{aligned} g(\lambda) &= \frac{2}{\sqrt{\nu(\lambda) + 1 - 2b_+\lambda} \sqrt{\nu(\lambda) + 1 - 2b_-\lambda}} \\ &\times \frac{2\nu(\lambda)}{\sqrt{\nu(\lambda) + 1 + 2b_+\lambda} \sqrt{\nu(\lambda) + 1 + 2b_-\lambda}}, \end{aligned} \quad (92)$$

with

$$b_{\pm} = \frac{\alpha}{2} \left[1 \pm \sqrt{1 + \frac{4}{\theta\delta}} \right]. \quad (93)$$

The first factor in the above expression of $g(\lambda)$ is due to the averaging over the initial conditions with respect to the steady-state distribution and the second factor is due to the integrating out of the final degrees of freedom.

2.7 ANALYSIS OF $g(\lambda)$

From Eq. (87) and Eq. (114) we recall that $v(\lambda_{\pm}) = 0$ and $v(\lambda) > 0$ (is a semicircle) for $\lambda \in (\lambda_-, \lambda_+)$. Moreover, all the four functions $1 \pm 2b_{\pm}\lambda$ are linear in λ with slopes $\pm 2b_{\pm}$ (where all four combinations of the two \pm signs are considered). Therefore, for example, if $(1 - 2b_+\lambda)$ has opposite signs at the two end points λ_{\pm} , then the function $[v(\lambda) + (1 - 2b_+\lambda)]$ must cross zero at some intermediate λ . This is also true for the other three cases. From Eqs. (93) and (113) respectively, we note that $b_+ > 0$, $b_- < 0$ and $\lambda_+ > 0$, $\lambda_- < 0$. One can therefore determine whether $g(\lambda)$ has a singularity as follows (see Fig. 4):

1. Evidently, $1 - 2b_+\lambda_- > 0$. Thus, $v(\lambda_a) + 1 - 2b_+\lambda_a = 0$ for a specific $\lambda_a \in (\lambda_-, \lambda_+)$ if and only if $1 - 2b_+\lambda_+ < 0$. When this happens [see Fig. 4 (a)], the position of the singularity can be found as

$$\lambda_a = (a + b_+)/(\alpha + b_+^2). \quad (94)$$

It is evident that $\lambda_a > 0$.

2. Evidently, $1 - 2b_-\lambda_+ > 0$. Thus, $v(\lambda_b) + 1 - 2b_-\lambda_b = 0$ for a specific $\lambda_b \in (\lambda_-, \lambda_+)$ if and only if $1 - 2b_-\lambda_- < 0$. When this happens [see Fig. 4 (b)], the position of the singularity can be found as

$$\lambda_b = (a + b_-)/(\alpha + b_-^2) \quad (95)$$

and it can be shown that $\lambda_b < 0$.

3. Evidently, $1 + 2b_+\lambda_+ > 0$. Thus, $\nu(\lambda_c) + 1 + 2b_+\lambda_c = 0$ for a specific $\lambda_c \in (\lambda_-, \lambda_+)$ if and only if $1 + 2b_+\lambda_- < 0$. When this happens [see Fig. 4 (c)], the position of the singularity can be found as

$$\lambda_c = (a - b_+)/ (a + b_+^2) \quad (96)$$

and it can be shown that $\lambda_c < 0$.

4. Evidently, $1 + 2b_-\lambda_- > 0$. Thus, $\nu(\lambda_d) + 1 + 2b_-\lambda_d = 0$ for a specific $\lambda_d \in (\lambda_-, \lambda_+)$ if and only if $1 + 2b_-\lambda_+ < 0$. When this happens [see Fig. 4 (d)], the position of the singularity can be found as

$$\lambda_d = (a - b_-)/ (a + b_-^2). \quad (97)$$

It is evident that $\lambda_d > 0$. Moreover, it can be shown that $\lambda_c + \lambda_d = 1$.

It is easily seen that the singularities of $g(\lambda)$ are branch points (square root singularities) and the function $f_w(\lambda)$ at these singularities is given by

$$h_i(w) := f_w(\lambda_i) = \frac{1}{2} [1 - \nu(\lambda_i)] + \lambda_i w, \quad (98)$$

where the index i stands for one of the indices from the set $\{a, b, c, d\}$. Substituting $\nu(\lambda_i)$ at the singularities using the conditions from above, we get

$$h_a(w) = (1 - b_+\lambda_a) + \lambda_a w, \quad (99)$$

$$h_b(w) = (1 - b_-\lambda_b) + \lambda_b w, \quad (100)$$

$$h_c(w) = (1 + b_+\lambda_c) + \lambda_c w, \quad (101)$$

$$h_d(w) = (1 + b_-\lambda_d) + \lambda_d w. \quad (102)$$

It is also useful to define the non-singular part of $g(\lambda)$ at a singularity as

$$\tilde{g}(\lambda_i) = \lim_{\lambda \rightarrow \lambda_i} |(\lambda - \lambda_i)^{1/2} g(\lambda)|. \quad (103)$$

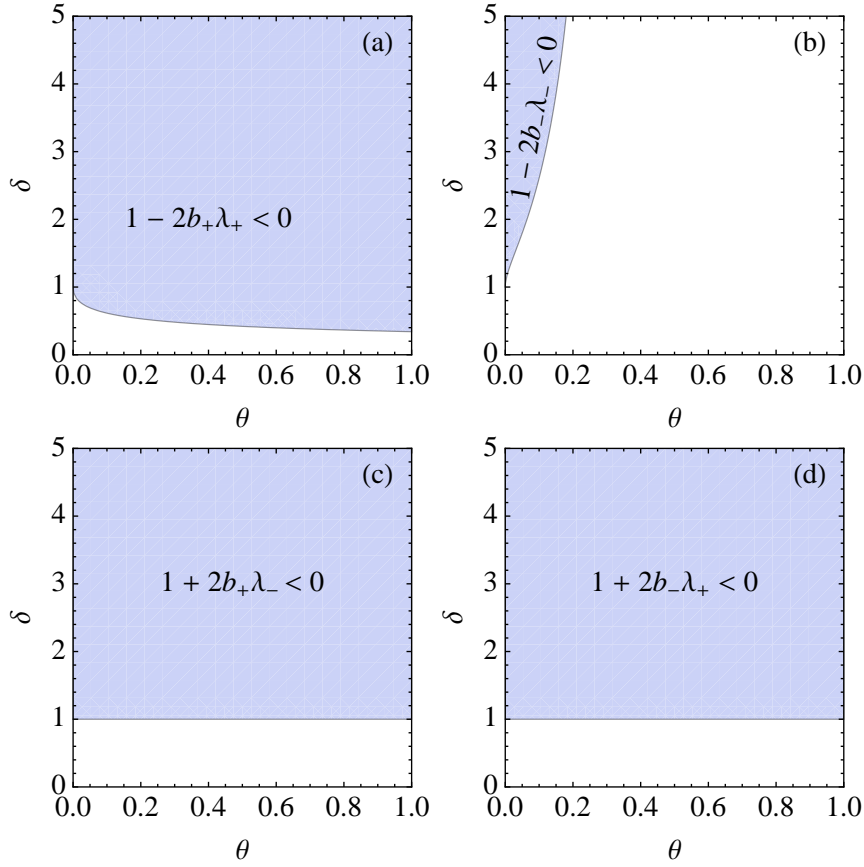


Figure 4: In the shaded regions of the (θ, δ) plane in the figures (a), (b), (c) and (d), the respective mathematical conditions given there are satisfied and consequently $g(\lambda)$ possesses singularities at $\lambda_a, \lambda_b, \lambda_c$, and λ_d respectively, given by Eqs. (94)–(97).

We note that for a given set of parameters θ (or α) and δ , the position of the singularities (whenever they exist) are fixed within the interval (λ_-, λ_+) . The specific values of w at which the saddle point coincides with one of the singularities is obtained by solving $\lambda^*(w_i^*) = \lambda_i$ as

$$w_i^* = \frac{(1 - 2\lambda_i)\sqrt{a}}{\sqrt{(1 + 1/a) - (2\lambda_i - 1)^2}}. \quad (104)$$

Since, $(1 + 1/a) = (2\lambda_{\pm} - 1)^2$ and $\lambda_- < \lambda_i < \lambda_+$, the term under the square root in the above equation is always positive.

2.7.1 The case: $\delta < 1$

For any $\delta < 1$, there exists a θ_{c_1} given by the solution of $1 - 2b_+\lambda_+ = 0$ as

$$\theta_{c_1}(\delta) = \frac{(1 - \delta^2)^2}{\delta^2 (3 + 10\delta + 3\delta^2)}, \quad (105)$$

and for $\theta < \theta_{c_1}$ the function $g(\lambda)$ has no singularities whereas it has one singularity for $\theta > \theta_{c_1}$. As $\delta \rightarrow 0$ we get $\theta_{c_1} \simeq 1/(3\delta^2)$ whereas $\theta_{c_1} \simeq (1 - \delta)^2/4$ as $\delta \rightarrow 1^-$.

The $\theta = \theta_{c_1}(\delta)$ line corresponds to the $\alpha = \alpha_{c_1}(\delta)$ line in the (α, δ) plane, where

$$\alpha_{c_1}(\delta) = \frac{(1 + \delta)(1 - \delta)^2}{3 + 10\delta + 3\delta^2}. \quad (106)$$

2.7.2 The case: $\delta > 1$

For $\delta > 1$, there again exists a θ_{c_2} given by the solution of $1 - 2b_-\lambda_- = 0$ as

$$\theta_{c_2}(\delta) = \frac{(\delta^2 - 1)^2}{\delta^2 (3 + 10\delta + 3\delta^2)}, \quad (107)$$

and $g(\lambda)$ has either three or four singularities depending on whether $\theta > \theta_{c_2}$ or $\theta < \theta_{c_2}$. In the limit $\delta \rightarrow \infty$ we get $\theta_{c_2} = 1/3$ and $\theta_{c_2} \rightarrow 0$ as $\delta \rightarrow 1$. More precisely, $\theta_{c_2} \simeq 1/3 - 10/(9\delta)$ as $\delta \rightarrow \infty$, whereas $\theta_{c_2} \simeq (\delta - 1)^2/4$ as $\delta \rightarrow 1^+$.

The $\theta = \theta_{c_2}(\delta)$ line corresponds to the $\alpha = \alpha_{c_2}(\delta)$ line in the (α, δ) plane, where

$$\alpha_{c_2}(\delta) = \frac{(1 + \delta)(\delta - 1)^2}{3 + 10\delta + 3\delta^2}. \quad (108)$$

2.7.3 The case: $\delta = 1$

It is instructive to illustrate the particular case of $\delta = 1$, for which we have $\alpha = \theta/2$ and $a = \theta/4$. Here from Eqs. (93) and (113) we get $2b_{\pm} = \theta\lambda_{\pm}$ and $\theta\lambda_+\lambda_- = -1$. It follows that:

1. $1 - 2b_+\lambda_- = 2$ and $1 - 2b_+\lambda_+ = -\theta\lambda_+ < 0$ for $\theta > 0$. This implies $g(\lambda)$ has a singularity at $\lambda = \lambda_a$. We get $\lambda_a = (1 + 2\lambda_+)/ (2 + \theta\lambda_+)$ and $\lambda_a \in (0, \lambda_+)$.
2. $1 - 2b_-\lambda_+ = 2$ and $1 - 2b_-\lambda_- = -\theta\lambda_- > 0$ for $\theta > 0$. This implies $g(\lambda)$ does not have any singularity at $\lambda = \lambda_b$.
3. $1 + 2b_+\lambda_+ = 2 + \theta\lambda_+ > 0$ and $1 + 2b_+\lambda_- = 0$. However, since $v(\lambda_-) = 0$, $g(\lambda)$ has a singularity at $\lambda = \lambda_c = \lambda_-$.
4. $1 + 2b_-\lambda_+ = 2 + \theta\lambda_- > 0$ as $\theta\lambda_- \in (-1, 0)$. Moreover, $1 + 2b_-\lambda_- = 0$ and $v(\lambda_+) = 0$. Therefore, $g(\lambda)$ has a singularity at $\lambda = \lambda_d = \lambda_+$.

However, we have already seen that $\lambda^* \rightarrow \lambda_{\pm}$ only when $w \rightarrow \mp\infty$. Therefore, for all practical purposes (any finite w) the singularities at λ_{\pm} are not relevant and hence we treat this case together with the case $\delta < 1$, $\theta > \theta_{c_1}$ where $g(\lambda)$ has only one singularity. However, for the $\delta = 1$ case, in principle, one can use the results of Sec. 2.8.3, where the case of the three singularities is discussed.

2.8 PROBABILITY DENSITY FUNCTION

The probability density function (PDF) of the work done W_{τ} can be obtained from the moment generating function $Z(\lambda, \tau)$, by taking the inverse ‘‘Fourier’’ (two-sided Laplace) transform

$$P(W_{\tau}) = \frac{1}{2\pi i} \int_{-i\infty}^{+i\infty} Z(\lambda, \tau) e^{\lambda W_{\tau}} d\lambda, \quad (109)$$

where the integration is done along the imaginary axis in the complex λ plane. Using the large- τ form of $Z(\lambda, \tau)$ given by Eq. (91) we write

$$P(W_\tau = w\tau) \approx \frac{1}{2\pi i} \int_{-i\infty}^{+i\infty} g(\lambda) e^{\tau f_w(\lambda)} d\lambda, \quad (110)$$

where

$$f_w(\lambda) = \frac{1}{2} [1 - v(\lambda)] + \lambda w. \quad (111)$$

and we have set $\tau_c = 1$ for convenience. This is completely equivalent to measuring the time in the unit of τ_c , that is, $\tau/\tau_c \rightarrow \tau$.

The large- τ form of $P(W_\tau)$ can be obtained from Eq. (110) by using the method of steepest descent. The saddle-point λ^* is obtained from the solution of the condition $f'_w(\lambda^*) = 0$ as

$$\lambda^*(w) = \frac{1}{2} \left[1 - \frac{w}{\sqrt{w^2 + a}} \sqrt{1 + \frac{1}{a}} \right]. \quad (112)$$

From the above expression one finds that $\lambda^*(w)$ is a monotonically decreasing function of w and $\lambda^*(w \rightarrow \mp\infty) \rightarrow \lambda_\pm$, where

$$\lambda_\pm = \frac{1}{2} \left[1 \pm \sqrt{1 + \frac{1}{a}} \right]. \quad (113)$$

Therefore, $\lambda^* \in (\lambda_-, \lambda_+)$. It is also useful to note that $v(\lambda)$ can be written in terms of λ_\pm as

$$v(\lambda) = \sqrt{4a(\lambda_+ - \lambda)(\lambda - \lambda_-)}. \quad (114)$$

This clearly shows that $v(\lambda)$ has two branch points on the real- λ line at λ_\pm . However, $v(\lambda)$ is real and positive in the (real) interval $\lambda \in (\lambda_-, \lambda_+)$. As a consequence, $f_w(\lambda)$ remains real in the interval (λ_-, λ_+) . At $\lambda = \lambda^*$ we find

$$v(\lambda^*) = \frac{\sqrt{a(1+a)}}{\sqrt{w^2 + a}}, \quad (115)$$

and

$$h_s(w) := f_w(\lambda^*) = \frac{1}{2} \left[1 + w - \sqrt{w^2 + a} \sqrt{1 + \frac{1}{a}} \right]. \quad (116)$$

One also finds that

$$f''_w(\lambda^*) = \frac{2(w^2 + a)^{3/2}}{\sqrt{a(1+a)}} > 0. \quad (117)$$

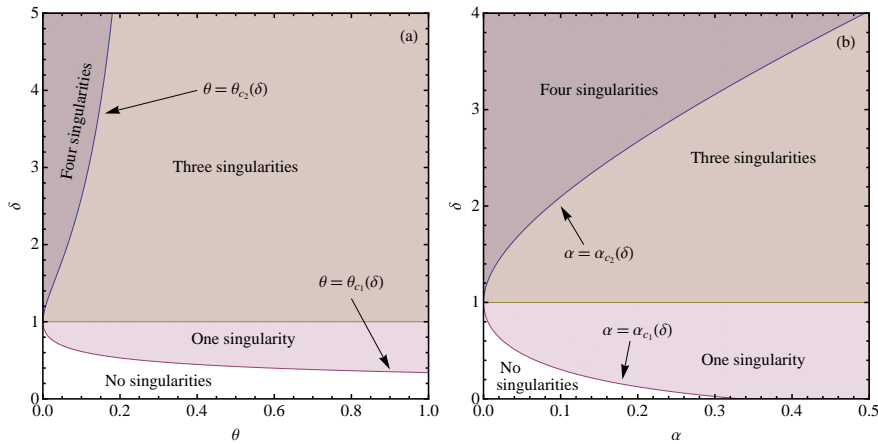


Figure 5: The regions in the (a) θ, δ and (b) α, δ spaces, where $g(\lambda)$ has the number of singularities mentioned in the figure. The equations of the boundary lines separating different regions are given in Section 2.7. $\alpha_{c_1} = 1/3$ for $\delta = 0$ and $\theta_{c_2} \rightarrow 1/3$ as $\delta \rightarrow \infty$. Each of the phase boundaries meet at $\theta = 0$ ($\alpha = 0$), $\delta = 1$.

This means that $f_w(\lambda)$ has a minimum at λ^* along real- λ , and hence the path of steepest descent is perpendicular to the real- λ axis at $\lambda = \lambda^*$.

Now, if $g(\lambda)$ is analytic for $\lambda \in (0, \lambda^*)$, one can deform the contour along the path of the steepest descent through the saddle-point, and obtain $P(W_\tau)$ using the usual saddle-point approximation method. However, if $g(\lambda)$ has any singularities, then the straightforward saddle-point method cannot be used, and one would require more sophisticated methods to obtain the asymptotic form of $P(W_\tau)$. Therefore, it is essential to analyze $g(\lambda)$ for possible singularities. In Section 2.7, we examine the terms under the four square roots in the denominator of $g(\lambda)$ in Eq. (92).

In Fig. 5, we show the regions in the (θ, δ) and (α, δ) planes, where $g(\lambda)$ possesses singularities.

2.8.1 The case of no singularities

In the singularity free region $\delta < 1$, $\theta < \theta_{c_1}$ ($\alpha < \alpha_{c_1}$), the asymptotic PDF of the work done is obtained by following the usual saddle-point approximation method. We get

$$P(W_\tau = w\tau) \approx \frac{g(\lambda^*) e^{\tau h_s(w)}}{\sqrt{2\pi\tau f''_w(\lambda^*)}}, \quad (118)$$

where $h_s(w)$ and $f''_w(\lambda^*)$ are given by Eqs. (116) and (117), respectively, and $g(\lambda^*)$ can be obtained from Eq. (92) while using λ^* from Eq. (112). Figure 6 shows very good agreement between the form given by Eq. (118) and numerical simulation results for $\theta < \theta_{c_1}$.

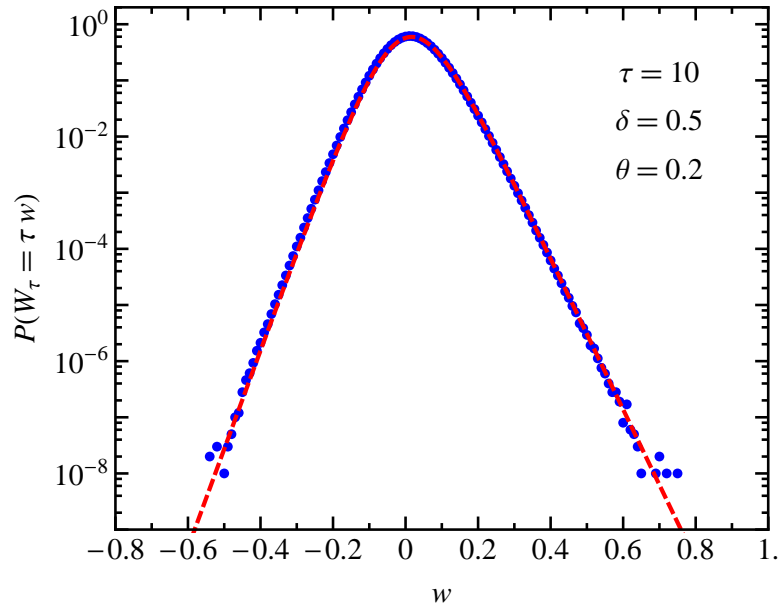


Figure 6: $P(W_\tau)$ against the scaled variable $w = W_\tau/\tau$ for $\tau = 10$, $\tau_c = 1$. The points (blue) are obtained from numerical simulation, and the dashed solid lines (red) plot the analytical asymptotic forms given by Eq. (118). $\theta_{c_1} = 9/35 = 0.257\dots$ for $\delta = 1/2$.

2.8.2 The case of one singularity

In the case $\delta < 1$, $\theta > \theta_{c_1}$ where $g(\lambda)$ has only one singularity, or the case $\delta = 1$ where only one singularity of $g(\lambda)$ is relevant, we can write

$$g(\lambda) = \frac{g_1(\lambda)}{\sqrt{\lambda_a - \lambda}}, \quad (119)$$

where $g_1(\lambda)$ is the analytical factor of $g(\lambda)$.

It is evident that for a given value of δ and θ , the position of the branch point λ_a is fixed somewhere between the origin and λ_+ . On the other hand, according to Eq. (112), even for a fixed θ , the saddle-point $\lambda^*(w)$ moves unidirectionally along the real- λ line from λ_- to λ_+ as one decreases w from $+\infty$ to $-\infty$ in a monotonic manner. Therefore, for sufficiently large w , the saddle-point lies in the interval (λ_-, λ_a) , and therefore, the contour of integration in Eq. (110) can be deformed into the steepest descent path (that passes through λ^*) without touching λ_a (see Fig. 18). However, as one decreases w , the saddle-point hits the branch-point, $\lambda^*(w_a^*) = \lambda_a$, at some specific value $w = w_a^*$ given by Eq. (104). For $w < w_a^*$, since $\lambda^* > \lambda_a$, the steepest descent contour wraps around the branch-cut between λ_a and λ^* as shown in Fig. 19. Leaving the details of the calculation to Appendix A.1, here we present the main results.

2.8.2.1 $w > w_a^*$

For $w > w_a^*$, following Appendix A.1.1, we get

$$P(W_\tau = w\tau) \approx \frac{g(\lambda^*)e^{\tau h_s(w)}}{\sqrt{2\pi\tau f''_w(\lambda^*)}} R_1\left(\sqrt{\tau[h_a(w) - h_s(w)]}\right), \quad (120)$$

where the function $R_1(z)$ is given by

$$R_1(z) = \frac{z}{\sqrt{\pi}} e^{z^2/2} K_{1/4}(z^2/2), \quad (121)$$

with $K_{1/4}(z)$ being the modified Bessel function of the second kind. It follows from the asymptotic form of $K_{1/4}(z)$ that $R_1(z \rightarrow \infty) \rightarrow 1$.

Therefore, for $w \gg w_a^*$, Eq. (120) approaches the form of the usual saddle-point approximation given by Eq. (118). On the other hand, using $K_{1/4}(z) \simeq (1/2)\Gamma(1/4)(z/2)^{-1/4}$ for small z , we get $R_1(z) \simeq \Gamma(1/4)\sqrt{z/2\pi}$. As $w \rightarrow w_a^*$ from above, i.e., when the saddle point approaches the branch point from below, $h_a(w) - h_s(w) \equiv f_w(\lambda_a) - f_w(\lambda^*) \simeq (\lambda_a - \lambda^*)^2 f''(\lambda^*)/2$. Therefore, the expression given by Eq. (120) remains finite, even when the saddle point approaches the singularity, i.e.,

$$P(W_\tau = w\tau) \approx \frac{\Gamma(1/4) g_1(\lambda^*) e^{\tau h_s(w)}}{2\pi [2\tau f''_w(\lambda^*)]^{1/4}} \quad \text{as } w \rightarrow w_a^*. \quad (122)$$

2.8.2.2 $w < w_a^*$

For $w < w_a^*$, following Appendix A.1.2, we write

$$P(W_\tau = w\tau) \approx P_B(w, \tau) + P_S(w, \tau), \quad (123)$$

where $P_B(w, \tau)$ is the contribution coming from the integrations along the branch cut and $P_S(w, \tau)$ is the saddle point contribution. Following Appendix A.1.2.1 we get,

$$P_B(w, \tau) \approx \frac{\tilde{g}(\lambda_a) e^{\tau h_a(w)}}{\sqrt{\pi\tau |f'_w(\lambda_a)|}} R_3 \left(\sqrt{\tau [h_a(w) - h_s(w)]} \right), \quad (124)$$

where

$$R_3(z) = \sqrt{\frac{2z}{\pi}} R_2(z), \quad (125)$$

with $R_2(z)$ being given by Eq. (407). Using the asymptotic forms of $R_2(z)$ given in Appendix A.1.2.1, we get $R_3(z) \rightarrow 1$ in the limit $z \rightarrow \infty$. Therefore,

$$P_B(w, \tau) \sim \frac{\tilde{g}(\lambda_a) e^{\tau h_a(w)}}{\sqrt{\pi\tau |f'_w(\lambda_a)|}} \quad \text{for } w \ll w_a^*. \quad (126)$$

As $w \rightarrow w_a^*$ (from below), $P_B(w, \tau) \rightarrow 0$.

The contribution coming from the saddle point is given by (see Appendix A.1.2.2),

$$P_S(w, \tau) \approx \frac{|g(\lambda^*)| e^{\tau h_s(w)}}{\sqrt{2\pi\tau f''_w(\lambda^*)}} R_4 \left(\sqrt{\tau [h_a(w) - h_s(w)]} \right), \quad (127)$$

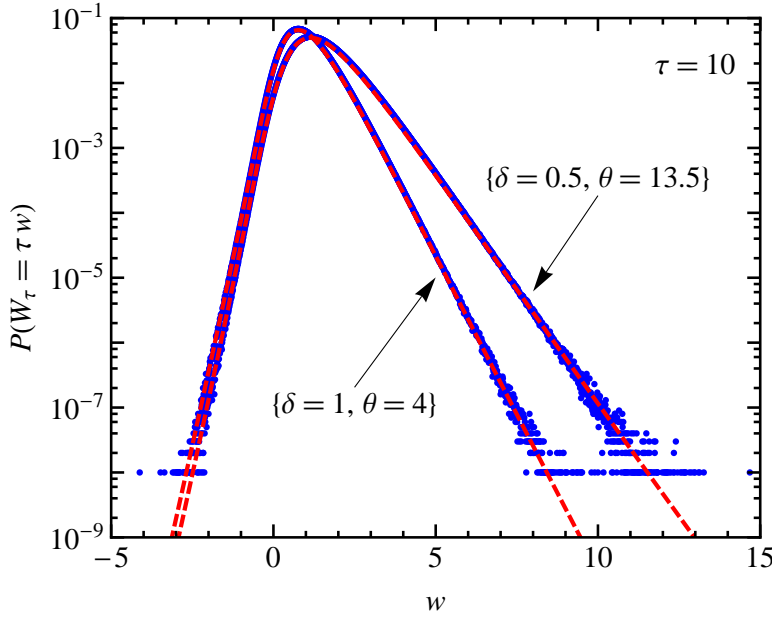


Figure 7: $P(W_\tau)$ against the scaled variable $w = W_\tau/\tau$ for $\tau = 10$, $\tau_c = 1$. The points (blue) are obtained from numerical simulation, and the dashed solid lines (red) plot the analytical asymptotic forms given by Eq. (120) for $w > w_a^*$ and Eqs. (123)–(127) for $w < w_a^*$, where $w_a^* = 0$ for $\delta = 1, \theta = 4$, and $w_a^* = -0.0135\dots$ for $\delta = 0.5, \theta = 13.5$.

where the function $R_4(z)$ is given by

$$R_4(z) = \sqrt{\frac{\pi}{2}} z e^{z^2/2} [I_{-1/4}(z^2/2) + I_{1/4}(z^2/2)] - \frac{4z}{\sqrt{\pi}} {}_2F_2(1/2, 1; 3/4, 5/4; z^2), \quad (128)$$

where $I_{\pm 1/4}(z)$ are modified Bessel functions of the first kind and ${}_2F_2(a_1, a_2; b_1, b_2; z)$ is the generalized hypergeometric function, defined by Eq. (416). The small and large z behaviors of $R_4(z)$ are given in Appendix A.1.2.2.

For $w \ll w_a^*$ we get $P_S(w, \tau) \ll P_B(w, \tau)$. On the other hand $P_S(w, \tau)$ acquires the same limiting form as in Eq. (122), when $w \rightarrow w_a^*$ (from below).

2.8.2.3 Numerical Simulation

We now compare the asymptotic forms presented in this subsection with numerical simulation. In one case, we choose $\delta = 1$ and $\theta = 4$, for which we get $\lambda_{\pm} = (1 \pm \sqrt{2})/2$, $\lambda^*(w) = (1 - \sqrt{2}w/\sqrt{1+w^2})/2$, $\lambda_a = 1/2$, and $w_a^* = 0$. In an another case, we choose $\delta = 1/2$ and $\theta = 13.5$, for which $w_a^* = -0.0135\dots$ Figure 7 shows very good agreement between the analytical and and simulation results.

2.8.3 The case of three singularities

Now we consider the case, $\delta > 1$ and $\theta > \theta_{c_2}$, in which case $g(\lambda)$ has three singularities (see Fig. 5) at λ_a , λ_c and λ_d given by Eqs. (94), (96) and (97) respectively; where $\lambda_- < \lambda_c < 0 < \lambda_a < \lambda_d < \lambda_+$. Therefore, $g(\lambda)$ can be written as

$$g(\lambda) = \frac{g_3(\lambda)}{\sqrt{\lambda - \lambda_c} \sqrt{\lambda_a - \lambda} \sqrt{\lambda_d - \lambda}}, \quad (129)$$

where $g_3(\lambda)$ is the analytical factor of $g(\lambda)$. We notice from Eq. (112) that $\lambda^* \rightarrow \lambda_-$ as $w \rightarrow +\infty$ and λ^* increases monotonically towards λ_+ with decreasing w . Therefore, there are specific values $+\infty > w_c^* > w_a^* > w_d^* > -\infty$ of w given by Eq. (104) at which the saddle point hits the corresponding branch point, i.e., $\lambda^*(w_c^*) = \lambda_c$, $\lambda^*(w_a^*) = \lambda_a$ and $\lambda^*(w_d^*) = \lambda_d$.

2.8.3.1 $w > w_c^*$

For $w > w_c^*$, the saddle point lies between λ_- and λ_c . Therefore, as in the case of one singularity discussed above in Sec. 2.8.2, the contributions comes from the branch point as well as from the saddle

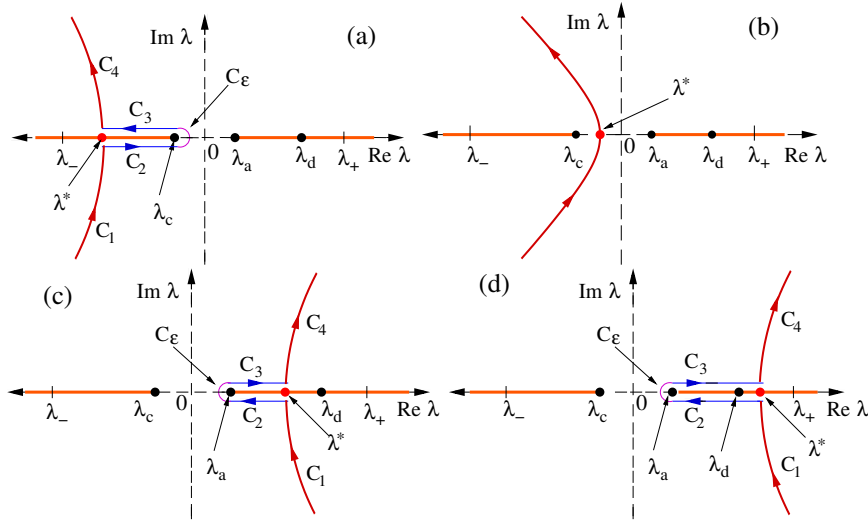


Figure 8: Schematic steepest descent contours for the case when there are three branch points at λ_a , λ_c and λ_d , where $\lambda_- < \lambda_c < 0 < \lambda_a < \lambda_d < \lambda_+$; and the saddle point λ^* lies between (a) λ_- and λ_c , (b) λ_c and λ_a , (c) λ_a and λ_d , and (d) λ_d and λ_+ respectively.

point, as shown in Fig. 8 (a). Following the procedure similar to that in the one singularity case (see Appendix A.1.2), we get

$$\begin{aligned}
 P(W_\tau = w\tau) &\approx \frac{\tilde{g}(\lambda_c) e^{\tau h_c(w)}}{\sqrt{\pi\tau|f'_w(\lambda_c)|}} R_3 \left(\sqrt{\tau[h_c(w) - h_s(w)]} \right) \\
 &\quad + \frac{|g(\lambda^*)| e^{\tau h_s(w)}}{\sqrt{2\pi\tau f''_w(\lambda^*)}} \\
 R_5 &\left(\sqrt{\tau[h_c(w) - h_s(w)]}, \sqrt{\tau[h_a(w) - h_s(w)]}, \sqrt{\tau[h_d(w) - h_s(w)]} \right),
 \end{aligned} \tag{130}$$

where $R_3(z)$ is given by Eq. (125), and

$$\begin{aligned}
 R_5(z_1, z_2, z_3) &= \sqrt{\frac{z_1 z_2 z_3}{\pi}} \int_0^\infty du e^{-u^2} \left[\frac{1}{\sqrt{z_1 + iu}\sqrt{z_2 + iu}\sqrt{z_3 + iu}} \right. \\
 &\quad \left. - \frac{1}{\sqrt{z_1 - iu}\sqrt{z_2 - iu}\sqrt{z_3 - iu}} \right] i.
 \end{aligned} \tag{131}$$

2.8.3.2 $w_a^* < w < w_c^*$

For $w_a^* < w < w_c^*$, the saddle point lies between λ_c and λ_a . Therefore, the contour of integration can be deformed through the saddle

point without crossing any singularity, as shown in Fig. 8 (b). Now, to compute the saddle point contribution one can follow the methods of Appendix A.1.1, while taking into account of both the singularities λ_a and λ_c . The calculation yields

$$P(W_\tau = w\tau) \approx \frac{g(\lambda^*) e^{\tau h_s(w)}}{\sqrt{2\pi\tau f''_w(\lambda^*)}}$$

$$R_6\left(\sqrt{\tau[h_c(w) - h_s(w)]}, \sqrt{\tau[h_a(w) - h_s(w)]}, \sqrt{\tau[h_d(w) - h_s(w)]}\right), \quad (132)$$

where

$$R_6(z_1, z_2, z_3) = \sqrt{\frac{z_1 z_2 z_3}{\pi}} \int_{-\infty}^{\infty} \frac{e^{-u^2} du}{\sqrt{z_1 + iu} \sqrt{z_2 - iu} \sqrt{z_3 - iu}}. \quad (133)$$

As $w \rightarrow w_c^*$, the first term of Eq. (130), coming from the integral along the branch cut, goes to zero. On the other hand, it can be shown that $R_5(z_1 \rightarrow 0, z_2, z_3) = R_6(z_1 \rightarrow 0, z_2, z_3)$. Therefore, Eqs. (130) and (132) approach the same limiting form as $w \rightarrow w_c^*$ from the two sides.

2.8.3.3 $w_d^* < w < w_a^*$

For $w_d^* < w < w_a^*$, the saddle point lies between λ_a and λ_d . Therefore, the deformed contour is as shown in Fig. 8 (c). Combining the contributions from the branch point λ_a and the saddle point, we get

$$P(W_\tau = w\tau) \approx \frac{\tilde{g}(\lambda_a) e^{\tau h_a(w)}}{\sqrt{\pi\tau |f'_w(\lambda_a)|}} R_7\left(\sqrt{\tau[h_a(w) - h_s(w)]}, \sqrt{\tau[h_d(w) - h_s(w)]}\right)$$

$$+ \frac{|g(\lambda^*)| e^{\tau h_s(w)}}{\sqrt{2\pi\tau f''_w(\lambda^*)}}$$

$$R_8\left(\sqrt{\tau[h_c(w) - h_s(w)]}, \sqrt{\tau[h_a(w) - h_s(w)]}, \sqrt{\tau[h_d(w) - h_s(w)]}\right), \quad (134)$$

where

$$R_7(z_1, z_2) = \sqrt{\frac{2z_1(z_1 + z_2)}{\pi}} \int_0^{z_1} \frac{e^{-2z_1 u + u^2}}{\sqrt{u} \sqrt{z_1 + z_2 - u}} du, \quad (135)$$

and

$$R_8(z_1, z_2, z_3) = \sqrt{\frac{z_1 z_2 z_3}{\pi}} \int_0^{\infty} du e^{-u^2} \left[\frac{1}{\sqrt{z_1 + iu} \sqrt{z_2 + iu} \sqrt{z_3 - iu}} - \frac{1}{\sqrt{z_1 - iu} \sqrt{z_2 - iu} \sqrt{z_3 + iu}} \right] i. \quad (136)$$

As $w \rightarrow w_a^*$, the first term of Eq. (134), coming from the integral along the branch cut, goes to zero. On the other hand, it can be shown that $R_6(z_1, z_2 \rightarrow 0, z_3) = R_8(z_1, z_2 \rightarrow 0, z_3)$. Therefore, Eqs. (132) and (134) approach the same limiting form as $w \rightarrow w_a^*$ from the two sides.

2.8.3.4 $w < w_d^*$

Finally, for $w < w_d^*$, the saddle point lies between λ_d and λ_+ . In this case, the integral along the branch cut can be divided into two parts: one, from λ_a to λ_d and another from λ_d to λ^* . Between λ_d and λ^* , the the integral above the branch cut exactly cancels the integral below the branch cut. Therefore, the net contribution is the sum of the contributions coming from the integral around the branch cut between λ_a and λ_d , and the contribution of the integral along the contour (C_1 and C_4) through the saddle point, for which the calculation is similar to the one given in Appendix A.1.1. Therefore, we get

$$P(W_\tau = w\tau) \approx \frac{\tilde{g}(\lambda_a) e^{\tau h_a(w)}}{\sqrt{\pi\tau|f'_w(\lambda_a)|}} R_9 \left(\sqrt{\tau[h_a(w) - h_s(w)]}, \sqrt{\tau[h_d(w) - h_s(w)]} \right) - \frac{|g(\lambda^*)| e^{\tau h_s(w)}}{\sqrt{2\pi\tau f''_w(\lambda^*)}} R_{10} \left(\sqrt{\tau[h_c(w) - h_s(w)]}, \sqrt{\tau[h_a(w) - h_s(w)]}, \sqrt{\tau[h_d(w) - h_s(w)]} \right), \quad (137)$$

where

$$R_9(z_1, z_2) = \sqrt{\frac{2z_1(z_1 - z_2)}{\pi}} \int_0^{z_1 - z_2} \frac{e^{-2z_1 u + u^2} du}{\sqrt{u}\sqrt{z_1 - z_2 - u}}, \quad (138)$$

$$R_{10}(z_1, z_2, z_3) = \sqrt{\frac{z_1 z_2 z_3}{\pi}} \int_{-\infty}^{\infty} \frac{e^{-u^2} du}{\sqrt{z_1 + iu}\sqrt{z_2 + iu}\sqrt{z_3 + iu}}. \quad (139)$$

It is evident from the above equations that $R_7(z_1, 0) = R_9(z_1, 0)$. Moreover, it can be shown that $R_{10}(z_1, z_2, z_3 \rightarrow 0) = -R_8(z_1, z_2, z_3 \rightarrow 0)$. Therefore, Eqs. (134) and (137) approach the same limiting form as $w \rightarrow w_d^*$ from the two sides.

2.8.4 The case of four singularities

Finally, we consider the case $\delta > 1$ and $\theta < \theta_{c_2}$, in which case $g(\lambda)$ has four singularities (see Fig. 5) at $\lambda_a, \lambda_b, \lambda_c$ and λ_d given by Eqs. (94)–(97) respectively; where $\lambda_- < \lambda_b < \lambda_c < 0 < \lambda_a < \lambda_d < \lambda_+$. Therefore, $g(\lambda)$ can be written as

$$g(\lambda) = \frac{g_4(\lambda)}{\sqrt{\lambda - \lambda_b} \sqrt{\lambda - \lambda_c} \sqrt{\lambda_a - \lambda} \sqrt{\lambda_d - \lambda}}, \quad (140)$$

where $g_4(\lambda)$ is the analytical factor of $g(\lambda)$.

Now as w varies from $+\infty$ to $-\infty$, the saddle point hits the branch points, $\lambda^*(w_i^*) = \lambda_i$ with $i \in \{b, c, a, d\}$, at specific values of w given by Eq. (104) and $+\infty > w_b^* > w_c^* > w_a^* > w_d^* > -\infty$. It is straightforward to generalize the above results to this case of four singularities. Therefore, we only give the results below, without repeating the details.

2.8.4.1 $w > w_b^*$

For $w > w_b^*$, the saddle point lies between λ_- and λ_b , and

$$\begin{aligned} P(W_\tau = w\tau) &\approx \frac{\tilde{g}(\lambda_c) e^{\tau h_c(w)}}{\sqrt{\pi\tau} |f'_w(\lambda_c)|} R_9 \left(\sqrt{\tau[h_c(w) - h_s(w)]}, \sqrt{\tau[h_b(w) - h_s(w)]} \right) \\ &- \frac{|g(\lambda^*)| e^{\tau h_s(w)}}{\sqrt{2\pi\tau} f''_w(\lambda^*)} R_{11} \left(\sqrt{\tau[h_b(w) - h_s(w)]}, \sqrt{\tau[h_c(w) - h_s(w)]}, \right. \\ &\quad \left. \sqrt{\tau[h_a(w) - h_s(w)]}, \sqrt{\tau[h_d(w) - h_s(w)]} \right), \end{aligned} \quad (141)$$

where $R_9(z_1, z_2)$ is given by Eq. (138) and

$$\begin{aligned} R_{11}(z_1, z_2, z_3, z_4) &= \sqrt{\frac{z_1 z_2 z_3 z_4}{\pi}} \int_{-\infty}^{\infty} \frac{e^{-u^2} du}{\sqrt{z_1 - iu} \sqrt{z_2 - iu} \sqrt{z_3 - iu} \sqrt{z_4 - iu}} \\ &= \sqrt{\frac{z_1 z_2 z_3 z_4}{\pi}} \int_{-\infty}^{\infty} \frac{e^{-u^2} du}{\sqrt{z_1 + iu} \sqrt{z_2 + iu} \sqrt{z_3 + iu} \sqrt{z_4 + iu}}. \end{aligned} \quad (142)$$

2.8.4.2 $w_c^* < w < w_b^*$

For $w_c^* < w < w_b^*$, the saddle point lies between λ_b and λ_c , and

$$\begin{aligned} P(W_\tau = w\tau) \approx & \frac{\tilde{g}(\lambda_c) e^{\tau h_c(w)}}{\sqrt{\pi\tau|f'_w(\lambda_c)|}} R_7 \left(\sqrt{\tau[h_c(w) - h_s(w)]}, \sqrt{\tau[h_b(w) - h_s(w)]} \right) \\ & + \frac{|g(\lambda^*)| e^{\tau h_s(w)}}{\sqrt{2\pi\tau f''_w(\lambda^*)}} R_{12} \left(\sqrt{\tau[h_b(w) - h_s(w)]}, \sqrt{\tau[h_c(w) - h_s(w)]}, \right. \\ & \left. \sqrt{\tau[h_a(w) - h_s(w)]}, \sqrt{\tau[h_d(w) - h_s(w)]} \right), \end{aligned} \quad (143)$$

where $R_7(z_1, z_2)$ is given by Eq. (135) and

$$\begin{aligned} R_{12}(z_1, z_2, z_3, z_4) = & \sqrt{\frac{z_1 z_2 z_3 z_4}{\pi}} \int_0^\infty du e^{-u^2} \left[\frac{1}{\sqrt{z_1 - iu}\sqrt{z_2 + iu}\sqrt{z_3 + iu}\sqrt{z_4 + iu}} \right. \\ & \left. - \frac{1}{\sqrt{z_1 + iu}\sqrt{z_2 - iu}\sqrt{z_3 - iu}\sqrt{z_4 - iu}} \right] i. \end{aligned} \quad (144)$$

2.8.4.3 $w_a^* < w < w_c^*$

For $w_a^* < w < w_c^*$, the saddle point lies between λ_c and λ_a , and the PDF is given by

$$\begin{aligned} P(W_\tau = w\tau) \approx & \frac{g(\lambda^*) e^{\tau h_s(w)}}{\sqrt{2\pi\tau f''_w(\lambda^*)}} R_{13} \left(\sqrt{\tau[h_b(w) - h_s(w)]}, \sqrt{\tau[h_c(w) - h_s(w)]}, \right. \\ & \left. \sqrt{\tau[h_a(w) - h_s(w)]}, \sqrt{\tau[h_d(w) - h_s(w)]} \right), \end{aligned} \quad (145)$$

where

$$R_{13}(z_1, z_2, z_3, z_4) = \sqrt{\frac{z_1 z_2 z_3 z_4}{\pi}} \int_{-\infty}^\infty \frac{e^{-u^2} du}{\sqrt{z_1 + iu}\sqrt{z_2 + iu}\sqrt{z_3 - iu}\sqrt{z_4 - iu}}. \quad (146)$$

2.8.4.4 $w_d^* < w < w_a^*$

For $w_d^* < w < w_a^*$, the saddle point lies between λ_a and λ_d , and

$$\begin{aligned} P(W_\tau = w\tau) &\approx \frac{\tilde{g}(\lambda_a) e^{\tau h_a(w)}}{\sqrt{\pi\tau|f'_w(\lambda_a)|}} R_7 \left(\sqrt{\tau[h_a(w) - h_s(w)]}, \sqrt{\tau[h_d(w) - h_s(w)]} \right) \\ &+ \frac{|g(\lambda^*)| e^{\tau h_s(w)}}{\sqrt{2\pi\tau f''_w(\lambda^*)}} R_{14} \left(\sqrt{\tau[h_b(w) - h_s(w)]}, \sqrt{\tau[h_c(w) - h_s(w)]}, \right. \\ &\quad \left. \sqrt{\tau[h_a(w) - h_s(w)]}, \sqrt{\tau[h_d(w) - h_s(w)]} \right), \end{aligned} \quad (147)$$

where $R_7(z_1, z_2)$ is given by Eq. (135) and

$$\begin{aligned} R_{14}(z_1, z_2, z_3, z_4) &= \sqrt{\frac{z_1 z_2 z_3 z_4}{\pi}} \int_0^\infty du e^{-u^2} \left[\frac{1}{\sqrt{z_1 + iu}\sqrt{z_2 + iu}\sqrt{z_3 + iu}\sqrt{z_4 - iu}} \right. \\ &\quad \left. - \frac{1}{\sqrt{z_1 - iu}\sqrt{z_2 - iu}\sqrt{z_3 - iu}\sqrt{z_4 + iu}} \right] i. \end{aligned} \quad (148)$$

2.8.4.5 $w < w_d^*$

Finally, for $w < w_d^*$, the saddle point lies between λ_d and λ_+ , and

$$\begin{aligned} P(W_\tau = w\tau) &\approx \frac{\tilde{g}(\lambda_a) e^{\tau h_a(w)}}{\sqrt{\pi\tau|f'_w(\lambda_a)|}} R_9 \left(\sqrt{\tau[h_a(w) - h_s(w)]}, \sqrt{\tau[h_d(w) - h_s(w)]} \right) \\ &- \frac{|g(\lambda^*)| e^{\tau h_s(w)}}{\sqrt{2\pi\tau f''_w(\lambda^*)}} R_{11} \left(\sqrt{\tau[h_b(w) - h_s(w)]}, \sqrt{\tau[h_c(w) - h_s(w)]}, \right. \\ &\quad \left. \sqrt{\tau[h_a(w) - h_s(w)]}, \sqrt{\tau[h_d(w) - h_s(w)]} \right). \end{aligned} \quad (149)$$

where $R_9(z_1, z_2)$ and $R_{11}(z_1, z_2, z_3, z_4)$ are given by Eqs. (138) and (142), respectively.

It can be shown that, when $w \rightarrow w_i^*$ with $i \in \{a, b, c, d\}$ from the two sides of w_i^* , the respective expressions of the PDFs, i.e, Eqs. (141) and (143), Eqs. (143) and (145), Eqs. (145) and (147), and Eqs. (147) and (149), respectively, approach the same limiting form.

2.8.4.6 Numerical simulation

We now compare the analytical results obtained in this section with numerical simulation. We consider $\delta = 5$, for which we have $\theta_{c_2} =$

0.18. Therefore, $g(\lambda)$ has three singularities for $\theta > \theta_{c_2}$, whereas for $\theta < \theta_{c_2}$ it has four singularities.

For $\theta = 0.5$ the three singularities are located at $\lambda_c = -0.3062\dots$, $\lambda_a = 0.3958\dots$ and $\lambda_d = 1.3062\dots$, whereas $\lambda_- = -0.4848\dots$ and $\lambda_+ = 1.4848\dots$. Figure 9 compares numerical simulation for this case with analytical results obtained above for the case of the three singularities.

On the other hand, for $\theta = 0.1$, the four singularities of $g(\lambda)$ are located at $\lambda_b = -10/7$, $\lambda_c = -1$, $\lambda_a = 13/11$, and $\lambda_d = 2$. Moreover, $\lambda_- = -1.4621\dots$ and $\lambda_+ = 2.4621\dots$. Figure 10 compares numerical simulation for this case with analytical results obtained above for the case of the four singularities.

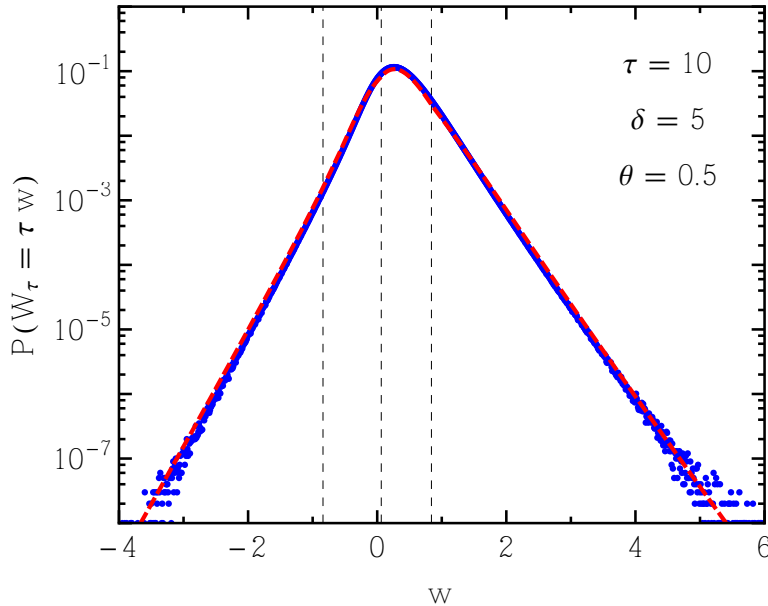


Figure 9: $P(W_\tau)$ against the scaled variable $w = W_\tau/\tau$ for $\tau = 10$, $\tau_c = 1$, $\delta = 5$, and $\theta = 0.5$. The points (blue) are obtained from numerical simulation, and the dashed solid line (red) plots the analytical asymptotic forms given in the text. The vertical dashed lines mark the positions $w_c^* = 0.8398\dots$, $w_a^* = 0.06269\dots$ and $w_d^* = -0.8398\dots$.

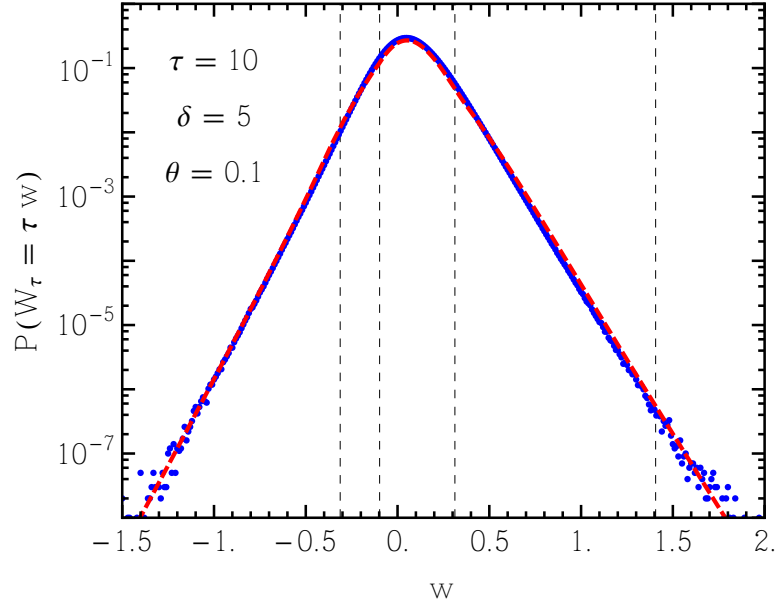


Figure 10: $P(W_\tau)$ against the scaled variable $w = W_\tau/\tau$ for $\tau = 10$, $\tau_c = 1$, $\delta = 5$ and $\theta = 0.1$. The points (blue) are obtained from numerical simulation, and the dashed solid line (red) plots the analytical asymptotic forms given in the text. The vertical dashed lines mark the positions $w_b^* = 1.4062\dots$, $w_c^* = 0.3125$, $w_a^* = -0.0976\dots$ and $w_d^* = -0.3125$.

2.9 LARGE DEVIATION FUNCTION AND FLUCTUATION THEOREM

The large deviation function is defined by

$$h(w) = \lim_{\tau \rightarrow \infty} \frac{1}{\tau} \ln P(W_\tau = w\tau). \quad (150)$$

In other words, the large deviation form of the PDF refers to the ultimate asymptotic form $P(W_\tau = w\tau) \sim e^{\tau h(w)}$ while ignoring the subleading corrections. Apart from being an interesting quantity on its own, the large deviation functions have found importance recently in the context of the fluctuation theorem. The latter refers to the relation

$$\lim_{\tau \rightarrow \infty} \frac{1}{\tau} \ln \left[\frac{P(W_\tau = +w\tau)}{P(W_\tau = -w\tau)} \right] = w. \quad (151)$$

When the above relation is valid, the large deviation function evidently satisfies the symmetry relation

$$h(w) - h(-w) = w. \quad (152)$$

Now, as we have seen in the above sections, when $g(\lambda)$ is analytic between the origin and the saddle point, the dominant contribution to $P(W_\tau)$ comes from the saddle point as given by Eq. (118). On the other hand, when there are singularities between the origin and the saddle point, the most dominant contribution to $P(W_\tau)$ comes from the singularity closest to the origin (farthest from the saddle point) and lies between the origin and the saddle point. This is because, evidently $-\nu(\lambda)$, and hence the function $f_w(\lambda)$, is convex on the interval $[\lambda_-, \lambda_+]$ and $f_w(\lambda)$ is minimum at the saddle point λ^* along the real- λ line.

Consequently, for the case $\delta < 1$ and $\theta < \theta_{c_1}$, where $g(\lambda)$ is analytic on the interval (λ_-, λ_+) , the large deviation function is $h(w) = h_s(w)$, given by Eq. (116). In this case, $h(w)$ satisfies the above symmetry relation (152), and therefore, the fluctuation theorem is valid. On the other hand, for $\delta < 1$ and $\theta > \theta_{c_1}$, where $g(\lambda)$ has one singularity at λ_a , (also for $\delta = 1$ and all values of θ , where only the singularity at λ_a is relevant), one has

$$h(w) = \begin{cases} h_s(w) & \text{for } w > w_a^* \\ h_a(w) & \text{for } w < w_a^*. \end{cases} \quad (153)$$

Therefore, it is only when $w_a^* < 0$ (e.g., when $\theta < 4$ for the $\delta = 1$ case), the symmetry relation Eq. (152) (and hence the fluctuation theorem) is satisfied only in the specific range $w_a^* < w < -w_a^*$. Otherwise it is not satisfied.

For the case $\delta > 1$, although there are either three or four singularities depending on whether $\theta > \theta_{c_2}$ or $\theta < \theta_{c_2}$, the singularities closest to the origin (one on each side), namely λ_c and λ_a are common

in both cases. Therefore, for both cases, the large deviation function is given by

$$h(w) = \begin{cases} h_c(w) & \text{for } w > w_c^*, \\ h_s(w) & \text{for } w_a^* < w < w_c^*, \\ h_a(w) & \text{for } w < w_a^*. \end{cases} \quad (154)$$

Since $\lambda_c < 0$, it is evident from Eq. (104) that $w_c^* > 0$. Therefore again, it is only when $w_a^* < 0$ (e.g., when $\theta < 0.365\dots$ for the $\delta = 5$ case), the symmetry relation Eq. (152) (and hence the fluctuation theorem) is satisfied only in the specific range $\max(w_a^*, -w_c^*) < w < \min(-w_a^*, w_c^*)$.

Therefore, for any δ , there exists a θ_c , given by $w_a^* = 0$ (equivalently $\lambda_a = 1/2$) as

$$\theta_c(\delta) = \frac{3 + 2\delta + 3\delta^2 + (1 - \delta)\sqrt{9 + 14\delta + 9\delta^2}}{2\delta^2}, \quad (155)$$

and the fluctuation theorem is not valid for $\theta > \theta_c$. The $\theta = \theta_c(\delta)$ line corresponds to the $\alpha = \alpha_c(\delta)$ line in the (α, δ) plane where

$$\alpha_c(\delta) = \frac{3 + 2\delta + 3\delta^2 + (1 - \delta)\sqrt{9 + 14\delta + 9\delta^2}}{2(1 + \delta)}. \quad (156)$$

Figure 11 summarizes the state of validity of the fluctuation theorem in the δ, θ and α, δ parameter spaces.

It is useful to discuss the analytical properties of the probability distribution functions or the large deviation functions of the thermodynamical observables near the singularities. We shall elaborate one case and the others will follow directly. Identifying the structures of $h_s(w)$ and $h_a(w)$, we immediately observe that,

$$\begin{aligned} h_s(w_a^*) &= h_a(w_a^*) \\ h'_s(w_a^*) &= h'_a(w_a^*) \\ \text{but } h''_s(w_a^*) &\neq h''_a(w_a^*). \end{aligned} \quad (157)$$

Therefore, we find the PDFs to be continuous and analytic in the singular points, however the second derivatives are discontinuous at

these singular points. Nevertheless, one has to identify this case to be non-identical to the one where LDFs themselves exhibit singular behavior. A detailed discussion on this has been made in Sec. 3.7.

2.10 CONCLUSION

Let us now summarize the main contents of this chapter. We have obtained analytical results for a system studied recently experimentally in [99]. The experimental system consists of a colloidal particle in water and confined in an optical trap which is modulated according to an Ornstein-Uhlenbeck process. This system is described by a set of

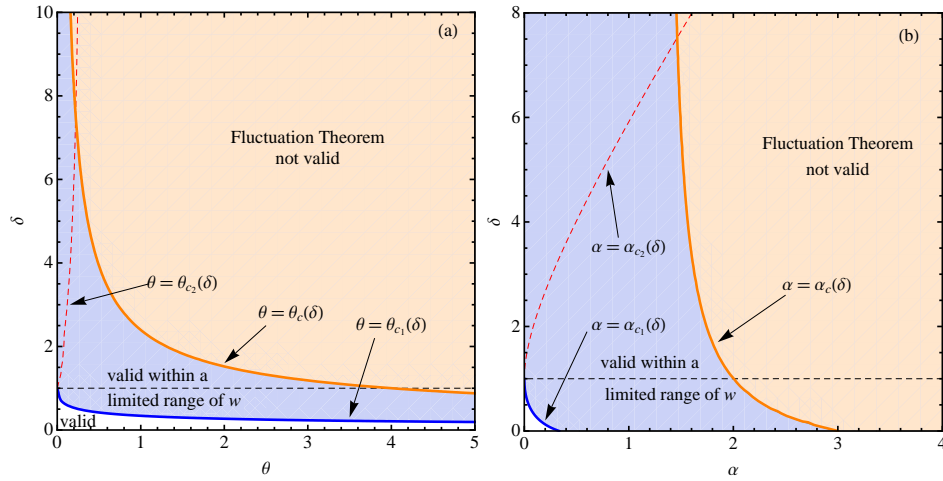


Figure 11: The phase diagrams in the parameters space showing the state of the validity of the fluctuation theorem. Apart from the $\theta = \theta_c$ and $\alpha = \alpha_c$ (orange) lines, the other lines are the same as in Fig. 5. In the (light orange) regions above the (orange) lines $\theta = \theta_c$ in (a) and $\alpha = \alpha_c$ in (b), the fluctuation theorem is not valid at all, whereas it is always valid in the white regions below the (blue) lines $\theta = \theta_{c_1}$ in (a) and $\alpha = \alpha_{c_1}$ in (b). In the intermediate (light blue) region, the fluctuation theorem is valid only within a limited range of w given by $w_a^* < w < -w_a^*$ for $\delta < 1$ and $\max(w_a^*, -w_c^*) < w < \min(-w_a^*, w_c^*)$ for $\delta > 1$. For $\delta = 0$, we have $\alpha_{c_1} = 1/3$ and $\alpha_c = 3$.

coupled Langevin equations. We have computed the PDF of the work done by the modulating trap on the Brownian particle in a given time τ , for large τ . The moment generating function of the work has the form $\langle e^{-\lambda W_\tau} \rangle \approx g(\lambda) e^{\tau \mu(\lambda)}$ for large τ . Inverting this, we obtain the PDF of the work within the saddle point approximation.

The results can be described in terms of two independent parameters: (1) the parameter θ that quantifies the relative strength of the external noise that generates the Ornstein-Uhlenbeck process for the trap modulation, with respect to the thermal fluctuations, and (2) the ratio δ of the correlation time of the trap modulation to the viscous relaxation time of the particle in the trap without any modulation. We find that the cumulant generating function $\mu(\lambda)$ is analytic in a (real) interval (λ_-, λ_+) and the saddle point lies within this interval. Here λ_\pm depends on the values of θ, δ . On the other hand, depending on the values of the pair (θ, δ) , the function $g(\lambda)$ behaves differently. For $\delta < 1$, there exists a value $\theta_{c_1}(\delta)$ such that $g(\lambda)$ is analytic in the interval (λ_-, λ_+) for $\theta < \theta_{c_1}$ whereas it has a branch point for $\theta > \theta_{c_1}$. For $\delta > 1$, there again exists a $\theta_{c_2}(\delta)$, and $g(\lambda)$ has either three or four branch points depending on whether $\theta > \theta_{c_2}$ or $\theta < \theta_{c_2}$. For $\delta = 1$, there are three branch points of which two coincide with λ_\pm . We have done the analysis in each of these regions and obtained the asymptotic form of the PDF accordingly. We have compared our analytical results with simulation results on this system and found very good agreement between the two.

The calculation also gives the large deviation function as a by-product, using which we check the validity of the so-called fluctuation theorem for this context. We find that in the region $\delta < 1, \theta < \theta_{c_1}$, it is always valid. Outside this parameter region, there exists a $\theta_c(\delta)$ and the fluctuation theorem is valid for a limited range of w around zero when $\theta < \theta_c$. For $\theta > \theta_c$, the fluctuation theorem is not valid at all (see Fig. 11).

This chapter therefore summarizes the effects of *stochastic driving* in a simple linear diffusive system namely the colloidal particle in

a driven harmonic trap. We have managed to compute the complete distribution functions of the observable which is, in this context, the mechanical work. In the next chapter, we shall extend our studies to other observables in the given set up. We will see the relations among the observables and the effects of stochastic modulation in the observable statistics. It is worth mentioning that the effects of stochastic driving is found to be more generic in the case of LC or RC circuit with Nyquist white noise. Usually, the voltage fluctuations due to the voltage generator is considered as the white noise (with an analogy to the noise due to the ambient medium for the colloidal system) while the electric circuit is considered to be connected with a nonfluctuating current source I (similar to the velocity v at which the trap is being pulled), when in parallel. But in practice, no current source is completely ideal i.e. eliminated from the small fluctuations due to the internal resistance and its compliance voltage. Thus, one indeed needs to model the current source with a stochastic term added to it. This should fit in perfectly within our framework and thus heat generated across the circuit and the power flux can also be measured. The results can be verified easily by table top experiments.

HEAT AND ENTROPY FLUCTUATIONS OF A GENERAL LANGEVIN SYSTEM

3.1 ABSTRACT

We study the heat and the entropy fluctuations in a general Langevin setup. We find that the construction of the total entropy production inherently allows it to be a suitable candidate for SSFT; however this is not generically true for the other relevant observables in a given system. If the observables of our interests are connected to each other through *boundary terms*, we provide a general framework which allows us to compute the PDFs of these observables by knowing only one among this family of observables. We also explicitly show the effects of the *boundary terms* while computing the PDFs and their role towards the validation of the SSFT. We verify our results in the following application: a Brownian particle diffusing in a stochastically modulated optical trap. Earlier we have studied work fluctuations in this set up [103]. We extend our studies to the heat and entropy fluctuations which are connected to work by the *boundary terms*. We show that our framework perfectly suits for such physical systems. We conclude with the fact that the observables such as work and heat are extensive in time while the energy difference (or boundary terms) is not, plays a crucial role in this derivation [66, 68, 94]. In pursuit of this, we add a simple derivation at the end of this chapter based on the probability theory and then show how the *boundary terms* play crucial role in the computation of the LDFs and eventually to the SSFT.

3.2 INTRODUCTION

We consider a system of $2n$ number of state variables in one dimension: positions (x_1, x_2, \dots, x_n) and momenta (p_1, p_2, \dots, p_n) , which is always kept in contact with the surrounding at certain temperature T . At $t = 0$, we switch on the external driving (which can be of deterministic or stochastic nature) and thus the system is driven away from its equilibrium or the steady state where it was initially prepared. We consider the driving to be a stationary process and therefore acting as a reversible source. The system trajectories fluctuate from one realization to the other because of three reasons: interactions with the surroundings, the presence of stochastic driving and the choice of initial condition.

In the foregoing chapter, we aimed to compute the mechanical work Eq. (40) for an overdamped model system of a Brownian particle diffusing in an optical trap. We will show that the heat dissipation and the total entropy production in this problem are differed to the mechanical work Eq. (40) defined in the last chapter by boundary terms (within the work and the heat, it is just the potential energy difference due to the second law constraint). Using this fact, we will compute the generating functions of the heat dissipation and the entropy production in a much efficient way. It will be shown that the moment generating function for the entropy will remain analytic in the entire phase space spanned by the system parameters while that of heat will not. The heat generating function, as we will see, are accompanied by singularities originating due to the exponential nature of the energy terms. The very presence of such singularities will lead to non identical distributions of these observables and shed light on the FT.

The entire chapter has been arranged in the following way. We develop the general formalism in the following section. Application to our model system and computation of the heat and the entropy has

been derived in the consecutive section. We have discussed the symmetry properties and the details of the fluctuation theorem in the last section.

3.3 A GENERAL FORMALISM

Consider a general set up of Langevin kind diffusive system

$$\frac{d\mathbf{U}}{dt} = \mathbf{F}(\mathbf{U}) + \boldsymbol{\eta}(t), \quad (158)$$

where the column matrix $\mathbf{U} = (x_i, p_i, f_i)^T$ contains all relevant state variables namely $(\{x_i : i = 1, \dots, n\}, \{p_i : i = 1, \dots, n\})$ of the system of interest and the external time dependent stochastic driving $\{f_i : i = 1, \dots, n\}$. We denote the initial condition as $\mathbf{U}(t = 0) = \mathbf{U}_0$ and this is not a fixed initial condition but chosen from a steady state distribution $P_{SS}(\mathbf{U}_0)$. We will often denote the end time state variable as $\mathbf{U}(t = \tau) = \mathbf{U}_\tau$. The force matrix $\mathbf{F}(\mathbf{U})$ takes into account of the internal interaction within the system of interest and that of with the external driving. Interaction with the bath has been modelled as a random noise added to the system. Both this noise and the stochasticity in the driving have been incorporated in the column matrix $\boldsymbol{\eta}(t)$. Let us consider the observables of our interests as the following:

$$\Omega_\tau = \int_0^\tau dt h[\mathbf{U}(t), \boldsymbol{\eta}(t)] \quad (159)$$

$$\Theta_\tau = \Omega_\tau + b_{\text{int}}[\mathbf{U}(0)] + b_{\text{fin}}[\mathbf{U}(\tau)], \quad (160)$$

where the observables depend on the state variables as a functional form $h[\mathbf{U}(t)]$ and are measured for the duration $[0, \tau]$. The boundary terms in Ω_τ are denoted by $b_{\text{int}}[\mathbf{U}(0)]$ and $b_{\text{fin}}[\mathbf{U}(\tau)]$ respectively. It is worth to note that the observables Eq. (160) are stochastic in nature due to the randomness present in \mathbf{U}_0 and the noise history $\{\boldsymbol{\eta}_i\}$. This leads one to have a statistical description of these observables such as: the mean, fluctuations or rather the full distribution. We compute the full density functions $P(\Omega_\tau)$, $P(\Theta_\tau)$ using the methods developed in the preceding chapter.

To compute the distribution of Ω_τ , we need to know the full history of the system trajectories $\{\mathbf{U}_t : t \in [0, \tau]\}$. To this purpose, it is instructive to write the full evolution equation of the joint distribution $P(\Omega_t, \mathbf{U}, t | \mathbf{U}_0, 0)$ using the Fokker-Planck operator such as

$$\partial_t P(\Omega_t, \mathbf{U}, t | \mathbf{U}_0, 0) = \mathcal{L}_\Omega P(\Omega_t, \mathbf{U}, t | \mathbf{U}_0, 0), \quad (161)$$

with the initial condition

$$P(\Omega_t, \mathbf{U}, t = 0) = \delta[\mathbf{U} - \mathbf{U}_0] \delta[\Omega_t], \quad (162)$$

since at $t = 0$, the observable is strictly zero. The corresponding Fokker-Planck operator can be derived by calculating the moments using Eq. (184):

$$\begin{aligned} \mathcal{L}_\Omega = & - \sum_{l=1}^{3n} \frac{\partial}{\partial \mathbf{U}_l} \frac{\langle \Delta \mathbf{U}_l \rangle}{\Delta t} - \frac{\partial}{\partial \Omega} \frac{\langle \Delta \Omega \rangle}{\Delta t} + \frac{1}{2} \sum_{m=1}^{3n} \sum_{m=1}^{3n} \frac{\partial^2}{\partial \mathbf{U}_l \partial \mathbf{U}_m} \frac{\langle \Delta \mathbf{U}_l \Delta \mathbf{U}_m \rangle}{\Delta t} \\ & + \sum_{l=1}^{3n} \frac{\partial^2}{\partial \mathbf{U}_l \partial \Omega} \frac{\langle \Delta \mathbf{U}_l \Delta \Omega \rangle}{\Delta t} + \frac{1}{2} \frac{\partial^2}{\partial \Omega^2} \frac{\langle \Delta \Omega^2 \rangle}{\Delta t}, \quad \text{with } \Delta t \rightarrow 0. \end{aligned} \quad (163)$$

The marginal distribution of the observable Ω is then simply obtained by integrating out the initial and final conditions such as

$$P(\Omega_t) = \int d\mathbf{U} \int d\mathbf{U}_0 P_{SS}(\mathbf{U}_0) P(\Omega_t, \mathbf{U}, t | \mathbf{U}_0, 0) \quad (164)$$

We now define the restricted moment generating function, constrained to fixed initial and final configurations \mathbf{U}_0 and \mathbf{U}_τ respectively, in the following way

$$Z(\lambda, \mathbf{U}, \tau | \mathbf{U}_0, 0) = \langle e^{-\lambda \Omega_\tau} \delta[\mathbf{U} - \mathbf{U}(\tau)] \rangle_\eta, \quad (165)$$

where the average is over the histories of the thermal noises starting from the fixed initial condition (\mathbf{U}_0) and λ is the conjugate variable. It is then simple to show that $Z(\lambda, \mathbf{U}, \tau | \mathbf{U}_0, 0)$ satisfies the Fokker-Planck equation

$$\frac{\partial Z}{\partial \tau} = \mathcal{L}_\lambda Z, \quad (166)$$

with the initial condition $Z(\lambda, \mathbf{U}, 0 | \mathbf{U}_0) = \delta(\mathbf{U} - \mathbf{U}_0)$ and the Fokker-Planck operator in the λ space is given by

$$\begin{aligned} \mathcal{L}_\lambda = & - \sum_{l=1}^{3n} \frac{\partial}{\partial U_l} \frac{\langle \Delta U_l \rangle}{\Delta t} - \lambda \frac{\langle \Delta \Omega \rangle}{\Delta t} + \frac{1}{2} \sum_{m=1}^{3n} \sum_{m=1}^{3n} \frac{\partial^2}{\partial U_l \partial U_m} \frac{\langle \Delta U_l \Delta U_m \rangle}{\Delta t} \\ & + \sum_{l=1}^{3n} \lambda \frac{\partial}{\partial U_l} \frac{\langle \Delta U_l \Delta \Omega \rangle}{\Delta t} + \frac{1}{2} \lambda^2 \frac{\langle \Delta \Omega^2 \rangle}{\Delta t}, \quad \text{with } \Delta t \rightarrow 0. \end{aligned} \quad (167)$$

Eq. (166) is a simple eigenvalue equation and the solution can be expanded in terms of the bi-orthogonal eigenstates

$$Z(\lambda, \mathbf{U}, \tau | \mathbf{U}_0, 0) = \sum_{k=1}^{\infty} \chi_k(\mathbf{U}_0, \lambda) \psi_k(\mathbf{U}, \lambda) e^{\tau \mu_k(\lambda)} \quad (168)$$

where $\psi_k(\mathbf{U}, \lambda)$ and $\chi_k(\mathbf{U}_0, \lambda)$ are the right and left eigenfunctions respectively and they satisfy

$$\mathcal{L}_\lambda \psi_k(\mathbf{U}, \lambda) = \mu_k(\lambda) \psi_k(\mathbf{U}, \lambda) \quad (169)$$

$$\mathcal{L}_\lambda^+ \chi_k(\mathbf{U}_0, \lambda) = \mu_k(\lambda) \chi_k(\mathbf{U}_0, \lambda) \quad (170)$$

where \mathcal{L}_λ^+ is the adjoint operator and $\mu_k(\lambda)$ are the eigenvalues. The orthonormality condition of the eigenfunctions is easy to state

$\int d\mathbf{U} \chi_k(\mathbf{U}, \lambda) \psi_k(\mathbf{U}, \lambda) = 1$. It is important to note the following points

- \mathcal{L}_λ and \mathcal{L}_λ^+ share the same eigenvalue.
- The stationary state corresponds to $\lambda = 0$ such that $\mathcal{L}_\lambda P_{SS} = 0$.
- The ground state eigenvalue which corresponds to $k = 1$ i.e. $\mu_1(0)$ is zero and the largest among all the other eigenvalues. Thus all other eigenvalues are strictly negative and they maintain the order $\mu_2(0) > \mu_3(0) > \mu_4(0) \dots$
- For $\lambda \neq 0$, one can still show that the ground state is the largest eigenvalue which is strictly positive and non degenerate as a consequence of the Perron-Frobenius theorem, but no order can be set for the rest eigenvalues.

However, we are interested in the large τ behavior which will be dominated by the the term containing the largest eigenvalue $\mu(\lambda)$ (for simplicity we will denote $\mu_1(\lambda)$ as $\mu(\lambda)$ now onwards). Thus, one can write

$$Z(\lambda, \mathbf{U}, \tau | \mathbf{U}_0) = \chi(\mathbf{U}_0, \lambda) \Psi(\mathbf{U}, \lambda) e^{\tau \mu(\lambda)} + \dots, \quad (171)$$

where $\psi(\mathbf{U}, \lambda)$ and $\chi(\mathbf{U}_0, \lambda)$ are the right and left eigenfunctions respectively corresponding to the largest eigenvalue $\mu(\lambda)$.

That said, the moment generating function can be obtained by averaging the restricted generating function over the initial variables \mathbf{U}_0 with respect to the steady state distribution $P_{SS}(\mathbf{U}_0)$ and also relaxing the the final degrees of freedom \mathbf{U} ,

$$Z(\lambda, \tau) = \int d\mathbf{U} \int d\mathbf{U}_0 P_{SS}(\mathbf{U}_0) Z(\lambda, \mathbf{U}, \tau | \mathbf{U}_0), \quad (172)$$

where $P_{SS}(\mathbf{U}_0) = \Psi(\mathbf{U}_0, 0)$. This yields

$$Z(\lambda, \tau) = \langle e^{-\lambda \Omega_\tau} \rangle = g(\lambda) e^{\tau \mu(\lambda)} + \dots, \quad (173)$$

where

$$g(\lambda) = \int d\mathbf{U} \Psi(\mathbf{U}, \lambda) \int d\mathbf{U}_0 \Psi(\mathbf{U}_0, 0) \chi(\mathbf{U}_0, \lambda), \quad (174)$$

is the prefactor which does not depend on time though depends on the choice of the initial condition (i.c.) explicitly. Therefore we can write

$$Z^{(\Omega)}(\lambda) = \langle e^{-\lambda \Omega_\tau} \rangle_{i.c.+noise} \sim g(\lambda) e^{\tau \mu(\lambda)} \quad (175)$$

where the superscript in $Z^{(\Omega)}(\lambda)$ stands for the generating function particular to the observable Ω_τ . The full probability distribution can now simply be obtained as

$$P(\Omega_\tau = \omega \tau) = \frac{1}{2\pi i} \int_{-i\infty}^{i\infty} d\lambda Z^{(\Omega)}(\lambda) e^{\lambda \omega} \quad (176)$$

$$\approx \frac{1}{2\pi i} \int_{-i\infty}^{i\infty} d\lambda g(\lambda) e^{\tau[\mu(\lambda) + \lambda \omega]}, \quad (177)$$

where $\mu(\lambda)$ is the largest eigenvalue and $g(\lambda)$ is the prefactor obtained from Eq. (174). Having said that, our aim is now to provide a detailed

statistical description of the other observable Θ_τ which is connected to Ω_τ by boundary terms Eq. (160)

$$\Theta_\tau = \Omega_\tau + b_{\text{int}}[\mathbf{U}_0] + b_{\text{fin}}[\mathbf{U}_\tau]. \quad (178)$$

We note two important points at this moment which are the following:

- \mathcal{L}_Ω and \mathcal{L}_Θ are completely identical due to the fact that Ω and Θ are related by the boundary terms and they do not contribute to the moments. As a result, the eigenvalue spectrum remains identical for both of them so as the largest eigenvalue $\mu(\lambda)$.
- The restricted moment generating function $Z(\lambda, \mathbf{U}, \tau|\mathbf{U}_0)$, constrained to fixed initial and final boundary conditions, for both the observables will now differ from each other. However, path average will remain same, changes will be on the boundaries.

We therefore find

$$Z_\Theta(\lambda, \mathbf{U}, \tau|\mathbf{U}_0) = Z_\Omega(\lambda, \mathbf{U}, \tau|\mathbf{U}_0) e^{-\lambda b_{\text{int}}[\mathbf{U}_0]} e^{-\lambda b_{\text{fin}}[\mathbf{U}_\tau]} \quad (179)$$

Since the eigenbases and the eigenspectrum remain identical for both the observables, the asymptotic analysis of the restricted generating function remains same

$$Z_\Theta(\lambda, \mathbf{U}, \tau|\mathbf{U}_0) \sim \chi(\mathbf{U}_0, \lambda) \Psi(\mathbf{U}, \lambda) e^{\tau\mu(\lambda)} e^{-\lambda b_{\text{int}}[\mathbf{U}_0]} e^{-\lambda b_{\text{fin}}[\mathbf{U}_\tau]}. \quad (180)$$

We can now relax the initial and final boundary conditions to obtain the moment generating function corresponding to the observable Θ_τ

$$Z^{(\Theta)}(\lambda) = \langle e^{-\lambda\Theta_\tau} \rangle_{\text{i.c.+noise}} \sim g_\Theta(\lambda) e^{\tau\mu(\lambda)} \quad (181)$$

where the prefactor has been modified as

$$g_\Theta(\lambda) = \int d\mathbf{U} \Psi(\mathbf{U}, \lambda) e^{-\lambda b_{\text{fin}}[\mathbf{U}]} \int d\mathbf{U}_0 \Psi(\mathbf{U}_0, 0) \chi(\mathbf{U}_0, \lambda) e^{-\lambda b_{\text{int}}[\mathbf{U}_0]}. \quad (182)$$

Therefore the distribution function of Θ can be obtained as sketched in Eq. (177)

$$P(\Theta_\tau = \theta\tau) \approx \frac{1}{2\pi i} \int_{-i\infty}^{i\infty} d\lambda g_\Theta(\lambda) e^{\tau[\mu(\lambda) + \lambda\theta]}, \quad (183)$$

where the prefactor is given by Eq. (182). The take home message from this section would be: given a stochastic dynamical system prepared from a well defined initial condition, if one constructs a set of observables of interests which differ by boundary terms, then the corresponding evolution operators will share the same eigenspectrum. However, the distributions will certainly differ and the method outlined here suggests an efficient way to connect these distribution functions. In the following section, we investigate a model system of a Brownian particle in an optical trap to make a connection with the theory developed in this section.

3.4 MODEL

For the sake of simplicity, we mostly focus on the linear systems where the force has been considered to be *linear* i.e. $F(\mathbf{U}) = -A\mathbf{U}$ so that the dynamics Eq. (158) is modified to

$$\frac{d\mathbf{U}}{dt} = -A\mathbf{U} + \boldsymbol{\eta}(t), \quad (184)$$

where the square matrix A is independent of \mathbf{U} and contains all the constant parameters of the dynamics. Such a system can be realized a set up which was introduced in the last chapter. Consider a Brownian particle suspended in an ambient medium at temperature T , with a viscosity γ . The particle is diffusing in an harmonic trap, with a stiffness k , around the mean position \mathbf{y} of the trap. The position $\mathbf{x}(t)$ of the particle is described by the overdamped Langevin equation

$$\frac{d\mathbf{x}}{dt} = -\frac{\mathbf{x} - \mathbf{y}}{\tau_\gamma} + \boldsymbol{\xi}(t), \quad (185)$$

where $\tau_\gamma = \gamma/k$ is the relaxation time of the harmonic trap. The thermal noise $\boldsymbol{\xi}(t)$ is taken to be Gaussian with mean $\langle \boldsymbol{\xi}(t) \rangle = 0$ and covariance $\langle \boldsymbol{\xi}(t)\boldsymbol{\xi}(s) \rangle = 2D\delta(t-s)$, where the diffusion coefficient $D = \gamma^{-1}k_B T$ with k_B being the Boltzmann constant. An external time-varying random force is exerted by the trap on the Brownian

particle by externally modulating the position of the trap according to an Ornstein-Uhlenbeck process

$$\frac{dy}{dt} = -\frac{y}{\tau_0} + \zeta(t), \quad (186)$$

where $\zeta(t)$ is an externally generated Gaussian white (non-thermal) noise with mean $\langle \zeta(t) \rangle = 0$ and covariance $\langle \zeta(t)\zeta(s) \rangle = 2\Lambda\delta(t-s)$. There is no correlation between the externally applied noise and the thermal noise, $\langle \zeta(t)\xi(s) \rangle = 0$. The system eventually reaches steady state, and in the steady state the trap exerts a correlated random force $ky(t)$ on the Brownian particle with mean $\langle y(t) \rangle = 0$ and covariance $\langle y(t)y(s) \rangle = \Lambda\tau_0 \exp(-|t-s|/\tau_0)$. In the last chapter, we were interested in investigating the statistical description of the mechanical work W_τ Eq. (40) by the random force on the Brownian particle

$$W_\tau = \frac{1}{k_B T} \int_0^\tau ky(t) \dot{x} dt, \quad (187)$$

with the initial condition (at $\tau = 0$) drawn from the steady state distribution. Some relevant parameters were introduced in Eq. (42), Eq. (43). A thorough investigation was made to compute the full distribution of the mechanical work in the last chapter. We recall few of the results derived in the last chapter for the sake of convenience

$$\begin{aligned} Z_{W_\tau}(\lambda, \mathbf{U}, \tau | \mathbf{U}_0) &= \langle e^{-\lambda W_\tau} \delta[\mathbf{U} - \mathbf{U}(\tau)] \rangle_\eta \\ &\sim \chi(\mathbf{U}_0, \lambda) \psi(\mathbf{U}, \lambda) e^{\tau\mu(\lambda)}, \end{aligned} \quad (188)$$

where we have

$$\mu(\lambda) = \frac{1}{2\tau_c} [1 - \nu(\lambda)], \quad \tau_c = \tau_0(1 + \delta)^{-1}, \quad (189)$$

in which $\nu(\lambda)$ is given by,

$$\nu(\lambda) = \sqrt{1 + 4a\lambda(1-\lambda)}, \quad a = \alpha(1 + \delta)^{-1}, \quad (190)$$

where the parameters are defined in Eq. (42), Eq. (43). The eigenfunctions were given by

$$\Psi(\mathbf{U}, \lambda) = \frac{1}{2\pi\sqrt{\det H_1(\lambda)}} \exp \left[-\frac{1}{2} \mathbf{U}^T \mathbf{L}_1(\lambda) \mathbf{U} \right], \quad (191)$$

$$\chi(\mathbf{U}_0, \lambda) = \exp \left[-\frac{1}{2} \mathbf{U}_0^T \mathbf{L}_2(\lambda) \mathbf{U}_0 \right], \quad (192)$$

where the matrices L_1 , and L_2 are given in Section 2.5. Finally, the moment generating function of the mechanical work W_τ in the steady was found to be

$$Z_W(\lambda, \tau) = \langle e^{-\lambda W_\tau} \rangle = g_W(\lambda) e^{\tau \mu(\lambda)} + \dots, \quad (193)$$

where

$$g_W(\lambda) = \frac{2}{\sqrt{\nu(\lambda) + 1 - 2b_+\lambda} \sqrt{\nu(\lambda) + 1 - 2b_-\lambda}} \times \frac{2\nu(\lambda)}{\sqrt{\nu(\lambda) + 1 + 2b_+\lambda} \sqrt{\nu(\lambda) + 1 + 2b_-\lambda}}, \quad (194)$$

with

$$b_\pm = \frac{\alpha}{2} \left[1 \pm \sqrt{1 + \frac{4}{\theta\delta}} \right]. \quad (195)$$

The first factor in the above expression of $g_W(\lambda)$ is due to the averaging over the initial conditions with respect to the steady-state distribution and the second factor is due to the integrating out of the final degrees of freedom. In this forthcoming section, we investigate the statistical properties of the heat dissipation into the medium Q_τ and the total entropy production ΔS_{tot} in the steady state for the duration $[0, \tau]$.

3.5 CHARACTERIZING THE HEAT DISSIPATION: A SYSTEMATIC STUDY

3.5.1 Definition of the heat dissipation

Following Sekimoto [107, 29], we can define the energy exchange of the system of interest with the surrounding reservoir as the heat dissipation like

$$Q_\tau = -\frac{1}{k_B T} \int_0^\tau k(x - y) \dot{x} dt. \quad (196)$$

We want to compute the distribution function $P(Q_\tau)$ for Q_τ . Before going into details, we notice that Q_τ will be connected to W_τ earlier by the second law of thermodynamics so that

$$\begin{aligned} Q_\tau &= W_\tau + \frac{1}{2D\tau_\gamma} [x^2(0) - x^2(\tau)] \\ &= W_\tau + \frac{1}{2} \mathbf{u}_0^T \mathbf{R}_1 \mathbf{u}_0 - \frac{1}{2} \mathbf{u}_\tau^T \mathbf{R}_1 \mathbf{u}_\tau, \end{aligned} \quad (197)$$

where the new matrix \mathbf{R}_1 has been defined as

$$\mathbf{R}_1 = \frac{1}{D\tau_\gamma} \begin{pmatrix} 1 & 0 \\ 0 & 0 \end{pmatrix}. \quad (198)$$

It is worth to note that Eq. (197) has an identical structure as Eq. (178) when the following quantities are suitably identified: $\Omega_\tau \equiv W_\tau$, $\Theta_\tau \equiv Q_\tau$, and the boundary terms are identified as

$$b_{\text{int}}[\mathbf{u}_0] \equiv \frac{1}{2} \mathbf{u}_0^T \mathbf{R}_1 \mathbf{u}_0, \quad b_{\text{fin}}[\mathbf{u}_\tau] \equiv -\frac{1}{2} \mathbf{u}_\tau^T \mathbf{R}_1 \mathbf{u}_\tau. \quad (199)$$

Therefore, the restricted generating function corresponding to Q_τ is simply given by

$$\begin{aligned} Z_{Q_\tau}(\lambda, \mathbf{u}, \tau | \mathbf{u}_0) &= \langle e^{-\lambda Q_\tau} \delta[\mathbf{u} - \mathbf{u}(\tau)] \rangle_\eta \\ &= Z_{W_\tau}(\lambda, \mathbf{u}, \tau | \mathbf{u}_0) e^{-\frac{\lambda}{2} \mathbf{u}_0^T \mathbf{R}_1 \mathbf{u}_0} e^{\frac{\lambda}{2} \mathbf{u}_\tau^T \mathbf{R}_1 \mathbf{u}_\tau}, \end{aligned} \quad (200)$$

where $Z_{W_\tau}(\lambda, \mathbf{u}, \tau | \mathbf{u}_0)$ is given by Eq. (188). Using the asymptotic expansion of the restricted generating function Eq. (188) of W_τ , we find

$$Z_{Q_\tau}(\lambda, \mathbf{u}, \tau | \mathbf{u}_0) \sim e^{\tau\mu(\lambda)} \psi(\mathbf{u}, \lambda) e^{\frac{\lambda}{2} \mathbf{u}^T \mathbf{R}_1 \mathbf{u}} \chi(\mathbf{u}_0, \lambda) e^{-\frac{\lambda}{2} \mathbf{u}_0^T \mathbf{R}_1 \mathbf{u}_0} \quad (201)$$

where the eigenfunctions and the corresponding eigenvalue remain same Eq. (192), Eq. (86). The moment generating function is obtained by taking average over the initial and final conditions

$$Z_Q(\lambda, \tau) = \langle e^{-\lambda Q_\tau} \rangle = g_Q(\lambda) e^{\tau\mu(\lambda)} + \dots, \quad (202)$$

where

$$\begin{aligned}
g_Q(\lambda) &= \det[\mathbf{H}_1(\lambda)\mathbf{L}_1(\lambda) - \lambda\mathbf{H}_1(\lambda)\mathbf{R}_1]^{-1/2} \\
&\quad \times \det[1 + \mathbf{H}_1(0)\mathbf{L}_2(\lambda) + \lambda\mathbf{H}_1(0)\mathbf{R}_1]^{-1/2} \\
&= \frac{1}{\nu(\lambda) + 1} \frac{2}{\sqrt{\nu(\lambda) + 1 + 2\lambda}} \frac{2\nu(\lambda)}{\sqrt{\nu(\lambda) + 1 - 2\lambda}}. \tag{203}
\end{aligned}$$

Therefore, probability distribution can be obtained by taking the inverse Fourier transform of $Z_Q(\lambda, \tau)$ Eq. (202).

3.5.2 Probability distribution

We can obtain the probability distribution function for the heat dissipation by taking the inverse Fourier transform of $Z_{Q_\tau}(\lambda, \tau)$ in Eq. (202)

$$\begin{aligned}
P(Q_\tau = q\tau) &= \frac{1}{2\pi i} \int_{-i\infty}^{i\infty} Z_Q(\lambda, \tau) e^{\lambda q\tau} d\lambda \\
&\approx \frac{1}{2\pi i} \int_{-i\infty}^{i\infty} g_Q(\lambda) e^{\tau f_q(\lambda)} d\lambda \tag{204}
\end{aligned}$$

where

$$f_q(\lambda) = \frac{1}{2}[1 - \nu(\lambda)] + \lambda q \tag{205}$$

where $g_Q(\lambda)$ is given by Eq. (203) and also we have set $\tau_c = 1$ for convenience. But an important point to notice that $g_Q(\lambda)$ contains singularities in the real λ -line similar to the one discussed in Sec. 2.7.

Now, if $g_Q(\lambda)$ is analytic for $\lambda \in (0, \lambda^*)$, one can deform the contour along the path of the steepest descent through the saddle-point, and obtain $P(Q_\tau)$ using the usual saddle-point approximation method. However, if $g_Q(\lambda)$ has any singularities, then the straightforward saddle-point method cannot be used, and one would require more sophisticated methods to obtain the asymptotic form of $P(Q_\tau)$. Therefore, it is essential to analyze $g_Q(\lambda)$ for possible singularities. We examine the terms under the square roots in the denominator of $g_Q(\lambda)$ in Eq. (203) in Section 3.5.2.1.

3.5.2.1 *singularities in $g_Q(\lambda)$*

As discussed in Sec. 2.7, we follow up the similar structure to identify the singularities in $g_Q(\lambda)$. Using Eq. (114) we recall that $v(\lambda_{\pm}) = 0$ and $v(\lambda) > 0$ (is a semicircle) for $\lambda \in (\lambda_-, \lambda_+)$. From Eq. (203), we find that $g_Q(\lambda)$ contains two functions, which are of our particular interests that can give rise to the singularities

$$\begin{aligned} f_1(\lambda) &= v(\lambda) + 1 + 2\lambda \\ f_2(\lambda) &= v(\lambda) + 1 - 2\lambda. \end{aligned} \quad (206)$$

Now, if $f_1(\lambda), f_2(\lambda)$ have opposite signs at the two end points λ_{\pm} , then the functions $f_1(\lambda), f_2(\lambda)$ must have crossed zero at some intermediate λ and those are the so-called singularities. It is easy to see that

$$\begin{aligned} f_1(\lambda_+) &= 2 + \sqrt{1 + \frac{(1 + \delta)^2}{\theta\delta^2}} > 0, \\ f_1(\lambda_-) &= 2 - \sqrt{1 + \frac{(1 + \delta)^2}{\theta\delta^2}}, \end{aligned} \quad (207)$$

where $f_1(\lambda_-)$ can be both positive or negative in the phase space spanned by (θ, δ) . So, the singularities lie on that region of the phase space where $f_1(\lambda_-)$ changes sign or precisely, it becomes negative. This has been depicted in Fig. 12. This term gives rise to one singularity given by

$$\lambda_a = \frac{\alpha - 1}{\alpha + 1} = \frac{\theta\delta^2 - (1 + \delta)^2}{\theta\delta^2 + (1 + \delta)^2}. \quad (208)$$

Now, we investigate the second term $f_2(\lambda)$ which has the following properties

$$\begin{aligned} f_2(\lambda_+) &= -\sqrt{1 + \frac{(1 + \delta)^2}{\theta\delta^2}} < 0, \\ f_2(\lambda_-) &= \sqrt{1 + \frac{(1 + \delta)^2}{\theta\delta^2}} > 0, \end{aligned} \quad (209)$$

which means that the function $f_2(\lambda)$ has always two opposite signs in the whole phase space meaning that the singularities emerging in this case lie in the whole phase space and not constrained to any condition. In this case, we find the singularity to be

$$\lambda_b = 1, \quad (210)$$

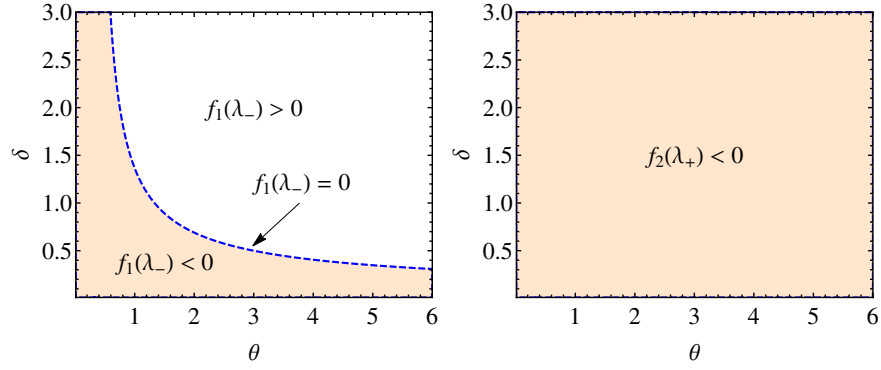


Figure 12: This plot summarizes the analytic properties of $g_Q(\lambda)$. The left panel depicts the properties of $f_1(\lambda)$ while the right one is for $f_2(\lambda)$. **Left panel:** In the shaded region of the (θ, δ) plane, $f_1(\lambda)$ possesses a singularity λ_a , where $f_1(\lambda_-) < 0$. On the other hand, in the unshaded region $f_1(\lambda)$ does not have any singularities, where $f_1(\lambda_-) > 0$. These two domains are separated by the boundary given by the equation $f_1(\lambda_-) = 0$. **Right panel:** $f_2(\lambda)$ possesses a singularity λ_b in the entire phase space spanned by (θ, δ) -plane.

which is independent of θ, δ and that means the singularity λ_b will be always present in $g_Q(\lambda)$ irrespective of any values of θ, δ .

To summarize this part, we note the following points:

- We have found that $g_Q(\lambda)$ indeed contains branch point singularities in the (θ, δ) -plane. The singularity given by λ_b will be always present for any values of θ, δ .
- The other singularity λ_a is parameter dependent and it will appear according to the condition in Eq. (207) and as given by Fig. 12. First we will deal with the case, when $f_1(\lambda)$ is non singular and thus $g_Q(\lambda)$ contains only one singularity. We will deal with the two singularities later.

3.5.2.2 *case of one singularity*

In this section, we will handle the case where $g_Q(\lambda)$ has only one singularity present namely λ_b . This case is identical to the one described in Sec. 2.8.2. Following Sec. 2.8.2, we can write $g_Q(\lambda)$ as

$$g_Q(\lambda) = \frac{g_b(\lambda)}{\sqrt{\lambda_b - \lambda}} \tag{211}$$

where $g_b(\lambda)$ is the analytical factor of $g_Q(\lambda)$

$$g_b(\lambda) = \frac{1}{\sqrt{a+1}} \frac{1}{\sqrt{\lambda}} \frac{\sqrt{\nu(\lambda) - 1 + 2\lambda}}{\sqrt{\nu(\lambda) + 1 + 2\lambda}} \frac{2\nu(\lambda)}{\nu(\lambda) + 1} \tag{212}$$

Since $\lambda_b > 0$, it is fixed between the origin and λ_+ . In the absence of a singularity, one can do this integral using the standard steepest descent method for large τ , where the contour of integration can be deformed into the steepest descent path through the saddle point given by $f'_q(\lambda^*) = 0$ which results in

$$\lambda^*(q) = \frac{1}{2} \left[1 - \frac{q}{\sqrt{q^2 + a}} \sqrt{1 + \frac{1}{a}} \right]. \tag{213}$$

However, in this case, we know that there is a branch point present in the real λ -line and therefore, the contour has to be deformed without touching the branch point. The saddle-point $\lambda^*(q)$ moves unidirectionally along the real- λ line from λ_- to λ_+ as one decreases q from $+\infty$ to $-\infty$ in a monotonic manner. However, as one decreases q , the saddle-point hits the branch-point, $\lambda^*(q_b^*) = \lambda_b$, at some specific value $q = q_b^*$ given by

$$q_b^* = -a. \tag{214}$$

Incorporating this fact, we now present the main results.

- When $q > q_b^*$, the PDF is given by

$$P(Q_\tau = q\tau) \approx \frac{g_Q(\lambda^*) e^{\tau h_s(q)}}{\sqrt{2\pi\tau f''_q(\lambda^*)}} R_1 \left(\sqrt{\tau [h_b(q) - h_s(q)]} \right), \tag{215}$$

where $R_1(z)$ is given by Eq. (121) and the large deviation functions $h_s(q)$, $h_b(q)$ are given by

$$\begin{aligned} h_s(q) &:= f_q(\lambda^*) = \frac{1}{2} \left[1 + q - \sqrt{q^2 + a} \sqrt{1 + \frac{1}{a}} \right], \\ h_b(q) &:= f_q(\lambda_b) = q, \end{aligned} \quad (216)$$

since $v(\lambda_b) = 1$. We also find that

$$f''_q(\lambda^*) = \frac{2(q^2 + a)^{3/2}}{\sqrt{a(1+a)}}, \quad (217)$$

and the prefactor $g_Q(\lambda^*)$ can be calculated by putting Eq. (213) in Eq. (203).

- When $q > q_b^*$, the PDF is given by

$$P(Q_\tau = q\tau) \approx P_B(q, \tau) + P_S(q, \tau), \quad (218)$$

where the branch point contribution can be obtained following Appendix A.1.2.1

$$P_B(q, \tau) \approx \frac{\tilde{g}(\lambda_b) e^{\tau h_b(q)}}{\sqrt{\pi\tau} |f'_q(\lambda_b)|} R_3 \left(\sqrt{\tau [h_b(q) - h_s(q)]} \right), \quad (219)$$

where $R_3(z)$ is given by Eq. (125) and Eq. (407). The nonsingular prefactor $\tilde{g}(\lambda_b)$ is simply given by

$$\tilde{g}(\lambda_b) = \lim_{\lambda \rightarrow \lambda_b} |(\lambda - \lambda_b)^{1/2} g_Q(\lambda)|. \quad (220)$$

Similarly, following Appendix A.1.2.2 the contribution coming from the saddle point is given by

$$P_S(q, \tau) \approx \frac{|g_Q(\lambda^*)| e^{\tau h_s(q)}}{\sqrt{2\pi\tau} f''_q(\lambda^*)} R_4 \left(\sqrt{\tau [h_b(q) - h_s(q)]} \right), \quad (221)$$

where $R_4(z)$ is given by Eq. (373) and $f''_q(\lambda^*)$ is given by Eq. (217).

3.5.2.3 case of two singularities

In this subsection, we consider the fact that there are two singularities in the real λ -line. It is however important to note that the singularity

λ_a can be either positive or negative. We first consider the case when λ_a is positive. Moreover, we shall note that $\lambda_a < \lambda_b$ such that the ordering can be made in the following way: $\lambda_- < 0 < \lambda_a < \lambda_b < \lambda_+$. In this case, we can rewrite $g_Q(\lambda)$ in the following way

$$g_Q(\lambda) = \frac{g_2(\lambda)}{\sqrt{\lambda_a - \lambda} \sqrt{\lambda_b - \lambda}}, \quad (222)$$

where $g_2(\lambda)$ is given by

$$g_2(\lambda) = \frac{\sqrt{v(\lambda) - 1 + 2\lambda} \sqrt{v(\lambda) - 1 - 2\lambda}}{(\alpha + 1)\lambda[v(\lambda) + 1]}. \quad (223)$$

The q -value corresponding to the branch point λ_a is given by $\lambda^*(q_a^*) = \lambda_a$, from which we obtain

$$q_a^* = \frac{(1 - 2\lambda_a)\sqrt{\alpha}}{\sqrt{(1 + 1/\alpha) - (1 - 2\lambda_a)^2}} \quad (224)$$

We now proceed to evaluate the integrals to obtain the heat PDF following the method developed in Sec. 2.8.2 and in Sec. 2.8.3.

- When $q > q_a^*$, the PDF is given by

$$P(Q_\tau = q\tau) \approx \frac{g_Q(\lambda^*) e^{\tau h_s(q)}}{\sqrt{2\pi\tau f_q''(\lambda^*)}} R_1 \left(\sqrt{\tau[h_a(q) - h_s(q)]} \right). \quad (225)$$

- When $q_a^* > q > q_b^*$, the heat PDF has contributions both from the branch point and the saddle point similar to Eq. (218). The branch point contribution can be written as

$$P_B(q, \tau) \approx \frac{\tilde{g}(\lambda_a) e^{\tau h_a(q)}}{\sqrt{\pi\tau |f_q'(\lambda_a)|}} R_7 \left(\sqrt{\tau[h_a(q) - h_s(q)]}, \sqrt{\tau[h_b(q) - h_s(q)]} \right), \quad (226)$$

where $R_7(z_1, z_2)$ is given by Eq. (135) and the large deviation function corresponding to λ_a is given by

$$h_a(q) := f_q(\lambda_a). \quad (227)$$

The saddle point contribution will be

$$P_S(q, \tau) \approx \frac{|g_Q(\lambda^*)| e^{\tau h_s(q)}}{\sqrt{2\pi\tau f_q''(\lambda^*)}} R_8 \left(\sqrt{\tau[h_a(q) - h_s(q)]}, \sqrt{\tau[h_b(q) - h_s(q)]} \right), \quad (228)$$

where $R'_8(z_1, z_2)$ is given by

$$R'_8(z_1, z_2) = \sqrt{\frac{z_1 z_2}{\pi}} \int_0^\infty du e^{-u^2} \left[\frac{1}{\sqrt{z_1 + iu}\sqrt{z_2 - iu}} - \frac{1}{\sqrt{z_1 - iu}\sqrt{z_2 + iu}} \right] i. \quad (229)$$

- When $q_b^* > q$, the heat PDF is obtained as a cumulative of both the branch point and the saddle point; the branch point contribution is given by

$$P_B(q, \tau) \approx \frac{\tilde{g}(\lambda_a) e^{\tau h_a(q)}}{\sqrt{\pi\tau} |f'_q(\lambda_a)|} R_9 \left(\sqrt{\tau[h_a(q) - h_s(q)]}, \sqrt{\tau[h_b(q) - h_s(q)]} \right), \quad (230)$$

where $R_9(z_1, z_2)$ is given by Eq. (138). The saddle contribution is

$$P_S(q, \tau) \approx \frac{|g_Q(\lambda^*)| e^{\tau h_s(q)}}{\sqrt{2\pi\tau} f''_q(\lambda^*)} R'_{10} \left(\sqrt{\tau[h_a(q) - h_s(q)]}, \sqrt{\tau[h_b(q) - h_s(q)]} \right), \quad (231)$$

where $R'_{10}(z_1, z_2)$ is given by

$$R'_{10}(z_1, z_2) = \sqrt{\frac{z_1 z_2}{\pi}} \int_{-\infty}^\infty du \frac{e^{-u^2}}{\sqrt{z_1 + iu}\sqrt{z_2 + iu}} \quad (232)$$

Next, we consider the case when λ_a is *negative* and it lies between λ_- and the origin. The ordering goes as: $\lambda_- < \lambda_a < 0 < \lambda_b < \lambda_+$. In this case, we rewrite $g_Q(\lambda)$ in the following way

$$g_Q(\lambda) = \frac{g_2(\lambda)}{\sqrt{\lambda - \lambda_a}\sqrt{\lambda_b - \lambda}}. \quad (233)$$

Following the same prescription, we summarize the results for the heat PDF.

- When $q > q_a^*$, the heat PDF constitutes of both the branch point and the saddle point. The branch point contribution is the following

$$P_B(q, \tau) \approx \frac{\tilde{g}(\lambda_a) e^{\tau h_a(q)}}{\sqrt{\pi\tau} |f'_q(\lambda_a)|} R_3 \left(\sqrt{\tau[h_a(q) - h_s(q)]} \right), \quad (234)$$

and the saddle contribution can be found as

$$P_S(q, \tau) \approx \frac{|g_Q(\lambda^*)| e^{\tau h_s(q)}}{\sqrt{2\pi\tau f_q''(\lambda^*)}} R'_5 \left(\sqrt{\tau[h_a(q) - h_s(q)]}, \sqrt{\tau[h_b(q) - h_s(q)]} \right), \quad (235)$$

where $R'_5(z_1, z_2)$ is given by

$$R'_5(z_1, z_2) = \sqrt{\frac{z_1 z_2}{\pi}} \int_0^\infty du e^{-u^2} \left[\frac{1}{\sqrt{z_1 + iu}\sqrt{z_2 + iu}} - \frac{1}{\sqrt{z_1 - iu}\sqrt{z_2 - iu}} \right] i. \quad (236)$$

- When $q_a^* > q > q_b^*$, the heat PDF has a contribution only from the saddle point:

$$P_S(q, \tau) \approx \frac{g_Q(\lambda^*) e^{\tau h_s(q)}}{\sqrt{2\pi\tau f_q''(\lambda^*)}} R'_6 \left(\sqrt{\tau[h_a(q) - h_s(q)]}, \sqrt{\tau[h_b(q) - h_s(q)]} \right), \quad (237)$$

where $R'_6(z_1, z_2)$ is given by

$$R'_6(z_1, z_2) = \sqrt{\frac{z_1 z_2}{\pi}} \int_{-\infty}^\infty du \frac{e^{-u^2}}{\sqrt{z_1 + iu}\sqrt{z_2 - iu}}. \quad (238)$$

- When $q_b^* > q$, the heat PDF again gets contributions from the branch point and the saddle point as well

$$P_B(q, \tau) \approx \frac{\tilde{g}(\lambda_b) e^{\tau h_b(q)}}{\sqrt{\pi\tau |f'_q(\lambda_b)|}} R_3 \left(\sqrt{\tau[h_b(q) - h_s(q)]} \right), \quad (239)$$

where $R_3(z)$ is given by Eq. (125) and Eq. (407). The saddle contribution has the form

$$P_S(q, \tau) \approx \frac{|g_Q(\lambda^*)| e^{\tau h_s(q)}}{\sqrt{2\pi\tau f_q''(\lambda^*)}} R'_5 \left(\sqrt{\tau[h_a(q) - h_s(q)]}, \sqrt{\tau[h_b(q) - h_s(q)]} \right), \quad (240)$$

where $R'_5(z_1, z_2)$ is given by Eq. (236).

3.5.3 Symmetry properties and the Fluctuation theorem

It was already observed in recent literatures that the heat PDF generically does not satisfy the SSFT [43, 44, 45, 108, 109, 110]. Our result

will turn out to be very consistent with this fact. From the detailed computation of the PDF of the heat dissipation, we note that the heat PDF has contributions both from the saddle point and the corresponding singularities. We have found the following

$$\begin{aligned} h_s(q) - h_s(-q) &= q \\ h_b(q) - h_b(-q) &= 2q \\ h_a(q) - h_a(-q) &= 2\lambda_a q \end{aligned} \tag{241}$$

It is therefore clear from this discussion that if the heat PDF takes support from the singular points, it will fail to satisfy the SSFT while in the absence of singular points, the contributions will come solely from the saddle point and in that case, the heat PDF will satisfy the SSFT. A tentative argument on the origin of the singularities has been discussed in the last section. It is quite often found that the systems with a bounded configuration space (such as energy or particle exchanging lattice exclusion models, multilevel systems with finite energy states) usually do not face such criticality [101, 102]. The finiteness of the phase space delimits the wave functions faster than exponentials and which results in the convergence of the integrals over the initial and the final configurations. This always results in an analytic $g(\lambda)$ and thus SSFT is always satisfied [101, 102].

3.6 CHARACTERIZING THE TOTAL ENTROPY PRODUCTION: A SYSTEMATIC STUDY

3.6.1 Definition of the total entropy production

We define the total entropy production as a cumulative of the entropy increase in the *medium* due to the heat dissipation plus the change in entropy of the *system* along with the entropy production in the *driving source*. To elaborate, we have considered the trapped Brownian particle as the *system*, the ambient surrounding kept at fixed temper-

ature T works as the *medium*. The motion of the trap (modelled as the Ornstein-Uhlenbeck process) is stochastic and this mechanism is the *driving source*. Therefore, the total entropy production of the universe is given by

$$\Delta S_{\text{tot}} = \Delta S_{\text{med}} + \Delta S_{\text{sys}} + \Delta S_{\text{sd}}^{\text{tot}}, \quad (242)$$

where change in the *medium* entropy is given by

$$\Delta S_{\text{med}} = \beta Q_{\tau} \quad (243)$$

where Q_{τ} is given by Eq. (196). Change in *system* entropy in the steady state is given by

$$\begin{aligned} \Delta S_{\text{sys}} &= -\ln p_{\text{ss}}[x_{\tau}|y_{\tau}] + \ln p_{\text{ss}}[x_0|y_0] \\ &= \ln \frac{p_{\text{ss}}[x_0|y_0]}{p_{\text{ss}}[x_{\tau}|y_{\tau}]} \\ &= \ln \frac{P_{\text{ss}}[x_0, y_0]}{p_{\text{eq}}[y_0]} \frac{p_{\text{eq}}[y_{\tau}]}{P_{\text{ss}}[x_{\tau}, y_{\tau}]} \\ &= \ln \frac{P_{\text{ss}}[U_0]}{P_{\text{ss}}[U_{\tau}]} + \ln \frac{p_{\text{eq}}[y_{\tau}]}{p_{\text{eq}}[y_0]}, \end{aligned} \quad (244)$$

where $p_{\text{ss}}[x_{\tau}|y_{\tau}]$ is the conditional steady state configuration of the *system* (denoted by x_{τ}) trajectories for a given realization of the *driving source* (denoted by y_{τ}). Each trajectory of the *driving source* complies with the initial $p_{\text{eq}}[y_0]$ and the final equilibrium distributions $p_{\text{eq}}[y_{\tau}]$.

This definition of *system* entropy, introduced by Seifert, is in unison with that of Shannon. The total entropy production due to the stochastic driving (sd) source $\Delta S_{\text{sd}}^{\text{tot}}$ is considered to be zero as it is a reversible source and a Gaussian process thus effectively relaxing to equilibrium,

$$\begin{aligned} \Delta S_{\text{sd}}^{\text{tot}} &= \Delta S_{\text{sd}}^{\text{med}} + \Delta S_{\text{sd}}^{\text{sys}} \\ &= \beta \Delta q_{\text{sd}} + \ln \frac{p_{\text{eq}}(y_0)}{p_{\text{eq}}(y_{\tau})} \\ &= \beta \Delta E_{\text{sd}} - \beta \Delta E_{\text{sd}}, \quad \text{since } p_{\text{eq}}(y) \propto e^{-\frac{y^2}{2\lambda\tau_0}} \\ &= 0. \end{aligned} \quad (245)$$

No additional perturbation is acting on the *driving source* (with internal energy ΔE_{sd}), which implies that the driving source will reach an

effective equilibrium through dissipation such that $\Delta q_{sd} = \Delta E_{sd}$, as $t > \tau_0$, where τ_0 is its own relaxation time.

Combining Eq. (243), Eq. (244) and Eq. (245), we obtain

$$\Delta S_{\text{tot}} = \beta Q_\tau - \frac{1}{2} \mathbf{u}_0^\top [\mathbf{H}_1^{-1}(0) - \mathbf{R}_2] \mathbf{u}_0 + \frac{1}{2} \mathbf{u}_\tau^\top [\mathbf{H}_1^{-1}(0) - \mathbf{R}_2] \mathbf{u}_\tau, \quad (246)$$

where the new matrix \mathbf{R}_2 has been defined as

$$\mathbf{R}_2 = \frac{1}{D\theta\tau_0} \begin{pmatrix} 0 & 0 \\ 0 & 1 \end{pmatrix}. \quad (247)$$

It is worth to note that Eq. (246) also follows an identical structure as Eq. (178) and as Q_τ when the following quantities are suitably identified: $\Omega_\tau \equiv Q_\tau$, $\Theta_\tau \equiv \Delta S_{\text{tot}}$, and the boundary terms are identified as

$$b_{\text{int}}[\mathbf{u}_0] \equiv \frac{1}{2} \mathbf{u}_0^\top [\mathbf{R}_2 - \mathbf{H}_1^{-1}(0)] \mathbf{u}_0, \quad b_{\text{fin}}[\mathbf{u}_\tau] \equiv -\frac{1}{2} \mathbf{u}_\tau^\top [\mathbf{R}_2 - \mathbf{H}_1^{-1}(0)] \mathbf{u}_\tau. \quad (248)$$

Therefore, the restricted generating function corresponding to ΔS_{tot} is simply given by

$$\begin{aligned} Z_{\Delta S_{\text{tot}}}(\lambda, \mathbf{u}, \tau | \mathbf{u}_0) &= \langle e^{-\lambda \Delta S_{\text{tot}}} \delta[\mathbf{u} - \mathbf{u}(\tau)] \rangle_\eta \\ &= Z_{Q_\tau}(\lambda, \mathbf{u}, \tau | \mathbf{u}_0) \\ &\quad \times e^{-\frac{\lambda}{2} \mathbf{u}_0^\top [\mathbf{R}_2 - \mathbf{H}_1^{-1}(0)] \mathbf{u}_0} e^{\frac{\lambda}{2} \mathbf{u}_\tau^\top [\mathbf{R}_2 - \mathbf{H}_1^{-1}(0)] \mathbf{u}_\tau}, \end{aligned} \quad (249)$$

where $Z_{Q_\tau}(\lambda, \mathbf{u}, \tau | \mathbf{u}_0)$ is given by Eq. (201). Using the asymptotic expansion of the restricted generating function Eq. (201) of Q_τ , we find

$$\begin{aligned} Z_{\Delta S_{\text{tot}}}(\lambda, \mathbf{u}, \tau | \mathbf{u}_0) &\sim e^{\tau\mu(\lambda)} \psi(\mathbf{u}, \lambda) e^{\frac{\lambda}{2} \mathbf{u}^\top [\mathbf{R}_1 + \mathbf{R}_2 - \mathbf{H}_1^{-1}(0)] \mathbf{u}} \\ &\quad \times \chi(\mathbf{u}_0, \lambda) e^{-\frac{\lambda}{2} \mathbf{u}_0^\top [\mathbf{R}_1 + \mathbf{R}_2 - \mathbf{H}_1^{-1}(0)] \mathbf{u}_0} \end{aligned} \quad (250)$$

where the eigenfunctions and the corresponding eigenvalue remain same as Eq. (192), Eq. (86) respectively. We are now ready to obtain

the moment generating function by taking average over the initial and final conditions

$$Z_{\Delta S_{\text{tot}}}(\lambda, \tau) = \langle e^{-\lambda \Delta S_{\text{tot}}} \rangle = g_{\Delta S_{\text{tot}}}(\lambda) e^{\tau \mu(\lambda)} + \dots, \quad (251)$$

where the prefactor is

$$\begin{aligned} g_{\Delta S_{\text{tot}}}(\lambda) &= \det[H_1(\lambda)L_1(\lambda) - \lambda H_1(\lambda)R_1 - \lambda H_1(\lambda)R_2 + \lambda \nu(\lambda)^{-1}]^{-1/2} \\ &\quad \times \det[1 + H_1(0)L_2(\lambda) + \lambda H_1(0)R_1 + \lambda H_1(0)R_2 - \lambda]^{-1/2} \\ &= \frac{4\nu(\lambda)}{[\nu(\lambda) + 1]^2}. \end{aligned} \quad (252)$$

3.6.2 Probability distribution

We are now ready to compute the probability distribution function for the total entropy production. The PDF can be obtained by taking the inverse Fourier transform of $Z_{\Delta S_{\text{tot}}}(\lambda, \tau)$ in Eq. (251)

$$\begin{aligned} P(\Delta S_{\text{tot}} = s\tau) &= \frac{1}{2\pi i} \int_{-i\infty}^{i\infty} Z_{\Delta S_{\text{tot}}}(\lambda, \tau) e^{\lambda s\tau} d\lambda \\ &\approx \frac{1}{2\pi i} \int_{-i\infty}^{i\infty} g_{\Delta S_{\text{tot}}}(\lambda) e^{\tau f_s(\lambda)} d\lambda \end{aligned} \quad (253)$$

where

$$f_s(\lambda) = \frac{1}{2}[1 - \nu(\lambda)] + \lambda s \quad (254)$$

and we have set $\tau_c = 1$ for convenience. The large τ form of the PDF can be obtained using the method of steepest descent. Before proceeding further, we notice that $g_{\Delta S_{\text{tot}}}(\lambda)$ is analytic in the interval $\lambda \in (\lambda_-, \lambda_+)$ so that we can deform the contour along the path of steepest descent through the saddle point given by Eq. (112) as obtained from the solution of the condition $f'_s(\lambda^*) = 0$

$$\lambda^*(s) = \frac{1}{2} \left[1 - \frac{s}{\sqrt{s^2 + a}} \sqrt{1 + \frac{1}{a}} \right]. \quad (255)$$

Using the saddle point approximation, the asymptotic form of the PDF can be written as

$$P(\Delta S_{\text{tot}} = s\tau) \approx \frac{g_{\Delta S_{\text{tot}}}(\lambda^*) e^{\tau h(s)}}{\sqrt{2\pi\tau f''_s(\lambda^*)}}, \quad (256)$$

where the large deviation function corresponding to the total entropy production is given by

$$h(s) := f_s(\lambda^*) = \frac{1}{2} \left[1 + s - \sqrt{s^2 + a} \sqrt{1 + \frac{1}{a}} \right]. \quad (257)$$

We also find that

$$f_s''(\lambda^*) = \frac{2(s^2 + a)^{3/2}}{\sqrt{a(1 + a)}}, \quad (258)$$

and the prefactor to be

$$g_{\Delta S_{\text{tot}}}(\lambda^*) = \frac{4\sqrt{a(1 + a)}\sqrt{s^2 + a}}{[\sqrt{a(1 + a)} + \sqrt{s^2 + a}]^2}. \quad (259)$$

3.6.3 Symmetry properties and the Fluctuation theorem

We have shown that the PDF of the total entropy can be expressed completely in terms of the large deviation function as obtained in Eq. (256) with Eq. (257). As mentioned in Sec. 1.4.3, it is well understood that an observable is said to satisfy the steady state fluctuation theorem if

$$\lim_{\tau \rightarrow \infty} \frac{1}{\tau} \ln \left[\frac{P(\Omega_\tau = \omega\tau)}{P(\Omega_\tau = -\omega\tau)} \right] = \omega \quad (260)$$

as also referred in Eq. (151). This translates to the large deviation function in the following form

$$h(\omega) - h(-\omega) = \omega. \quad (261)$$

Within the current context, using Eq. (256) and Eq. (257), we infer that

$$h(s) - h(-s) = s, \quad (262)$$

which means that the total entropy production if properly defined as that of the system plus its surroundings will satisfy the SSFT at all times. This differs from the actual version of the steady state fluctuation theorem as derived by Evans-Searles in dynamical systems and Gallavotti-Cohen for *Ansov* systems and later extended to stochastic dynamics by Kurchan and Lebowitz-Spohn. In these early works,

only the *entropy of the medium* was considered while the *system entropy* was neglected since at large times, the former dominates (for it is extensive) over the later one. However, incorporating the *system entropy* part, Crooks, Maes, Seifert and others have shown that the *total entropy production* satisfies the FT for any finite length of time, which is indeed a stronger statement than the earlier one [57, 59, 64].

Though it was indeed shown before that the total entropy production in such kind of driven and dissipative systems should always follow the SSFT, its validation in stochastically driven system was not anticipated till recently. We extended the study to such stochastically driven systems and found that indeed the fluctuation theorem for total entropy production remains intact to any generic systems.

3.7 A SIMPLE DESCRIPTION OF THE HEAT AND THE TOTAL ENTROPY FLUCTUATIONS

In this section, we describe a simple probabilistic model that mimics the case of heat and total entropy production fluctuations for the linear Langevin stochastic models as described in the framework of an example in the preceding sections [105]. Let us recall Eq. (160) in a general framework in the following way

$$\Omega_n = \Theta_n - \Delta U_n , \quad (263)$$

where let us say that Θ_n is like the total entropy production which satisfies the SSFT while Ω_n is the heat part which does not satisfy SSFT in general but in a restricted phase space. Let us consider all the boundary terms (difference in kinetic energy or the quadratic potential energy) cumulatively as ΔU_n and the suffix index 'n' refers to the random variable index. Here I simply present a probabilistic description to depict these features. Let us consider $\Theta_n = n\theta$ has the following form

$$Z_{\Theta}(\lambda, n) = \langle e^{-\lambda\Theta} \rangle = \langle e^{-\lambda n\theta} \rangle \sim g_{\theta}(\lambda) e^{n\mu_{\theta}(\lambda)} \quad (264)$$

where $g_\theta(\lambda)$ is the prefactor. Let us assume that $g_\theta(\lambda)$ is analytic and the PDF for Θ satisfies the symmetry of the FT. Consider the energy term defined in terms of random variables in the following way

$$\Delta U_n = X_n^2 - X_1^2. \quad (265)$$

Here we shall assume that the $\{X_i\}$'s are *independent* and *identically distributed* (IID) random variables. For simplicity, we choose them from a Gaussian distribution with unit mean and unit variance

$$P(X = x) = \frac{1}{\sqrt{2\pi}} e^{-\frac{(x-1)^2}{2}}. \quad (266)$$

It is important to note that in real Langevin models, entropy production or the heat dissipation is not a simple sum or an integrated function of IID random variables but they are rather Markovian (exponentially correlated) or non-Markovian (long range correlation) random variables. However, these differences will turn out to be irrelevant to our discussions and inclusion of correlated random variables in this context are not going to differ the basic results. In general, we are interested in computing the probability distribution of the *mean* or the scaled observables such as $\omega_n = \Omega_n/n$, or $\theta_n = \Theta_n/n$, so that

$$\begin{aligned} \omega_n &= \theta_n - \frac{\Delta U_n}{n} \\ &= \theta_n - \frac{X_n^2}{n} + \frac{X_1^2}{n}. \end{aligned} \quad (267)$$

As described in the earlier chapters, we define the moment generating function (MGF) $Z(\lambda)$ and the cumulant generating function (CGF) $\mu(\lambda)$ corresponding to these observables in the following way

$$\begin{aligned} Z(\lambda) &= \langle e^{-\lambda n \omega_n} \rangle \sim g(\lambda) e^{n\mu(\lambda)}, \\ \mu(\lambda) &= \lim_{n \rightarrow \infty} \frac{1}{n} \ln \langle e^{-\lambda n \omega_n} \rangle. \end{aligned} \quad (268)$$

This allows us to represent the PDF of these observables $P(\omega)$ in terms of the large deviation functions (LDF) $h(\omega)$ as prescribed in the following

$$\begin{aligned} P(\omega_n = \omega) &\approx e^{n h(\omega)}, \\ h(\omega) &= \sup_{\lambda \in \mathcal{R}} [\mu(\lambda) + \lambda \omega]. \end{aligned} \quad (269)$$

In the current context, we then write the moment generating function as

$$\begin{aligned}\langle e^{-\lambda n \omega_n} \rangle &= \langle e^{-\lambda n [\theta - \frac{X_n^2}{n} + \frac{X_1^2}{n}]} \rangle \\ &= \langle e^{-\lambda n \theta} \rangle \langle e^{\lambda X_n^2} \rangle \langle e^{-\lambda X_1^2} \rangle \\ &= g_\theta(\lambda) e^{n \mu_\theta(\lambda)} \langle e^{\lambda X^2} \rangle \langle e^{-\lambda X^2} \rangle ,\end{aligned}\quad (270)$$

since X 's are IID variables and the indices are dropped since all the random variables are identically distributed. Using the definition in Eq. (268), we write the corresponding CGF as

$$\begin{aligned}\mu(\lambda) &= \mu_\theta(\lambda) + \lim_{n \rightarrow \infty} \frac{1}{n} \left[\ln \langle e^{\lambda X^2} \rangle + \ln \langle e^{-\lambda X^2} \rangle \right] \\ &= \mu_\theta(\lambda) + \lim_{n \rightarrow \infty} \frac{1}{n} \left[\mu_X(-\lambda) + \mu_X(\lambda) \right] ,\end{aligned}\quad (271)$$

where we have defined the CGFs respectively

$$\mu_X(\lambda) = \ln \langle e^{-\lambda X^2} \rangle , \mu_X(-\lambda) = \ln \langle e^{\lambda X^2} \rangle . \quad (272)$$

A simple calculation yields the following results for the CGFs

$$\mu_X(\lambda) = \begin{cases} -\frac{\lambda}{1+2\lambda} - \frac{1}{2} \ln(1+2\lambda) & \text{if } \lambda > -\frac{1}{2} \\ \infty & \text{otherwise} \end{cases} \quad (273)$$

and

$$\mu_X(-\lambda) = \begin{cases} \frac{\lambda}{1-2\lambda} - \frac{1}{2} \ln(1-2\lambda) & \text{if } \lambda < \frac{1}{2} \\ \infty & \text{otherwise .} \end{cases} \quad (274)$$

Therefore, we can infer that

$$\mu_X(\lambda) + \mu_X(-\lambda) = \begin{cases} \text{finite} & \text{if } \lambda \in (-\frac{1}{2}, \frac{1}{2}) \\ \infty & \text{otherwise .} \end{cases} \quad (275)$$

Since, within this range, the above function stays finite and also does not depend on n , the following condition holds

$$\lim_{n \rightarrow \infty} \frac{1}{n} \left[\mu_X(\lambda) + \mu_X(-\lambda) \right] = 0 . \quad (276)$$

This allows us to write the CGF corresponding to ω_n as in Eq. (271)

$$\mu(\lambda) = \begin{cases} \mu_\theta(\lambda) & \text{if } \lambda \in (-\frac{1}{2}, \frac{1}{2}) \\ \infty & \text{otherwise .} \end{cases} \quad (277)$$

We now discuss the above result in details.

- CGF $\mu(\lambda)$ corresponding to ω_n gets most of the contribution from $\mu_\theta(\lambda)$ corresponding to the observable θ_n within certain allowed domain of λ . This means that within this domain, the boundary terms consisting of $\{X\}$'s do not play any role and they cancel as we take the limit $n \rightarrow \infty$.
- In order to set up this rule, we note that one does not need an exact expression for $\mu_\chi(\lambda)$ which is a salient feature of this problem. This is because we need to know only where $\mu_\chi(\lambda)$ is finite or infinite and then within that finite domain of $\mu_\chi(\lambda)$, the CGF $\mu_\theta(\lambda)$ contributes to $\mu(\lambda)$.

We now move to compute the LDF, $h(\omega)$ corresponding to the observable ω in the full domain. We recall that the LDF is given by

$$h(\omega) = \sup_{\lambda \in \mathcal{R}} [\mu(\lambda) + \lambda\omega] . \quad (278)$$

Within the domain $\lambda \in (-\frac{1}{2}, \frac{1}{2})$, we have found that $\mu(\lambda) = \mu_\theta(\lambda)$ and the method of supremum allows us to compute the supremum in λ given by

$$\lambda^* : \mu'(\lambda^*) + \omega = 0, \quad (279)$$

which results in the LDF

$$h_s(\omega) = \mu_\theta(\lambda^*) + \lambda^*\omega , \quad (280)$$

where the corresponding range of ω follows straightforward from the condition

$$\lambda^* \in (-\frac{1}{2}, \frac{1}{2}) \implies \omega \in (\frac{1}{2}, \frac{3}{2}) . \quad (281)$$

However, this method breaks down once we are interested outside the domain $\lambda \in (-\frac{1}{2}, \frac{1}{2})$. First, we concentrate when $\lambda < -\frac{1}{2}$. This corresponds to $\omega > \frac{3}{2}$. In this case, the LDF will not be determined by the supremum. It is decided by the end point where the CGF, $\mu_X(\lambda)$ diverges and thus one can not neglect its contribution any more. As a matter of fact, in this case, the end point is given by $\lambda_a = -\frac{1}{2}$ and LDF will be determined by λ_a which implies

$$h_a(\omega) = \mu_\theta(\lambda_a) + \lambda_a \omega . \quad (282)$$

Now we consider the other range out of the allowed domain which is $\lambda > \frac{1}{2}$. As before, this corresponds to the domain of $\omega : \omega < \frac{1}{2}$. In this case, we notice that the CGF, $\mu_X(-\lambda)$ diverges because of the end point defined by $\lambda_b = \frac{1}{2}$. This singular point results in a modification in the LDF in this certain domain as the following

$$h_b(\omega) = \mu_\theta(\lambda_b) + \lambda_b \omega . \quad (283)$$

To summarize, the rate functions are then given by

$$h(\omega) = \begin{cases} h_a(\omega) & \omega > \frac{3}{2} \\ h_s(\omega) & \frac{1}{2} \leq \omega \leq \frac{3}{2} \\ h_b(\omega) & \omega < \frac{1}{2} . \end{cases} \quad (284)$$

Since the PDF is associated with the LDF as the following $P(\Omega_n = n\omega) \sim e^{nh(\omega)}$, we note that the PDF is determined by $\mu_\theta(\lambda)$ within the allowed analytical range $\frac{1}{2} \leq \omega \leq \frac{3}{2}$. However, this is not the case when one computes the PDF outside this domain. We note that the PDF picks up the exponential tails corresponding to the singularities present in the CGF. Moreover, it is also to note that these exponential tails are only a product of the boundary terms appearing in Eq. (263) and in Eq. (264), Eq. (265). Therefore, we conclude that

$$\begin{aligned} P(\Omega_n = n\omega) &\approx P(\Theta_n = n\omega) \quad \text{as } \omega \in \left(\frac{1}{2}, \frac{3}{2}\right) \\ &\approx P(\Delta U_n = \omega) \quad \text{otherwise} . \end{aligned} \quad (285)$$

From the physical point of view, we notice that in a Langevin kind set up, the observables Θ, Ω s are usually the family of applied work, Jarzynski work, dissipated heat, power flux, total entropy generated etc. An important point to note is that these observables are usually extensive with time (analogous to n) but the boundary terms are not. For example, the second law of thermodynamics relates the change in heat energy ΔQ to the work difference ΔW by the energy difference ΔU . Though both work and heat are extensive in time, energy difference is not and thus the fluctuations order of ΔU is smaller than that of the order of $\Delta Q, \Delta W$ which are linear in time (or n). We thus will have

$$\Delta Q \sim \Delta W \sim n , \quad (286)$$

so that the statistics of Q, W will be identical. Nevertheless this relation might break down if $\Delta U \sim O(n)$ and then

$$\Delta Q \sim \Delta U \quad (287)$$

which results in an exponential tail in the PDF similar to the case as shown above. The effects of these tails arising from the decay constants or the singularities in the prefactor result in a major difference in the validation of SSFT which is in this case will be depicted in terms of the CGF from Eq. (277)

$$\mu(\lambda) = \mu(2 - \lambda) , \quad (288)$$

which is sometimes known as the Gallavotti-Cohen eigenvalue symmetry. This translates to the symmetry of the LDF as

$$h(\omega) - h(-\omega) = 2\omega . \quad (289)$$

As we note from Eq. (284), only within the restricted domain of $\omega \in (\frac{1}{2}, \frac{3}{2})$, the LDF of the dissipated heat satisfies the symmetry or the SSFT, but outside this domain, it fails to satisfy the SSFT. So, the boundary terms (or the energy terms, initial conditions etc. in the Langevin setup) have a major role to play in the failure of the SSFT. In

a series of examples both theoretical and experimental, these effects have been observed. Consider the example of a Brownian particle confined in an optical trap with the trap being moved with a uniform velocity studied by Van Zon *et al.* It was shown that the work PDF always has a Gaussian form and always satisfies the SSFT. But the heat (differed by the energy difference) satisfies the SSFT in a restricted regime [43, 44, 45, 85, 68] which is exactly the case here. The failure of SSFT in the case of heat fluctuations was also observed in several other cases like the heat transport between two reservoirs along a carrier or a harmonic chain [111, 69, 70, 75, 73], cantilever fluctuations, trapped particle system etc. [71, 72, 109, 104]. Extending the paradigm problem of a colloidal particle in a trap with a stochastic driving was carefully considered in an experiment and within a theoretical framework in this thesis. It was found that the total entropy production invariantly satisfies the SSFT while the heat or the mechanical work fails to satisfy the SSFT [99, 103]. We should emphasize again that this failure is a straightforward consequence of the singularities appearing in the MGF due to the unboundedness of the phase space identical to the cases discussed in the thesis. An apparent resemblance might be the the singularities appeared in the LDFs for current in the periodic asymmetric exclusion process [62], or the weakly asymmetric simple exclusion process with open boundaries, the periodic total asymmetric exclusion process, in the boundary driven diffusive models such as the Ising model driven in the boundaries, the Quadratic- σ (QS) model [112]. Also there are models such as the weakly driven asymmetric simple exclusion process in the limit of large bulk driving field and the partially asymmetric simple exclusion process in the hydrodynamic limit. In such systems, the LDFs are a direct analogue of free energies in equilibrium systems and perhaps the presence of long range correlations lead to the non-differentiable LDFs [112] and phenomenas such as non-equilibrium phase transitions. On the other hand, we have obtained complete analytic LDFs which are continuous and differentiable (first derivatives are continuous) at the singular

points though the second derivatives are found to be discontinuous at the singularities. It is worth pointing out that our systems of interest typically span unbounded phase space resulting in the singularities setting up the energy scale. On the contrary, the systems discussed above show singular behavior even in a finite dimensional space (e.g. exclusion processes in a finite lattice). This underlying difference is a major one giving rise to two entirely different scenarios. Henceforth, we should emphasize that our cases are not identical to the ones discussed just above since the singularities we obtain are determined by the generating functions (a consequence of an infinite-dimensional configuration space) resulting in the LDFs determined by the singularities (as the cases discussed in the thesis, cases studied by Van Zon *et al*, Baesi *et al*) in contrast to the LDFs determining the singularities (as discussed above) themselves.

3.8 SUMMARY

Let us now summarize the main contents of this chapter. Using the model introduced in the preceding chapter, we have studied the heat and the entropy fluctuations in the NESS. We have computed the full PDFs of these observables in terms of the LDFs. We have also derived a simple method to incorporate the boundary effects while operating within a set of observables like mechanical work, heat and the total entropy production. We have shown that if the observables are related to each other by boundary terms, then the corresponding operator and the eigensystem (eigenvalues and the eigenvectors) remain indifferent. However, while computing the moment generating function, the sub dominant prefactor $g(\lambda)$ differs resulting in different statistics. We observe that this leads to non universal symmetry properties among the class of PDFs and so the validation of the SSFT is restricted. Finally, we illustrate a simple model based on the probability theory which can capture the general behavior such as symmetries in the

LDFs, singularities in the prefactor, exponential tails in the PDFs of the observables usually observed within the Langevin set up.

WORK FLUCTUATIONS OF A BROWNIAN PARTICLE DRAGGED THROUGH A MEDIUM

4.1 ABSTRACT

This chapter depicts the situation of an underdamped Brownian particle diffusing through an ambient medium. We have further considered its motion in the presence of a correlated external random force. The force is modelled by an Ornstein-Uhlenbeck process. We investigate the fluctuations of the work done by the external force on the Brownian particle in a given time interval in the steady state. We calculate the large deviation functions as well as the complete asymptotic form of the probability density function of the performed work. At certain limit, this model mimics a very simple system of a Brownian particle coupled to two thermostats and there one is more interested in computing the full distribution of the heat flowing from one end to the other. We give a full description of this observable in terms of the large deviation functions same as before. Moreover, we discuss the symmetry properties of the large deviation functions for these systems. Finally we perform numerical simulations and they are in a very good agreement with the analytic results.

4.2 INTRODUCTION

Transport of any kind being energy or matter or charges is an important phenomena to understand how two physical systems react when kept in contact to each other. In recent times, successful experiments conducted in micro-sized systems have gained a lot of attention. The

reason being it has vast applications towards numerous disciplines and their commercial usage. This includes automotive engineering, thermal management of electronic devices and systems, climate control, insulation, materials processing, and power station engineering. It is therefore of immense importance to understand these phenomena from microscopic scale. In microscopic scale, transport can be of various forms: electron transport through quantum dots or wires; heat transport in (electrically) insulating nanotubes, nanowires; ballistic thermal conductance using single wall or multi-walled carbon nanotubes; heat current measurements in a boron-nitride nanotube based on thermal rectifier models. One can ask a whole set of questions in this kind of model: properties of the currents (heat, phonon, charge), universality of the steady state measure of the energies, variation of temperature or the the energy profile with the system size, the average flow of energy being transmitted, a complete information about the distribution of the particle or heat energy.

In this chapter, we will address few questions raised in the preceding paragraph using a model system. Consider a simplified version of a metal rod being implemented as a ordered (disordered) harmonic (anharmonic) chain [73] or take simply a Brownian particle [111] attached with the reservoirs kept at different temperatures at the extreme two ends. The aim is to calculate the full description of the heat energy being transported from one end to the other one. Though a few attempts have been made to compute the average heat current [69] or the fluctuations [70], the full distribution of the heat current is not known yet. Since, the heat energy is accompanied by non-Gaussian fluctuations, it is not sufficient to know about the mean and variance to get the detailed distribution. So, one has to go beyond the linear probability theory to incorporate these non-Gaussian fluctuations. We answer to this question using the formalism developed in the last two chapters and in unison with the theory of large deviations. We restrict ourselves within the single particle model; however, an extension to the harmonic chain should not offer more insights.

To this quest, we initially study a more general model and the problem of a bound particle connected with two thermostats appears as a subclass of this illustrated model. This correspondence will be made later as we go along. Our model system is described as following: consider an underdamped Brownian particle diffusing in an ambient medium at certain temperature. We apply a random external field to the system thus driving it away from equilibrium. In such way, the external random field does a work on the system and we are interested to quantify this quantity. We note that this observable is a trajectory dependent stochastic quantity and varies from one realization to the other one. The origin of its stochasticity is the following: initial conditions are chosen from a distribution and the observable depends on the noise history. So, one has to look into its distribution for the complete information. We compute the distribution of this work done in a given duration using the method developed in the preceding chapters. We find that the distribution function can be completely represented in terms of the large deviation functions at large time. By taking a suitable limit, we show that this model represents the system of the Brownian particle connected with two reservoirs and it is therefore simple hereafter to find the detailed description of the corresponding observable we were interested in. As a corollary, we can also explore the validity of the so called steady state fluctuation theorem in the context of this problem.

The chapter is organized as follows. In the following section, we define the model. In Sec. 4.4 we compute the moment generating function (MGF) of work W_τ performed in a given time τ in steady state. Some details of this calculation has been relegated to Sec. 4.5. Explicit results of $\mu(\lambda)$ and $g(\lambda)$ are given in the subsequent section Sec. 4.6. In Sec. 4.7, we invert the MGF to obtain the asymptotic form (for large τ) of the PDF of the work. In Sec. 4.8, we have considered the case of a Brownian particle connected to two heat baths, which appears to be a corollary set up of the general problem in certain limits. We have analyzed the heat PDF using the method developed

in the section in great details. We discuss the symmetry properties of the large deviation functions, obtained in this chapter, and their connection with the FT in Sec. 4.9. Finally we conclude in Sec. 4.10.

4.3 MODEL

Consider a Brownian particle of mass m , in the presence of an external fluctuating time dependent field, at a temperature T . The velocity $v(t)$ of the particle evolves according to the underdamped Langevin equation, given by,

$$m \frac{dv}{dt} + \gamma v = f(t) + \eta_1, \quad (290)$$

where γ is the friction coefficient. The viscous relaxation time scale for the particle is $\tau_\gamma = m/\gamma$. The thermal noise η_1 is taken to be a Gaussian white noise with mean zero and correlation $\langle \eta_1(t)\eta_1(s) \rangle = 2D\delta(t-s)$, where diffusion constant $D = \gamma k_B T$ and k_B is the Boltzmann constant. The external stochastic field f is modelled by an Ornstein-Uhlenbeck process,

$$\frac{df}{dt} = -\frac{f}{\tau_0} + \eta_2, \quad (291)$$

where η_2 is another Gaussian white noise with mean zero and correlation $\langle \eta_2(t)\eta_2(s) \rangle = 2A\delta(t-s)$. This system reaches a steady state and in the steady state the external force has zero mean and covariance $\langle f(t)f(s) \rangle = A\tau_0 \exp(-|t-s|/\tau_0)$.

The heat current flowing from the bath to the particle is the force exerted by the bath times the velocity of the particle [107, 29]. Therefore, in a given time τ , the total amount of heat flow (in the unit of $k_B T$) is given by,

$$Q_\tau = \frac{1}{k_B T} \int_0^\tau (-\gamma v + \eta_1)v(t) dt. \quad (292)$$

On the other hand, the change in the internal energy of the particle in this finite interval τ is given by

$$\Delta U(\tau) = \frac{1}{k_B T} \left[\frac{1}{2} m v^2(\tau) - \frac{1}{2} m v^2(0) \right]. \quad (293)$$

Then the first law of the thermodynamics (conservation of energy) gives $\Delta U(\tau) = W_\tau + Q_\tau$, where W_τ is the work done on the particle by the external force, which is given by

$$W_\tau = \frac{1}{k_B T} \int_0^\tau f(t)v(t) dt . \quad (294)$$

This work is a stochastic quantity and our goal is to compute its PDF $P(W_\tau)$.

For later convenience, we will introduce two dimensionless parameters in the following:

$$\theta = \frac{\tau_0^2 A}{D}, \quad \text{and} \quad \delta = \frac{\tau_0}{\tau_\gamma} . \quad (295)$$

4.4 MOMENT GENERATING FUNCTION

We begin by writing Eqs. (290) and (291) in the matrix form

$$\frac{d\mathbf{U}}{dt} = -\mathbf{A}\mathbf{U} + \mathbf{B}\boldsymbol{\eta} , \quad (296)$$

where $\mathbf{U} = (v, f)^T$ and $\boldsymbol{\eta} = (\eta_1, \eta_2)^T$ are column vectors, and \mathbf{A} and \mathbf{B} are 2×2 matrices given by

$$\mathbf{A} = \begin{pmatrix} 1/\tau_\gamma & -1/m \\ 0 & 1/\tau_0 \end{pmatrix}, \quad \mathbf{B} = \begin{pmatrix} 1/m & 0 \\ 0 & 1 \end{pmatrix}. \quad (297)$$

To compute the PDF of W_τ , we first consider its moment generating function, constrained to fixed initial and final configurations \mathbf{U}_0 and \mathbf{U} respectively:

$$Z(\lambda, \mathbf{U}, \tau | \mathbf{U}_0) = \langle e^{-\lambda W_\tau} \delta[\mathbf{U} - \mathbf{U}(\tau)] \rangle_{\mathbf{U}_0} , \quad (298)$$

where the averaging is over the histories of the thermal noises starting from the initial condition \mathbf{U}_0 . It is easy to show that this restricted moment generating function satisfies the Fokker-Planck equation

$$\frac{\partial Z}{\partial \tau} = \mathcal{L}_\lambda Z , \quad (299)$$

with the initial condition $Z(\lambda, \mathbf{U}, 0|\mathbf{U}_0) = \delta(\mathbf{U} - \mathbf{U}_0)$. The Fokker-Planck operator is given by

$$\mathcal{L}_\lambda = \frac{D}{m^2} \frac{\partial^2}{\partial v^2} + \frac{D\theta}{\tau_0^2} \frac{\partial^2}{\partial f^2} + \frac{1}{\tau_\gamma} \frac{\partial}{\partial v} v + \frac{1}{\tau_0} \frac{\partial}{\partial f} f - \frac{f}{m} \frac{\partial}{\partial v} - \frac{\lambda\gamma}{D} f v. \quad (300)$$

The solution of this equation can be formally expressed in the eigenbases of the operator \mathcal{L}_λ and the large- τ behavior is dominated by the term containing the largest eigenvalue. Thus, for large τ , one can write,

$$Z(\lambda, \mathbf{U}, \tau|\mathbf{U}_0) = \chi(\mathbf{U}_0, \lambda) \Psi(\mathbf{U}, \lambda) e^{\tau\mu(\lambda)} + \dots, \quad (301)$$

where $\mu(\lambda)$ is the largest eigenvalue, $\mathcal{L}_\lambda \Psi(\mathbf{U}, \lambda) = \mu(\lambda) \Psi(\mathbf{U}, \lambda)$ and $\int d\mathbf{U} \chi(\mathbf{U}, \lambda) \Psi(\mathbf{U}, \lambda) = 1$.

The moment generating function can be obtained by averaging the restricted generating function over the initial variables \mathbf{U}_0 with respect to the steady state distribution $P_{SS}(\mathbf{U}_0)$ and integrating out the the final variables \mathbf{U} ,

$$Z(\lambda, \tau) = \int d\mathbf{U} \int d\mathbf{U}_0 P_{SS}(\mathbf{U}_0) Z(\lambda, \mathbf{U}, \tau|\mathbf{U}_0), \quad (302)$$

where $P_{SS}(\mathbf{U}_0) = \Psi(\mathbf{U}_0, 0)$. This yields

$$Z(\lambda, \tau) = \langle e^{-\lambda W_\tau} \rangle = g(\lambda) e^{\tau\mu(\lambda)} + \dots, \quad (303)$$

where

$$g(\lambda) = \int d\mathbf{U} \int d\mathbf{U}_0 \Psi(\mathbf{U}_0, 0) \chi(\mathbf{U}_0, \lambda) \Psi(\mathbf{U}, \lambda). \quad (304)$$

The full forms of $\Psi(\mathbf{U}, \lambda)$ and $\chi(\mathbf{U}_0, \lambda)$ are given by Eq. (335) computed in the next section in details. The explicit results for $\mu(\lambda)$ and $g(\lambda)$ are given in Sec. 4.6 following Sec. 4.5.

4.5 DETAILED CALCULATION OF THE MGF

We recall Eq. (296) and Eq. (297)

$$\frac{d\mathbf{U}}{dt} = -A\mathbf{U} + B\eta, \quad (305)$$

where $\mathbf{U} = (v, f)^\top$ and $\boldsymbol{\eta} = (\eta_1, \eta_2)^\top$ are column vectors and A, B are 2×2 matrices given by

$$A = \begin{pmatrix} 1/\tau_\gamma & -1/m \\ 0 & 1/\tau_0 \end{pmatrix}, \quad B = \begin{pmatrix} 1/m & 0 \\ 0 & 1 \end{pmatrix}. \quad (306)$$

The expression for W_τ can then be expressed in terms of these matrices

$$W_\tau = \frac{\gamma}{2D} \int_0^\tau dt \mathbf{U}^\top A_1 \mathbf{U}, \quad (307)$$

where A_1 is a real symmetric matrix

$$A_1 = \begin{pmatrix} 0 & 1 \\ 1 & 0 \end{pmatrix}. \quad (308)$$

Using the integral representation of the delta-function Eq. (51), we rewrite the moment generating function

$$Z(\lambda, \mathbf{U}, \tau | \mathbf{U}_0) = \int \frac{d^2\sigma}{(2\pi)^2} e^{i\sigma^\top \mathbf{U}} \langle e^{-\lambda W_\tau - i\sigma^\top \mathbf{U}(\tau)} \rangle_{\mathbf{U}, \mathbf{U}_0}. \quad (309)$$

Now, we proceed by defining the finite time Fourier transforms and inverses as follows:

$$[\tilde{\mathbf{U}}(\omega_n), \tilde{\boldsymbol{\eta}}(\omega_n)] = \frac{1}{\tau} \int_0^\tau dt [\mathbf{U}(t), \boldsymbol{\eta}(t)] \exp(-i\omega_n t), \quad (310a)$$

$$[\mathbf{U}(t), \boldsymbol{\eta}(t)] = \sum_{n=-\infty}^{\infty} [\tilde{\mathbf{U}}(\omega_n), \tilde{\boldsymbol{\eta}}(\omega_n)] \exp(i\omega_n t), \quad (310b)$$

with $\omega_n = 2\pi n/\tau$.

In the frequency domain, the Gaussian noise configurations denoted by $\{\boldsymbol{\eta}(t) : 0 < t < \tau\}$ can be well described by the infinite sequence $\{\tilde{\boldsymbol{\eta}}(\omega_n) : n = -\infty, \dots, -1, 0, +1, \dots, \infty\}$ of Gaussian random variables having the following correlations

$$\langle \tilde{\boldsymbol{\eta}}(\omega) \tilde{\boldsymbol{\eta}}^\top(\omega') \rangle = \frac{2D}{\tau} \delta(\omega + \omega') \text{diag}(1, \theta/\tau_0^2). \quad (311)$$

The Fourier transform of $\mathbf{U}(t)$ is then straightforward and henceforth the expression for W_τ becomes

$$\tilde{\mathbf{U}} = GB\tilde{\boldsymbol{\eta}} - \frac{1}{\tau} G\Delta\mathbf{U} \quad W_\tau = \frac{\gamma\tau}{2D} \sum_{n=-\infty}^{\infty} \tilde{\mathbf{U}}^\top(\omega_n) A_1 \tilde{\mathbf{U}}^*(\omega_n), \quad (312)$$

where $G(\omega) = (i\omega I + A)^{-1}$ and $\Delta U = U(\tau) - U(0)$, with I being the identity matrix. The elements of G are $G_{11} = \tau_\gamma(i\omega\tau_\gamma + 1)^{-1}$, $G_{22} = \tau_0(i\omega\tau_0 + 1)^{-1}$, $G_{12} = G_{11}G_{22}/m$, $G_{21} = 0$. Substituting \tilde{U} from the above expression in W_τ and grouping the negative indices into their positive counterparts, we obtain

$$\begin{aligned} W_\tau = & \frac{\gamma\tau}{2D} \left[\tilde{\eta}_0^T (B G_0^T A_1 G_0 B) \tilde{\eta}_0 - \frac{2}{\tau} \Delta U^T (G_0^T A_1 G_0 B) \tilde{\eta}_0 \right. \\ & \left. + \frac{1}{\tau^2} \Delta U^T (G_0^T A_1 G_0) \Delta U \right] \\ & + \frac{\gamma\tau}{D} \sum_{n=1}^{\infty} \left[\tilde{\eta}^T (B G^T A_1 G^* B) \tilde{\eta}^* - \frac{1}{\tau} \Delta U^T (G^T A_1 G^* B) \tilde{\eta}^* \right. \\ & \left. - \frac{1}{\tau} \tilde{\eta}^T (B G^T A_1 G^*) \Delta U + \frac{1}{\tau^2} \Delta U^T (G^T A_1 G^*) \Delta U \right], \quad (313) \end{aligned}$$

where $G_0 = G(\omega = 0) = A^{-1}$, $\tilde{\eta}_0 = \tilde{\eta}(0)$. The finite time Fourier series can be written for $U(\tau)$ as well

$$\begin{aligned} U(\tau) &= \lim_{\epsilon \rightarrow 0} \sum_{n=-\infty}^{\infty} \tilde{U}(\omega_n) e^{-i\omega_n \epsilon} \\ &= \lim_{\epsilon \rightarrow 0} \sum_{n=-\infty}^{\infty} (GB\tilde{\eta} - \frac{1}{\tau} G\Delta U) e^{-i\omega_n \epsilon} \\ &= \lim_{\epsilon \rightarrow 0} \sum_{n=-\infty}^{\infty} (GB\tilde{\eta}) e^{-i\omega_n \epsilon}, \quad (314) \end{aligned}$$

where we observe that $\tau^{-1} \sum_n G(\omega_n) e^{-i\omega_n \epsilon} = 0$ for large τ . This is because while converting the summation into an integral we note that all the poles of $G(\omega)$ lie in the upper half plane. In other words, the function $G(\omega)$ is analytic in the lower half. Using this expression we obtain

$$\begin{aligned} \sigma^T U(\tau) &= \sigma^T G_0 B \tilde{\eta}_0 \\ &+ \sum_{n=1}^{\infty} \left[e^{-i\omega_n \epsilon} \tilde{\eta}^T (B G^T \sigma) + e^{i\omega_n \epsilon} (\sigma^T G^* B) \tilde{\eta}^* \right]. \quad (315) \end{aligned}$$

The average quantity then can be rewritten as

$$\langle e^{-\lambda W_\tau - i\sigma^T U(\tau)} \rangle = \prod_{n=0}^{\infty} \langle e^{s_n} \rangle, \quad (316)$$

where

$$s_n = -\lambda\tau\tilde{\eta}^T c_n \tilde{\eta}^* + \tilde{\eta}^T \alpha_n + \alpha_{-n}^T \tilde{\eta}^* - \frac{\lambda}{\tau} \frac{\gamma}{D} \Delta U^T (G^T A_1 G^*) \Delta U \quad \text{for } n \geq 1, \quad (317)$$

and

$$s_0 = -\frac{\lambda\tau}{2} \tilde{\eta}_0^T c_0 \tilde{\eta}_0 + \alpha_0^T \tilde{\eta}_0 - \frac{\lambda}{2\tau} \frac{\gamma}{D} \Delta U^T (G_0^T A_1 G_0) \Delta U, \quad (318)$$

in which we have used the following definitions

$$c_n = \frac{\gamma}{D} B G^T A_1 G^* B, \quad (319)$$

$$\alpha_n = \lambda \frac{\gamma}{D} (B G^T A_1 G^*) \Delta U - i e^{-i\omega_n \epsilon} B G^T \sigma. \quad (320)$$

We can now calculate the average $\langle e^{s_n} \rangle$ independently for each $n \geq 1$ with respect to the Gaussian PDF $P(\tilde{\eta}) = \pi^{-2} (\det \Lambda)^{-1} \exp(-\tilde{\eta}^T \Lambda^{-1} \tilde{\eta}^*)$ with $\Lambda^{-1} = \frac{2D}{\tau} \text{diag}(1, \theta/\tau_0^2)$, which gives,

$$\langle e^{s_n} \rangle = \frac{\exp[\alpha_{-n}^T \Omega_n^{-1} \alpha_n - \frac{\lambda}{\tau} \frac{\gamma}{D} \Delta U^T (G^T A_1 G^*) \Delta U]}{\det(\Lambda \Omega_n)}, \quad (321)$$

where $\Omega_n = \lambda\tau c_n + \Lambda^{-1}$. Similarly, calculating the average of $n = 0$ term with respect to the Gaussian PDF $P(\tilde{\eta}_0) = (2\pi)^{-1} (\det \Lambda)^{-1/2} \exp(-\frac{1}{2} \tilde{\eta}_0^T \Lambda^{-1} \tilde{\eta}_0)$, we get

$$\langle e^{s_0} \rangle = \frac{\exp[\frac{1}{2} \alpha_0^T \Omega_0^{-1} \alpha_0 - \frac{\lambda}{2\tau} \frac{\gamma}{D} \Delta U^T (G_0^T A_1 G_0^*) \Delta U]}{\sqrt{\det(\Lambda \Omega_0)}}. \quad (322)$$

The restricted moment generating function can now be rewritten as

$$Z(\lambda, u, \tau | u_0) = \int \frac{d^2\sigma}{(2\pi)^2} e^{i\sigma^T u} \prod_{n=0}^{\infty} \langle e^{s_n} \rangle, \quad (323)$$

where using the fact $\langle e^{s_n} \rangle = \langle e^{s_{-n}} \rangle$, we can write

$$\begin{aligned} \prod_{n=0}^{\infty} \langle e^{s_n} \rangle &= \exp\left(-\frac{1}{2} \sum_{n=-\infty}^{\infty} \ln[\det(\Lambda \Omega_n)]\right) \\ &\times \exp\left(\frac{1}{2\tau} \sum_{n=-\infty}^{\infty} [\alpha_{-n}^T \tau \Omega_n^{-1} \alpha_n - \lambda \frac{\gamma}{D} \Delta U^T G^T A_1 G^* \Delta U]\right). \end{aligned} \quad (324)$$

The determinant in Eq. (324) is found to be

$$\det(\Lambda \Omega_n) = 1 + \frac{4\theta\lambda(1-\lambda)}{\tau_0^2 \tau_\gamma^2} |G_{11}|^2 |G_{22}|^2. \quad (325)$$

Now in large- τ limit, we can replace the summations over n into an integral over ω i.e. $\sum_n \rightarrow \tau \int \frac{d\omega}{2\pi}$. The first part of the summation is then

$$\tau\mu(\lambda) = -\frac{\tau}{2} \int \frac{d\omega}{2\pi} \ln \left[\det(\Lambda\Omega(\omega)) \right], \quad (326)$$

where $\mu(\lambda)$ is given by Eq. (339a). Similarly, the second part of the summation can be converted into an integral. Finally, after doing some manipulations, we obtain

$$\prod_{n=0}^{\infty} \langle e^{s_n} \rangle \approx e^{\tau\mu(\lambda)} \exp \left[-\frac{1}{2} \sigma^T H_1 \sigma + i \Delta U^T H_2 \sigma + \frac{1}{2} \Delta U^T H_3 \Delta U \right], \quad (327)$$

in which we have defined the following matrices

$$H_1 = \int_{-\infty}^{\infty} \frac{d\omega}{2\pi} G^* B(\tau\Omega^{-1}) B G^T, \quad (328)$$

$$H_2 = -\lim_{\epsilon \rightarrow 0} \frac{\lambda}{2\pi} \frac{\gamma}{D} \int_{-\infty}^{\infty} d\omega e^{i\omega\epsilon} G^+ A_1 G B(\tau\Omega^{-1})^* B G^+, \quad (329)$$

and

$$H_3 = -\frac{\lambda}{2\pi} \frac{\gamma}{D} \int_{-\infty}^{\infty} d\omega G^T A_1 G^* + \frac{\lambda^2}{2\pi} \frac{\gamma^2}{D^2} \int_{-\infty}^{\infty} d\omega G^T A_1 G^* B(\tau\Omega^{-1}) B G^T A_1 G^*. \quad (330)$$

We then evaluate the matrices by performing the integral by the method of contours. For convenience, we write down the elements of the matrices respectively.

$$H_1^{11} = \frac{D\tau\gamma}{m^2} \frac{1}{1+\delta\bar{\nu}} \left(\delta + \frac{1+\theta}{\nu} \right), \quad (331a)$$

$$H_1^{12} = H_1^{21} = \frac{D\theta}{m} \frac{1-2\lambda}{\nu(1+\delta\bar{\nu})}, \quad (331b)$$

$$H_1^{22} = \frac{D\theta}{\tau_0} \frac{1}{1+\delta\bar{\nu}} \left(1 + \frac{\delta}{\nu} \right). \quad (331c)$$

The elements of H_2 matrix are

$$H_2^{11} = \frac{1}{\nu(1+\delta\bar{\nu})} \left[\lambda\theta + \frac{1}{2}(1-\nu) + \frac{1}{2}\delta\nu(1-\bar{\nu}) \right], \quad (332a)$$

$$H_2^{12} = -\frac{\lambda\gamma\theta}{\nu(1+\delta\bar{\nu})}, \quad (332b)$$

$$H_2^{21} = -\frac{\lambda\delta}{\gamma\nu(1+\delta\bar{\nu})} + \frac{\delta(1-\nu)}{2\gamma\nu(1+\delta\bar{\nu})}, \quad (332c)$$

$$H_2^{22} = \frac{\delta(1-\nu\bar{\nu})}{2\nu(1+\delta\bar{\nu})}. \quad (332d)$$

The elements of H_3 matrix are given by

$$H_3^{11} = \frac{\lambda^2 \theta \gamma^2 \tau_\gamma}{D\nu(1 + \delta\bar{\nu})}, \quad (333a)$$

$$H_3^{12} = H_3^{21} = \frac{4\lambda^2(1 - \lambda)\gamma\theta}{D\tau_0\tau_\gamma} \frac{1 + \nu + (1 + \delta\bar{\nu})(1 - \bar{\nu} - \frac{2}{\delta})}{[1 + (1 + \delta\bar{\nu}) + \delta\nu] \times [1 - \frac{1}{\delta}(1 + \delta\bar{\nu}) + \frac{\nu}{\delta}]}, \quad (333b)$$

$$H_3^{22} = -\frac{\lambda(1 - \lambda)\delta\tau_0}{D\nu(1 + \delta\bar{\nu})}. \quad (333c)$$

We note that the matrices H_1 and H_3 are symmetric and they satisfy the relation $H_3 = (I + H_2)H_1^{-1}H_2^T$. Inserting Eq. (327) into Eq. (323) and performing the Gaussian integral over σ , we obtain

$$Z(\lambda, \mathbf{u}, \tau|\mathbf{u}_0) \approx \frac{e^{\tau\mu(\lambda)}}{2\pi\sqrt{\det(H_1(\lambda))}} \times e^{-\frac{1}{2}\mathbf{u}^T L_1(\lambda)\mathbf{u}} e^{-\frac{1}{2}\mathbf{u}_0^T L_2(\lambda)\mathbf{u}_0}, \quad (334)$$

where $L_1(\lambda) = H_1^{-1}(I + H_2^T)$ and $L_2(\lambda) = -H_1^{-1}H_2^T$. We immediately identify the right and left eigenfunctions respectively as

$$\Psi(\mathbf{u}, \lambda) = \frac{1}{2\pi\sqrt{\det(H_1(\lambda))}} \exp\left[-\frac{1}{2}\mathbf{u}^T L_1(\lambda)\mathbf{u}\right], \quad (335a)$$

$$\chi(\mathbf{u}_0, \lambda) = \exp\left[-\frac{1}{2}\mathbf{u}_0^T L_2(\lambda)\mathbf{u}_0\right]. \quad (335b)$$

It is then straightforward to verify $\mathcal{L}_\lambda \Psi(\mathbf{u}, \lambda) = \mu(\lambda)\Psi(\mathbf{u}, \lambda)$ and $\int d\mathbf{u} \chi(\mathbf{u}, \lambda)\Psi(\mathbf{u}, \lambda) = 1$. The steady state distribution is given by

$$P_{SS}(\mathbf{u}) = Z(\lambda = 0, \mathbf{u}, \tau \rightarrow \infty|\mathbf{u}_0) = \Psi(\mathbf{u}, \lambda = 0) = \frac{1}{2\pi\sqrt{\det(H_1(0))}} \exp\left[-\frac{1}{2}\mathbf{u}^T L_1(0)\mathbf{u}\right], \quad (336)$$

where $L_1(0)$ and given by

$$L_1(0) = \frac{1}{\det H_1(0)} \frac{D}{1 + \delta} \begin{pmatrix} \frac{\theta}{\tau_0}(1 + \delta) & -\frac{\theta}{m} \\ -\frac{\theta}{m} & \frac{\tau_\gamma}{m^2}(1 + \delta + \theta) \end{pmatrix}. \quad (337)$$

It is worth noting that the deviation of the system from equilibrium can also be measured using Eq. (336)

$$\alpha = \frac{\langle v^2 \rangle_{ss}}{\langle v^2 \rangle_{eq}} - 1, \quad (338)$$

where $\langle v^2 \rangle_{ss}$ is the velocity variance in the steady state which can be found from Eq. (337) and $\langle v^2 \rangle_{eq}$ is that of in equilibrium in the absence of the external driving. Hence, one finds, $\alpha = \theta/(1 + \delta)$.

4.6 EXPLICIT RESULTS FOR $\mu(\lambda)$ AND $g(\lambda)$

Following the detail calculation given in Sec. 4.5, we find that

$$\mu(\lambda) = \frac{1}{2\tau_\gamma} [1 - \bar{v}(\lambda)] , \quad (339a)$$

where

$$\bar{v}(\lambda) = \frac{1}{\delta} \left[\sqrt{1 + \delta^2 + 2\delta v(\lambda)} - 1 \right] , \quad (339b)$$

with

$$v(\lambda) = \sqrt{1 + 4\theta\lambda(1 - \lambda)} . \quad (339c)$$

We note that $\mu(\lambda)$ obeys the so-called Gallavotti-Cohen symmetry, $\mu(\lambda) = \mu(1 - \lambda)$.

Using Eq. (304), we find

$$\begin{aligned} g(\lambda) &= [\det(I + H_2^T)]^{-1/2} [\det(I - H_1(0)H_1^{-1}(\lambda)H_2^T(\lambda))]^{-1/2} , \\ &= [f_1(\lambda, \theta, \delta)]^{-1/2} [f_2(\lambda, \theta, \delta)]^{-1/2} \end{aligned} \quad (340)$$

where the first and second terms are due to tracing out the final and initial variables respectively. Using the forms of the matrices given by Eq. (331) and Eq. (332), we obtain

$$\begin{aligned} f_1(\lambda, \theta, \delta) &:= \det(I + H_2^T) \\ &= \frac{1}{4v(1 + \delta\bar{v})^2} [p(\lambda) + 2\theta\lambda q(\lambda)] , \end{aligned} \quad (341a)$$

$$\begin{aligned} f_2(\lambda, \theta, \delta) &:= \det[I - H_1(0)H_1^{-1}(\lambda)H_2^T(\lambda)] \\ &= \frac{1}{4(1 + \delta)^2} \frac{1}{\theta + (1 + \delta\bar{v})^2} [r(\lambda) + 2\theta\lambda s(\lambda)] . \end{aligned} \quad (341b)$$

where

$$p(\lambda) = 2 + 2v + \delta(1 + \bar{v})(1 + \delta + 3v + \delta v\bar{v}) , \quad (342a)$$

$$q(\lambda) = 2 + \delta(\bar{v} - 1) = 1 + \sqrt{1 + \delta^2 + 2\delta v} - \delta . \quad (342b)$$

and

$$\begin{aligned} r(\lambda) &= 2\theta(1 + \nu) + 2(1 + \nu)(1 + \delta)^2 \\ &\quad + \left[\theta + (1 + \delta)^2 \right] \left[\delta(1 + \bar{\nu})^2 + \delta(1 + \bar{\nu})(1 + \delta\bar{\nu})(\nu + \bar{\nu}) \right], \end{aligned} \quad (343a)$$

$$\begin{aligned} s(\lambda) &= - \left[2 + 2\theta + 3\theta\delta + \delta\bar{\nu} + \theta\delta\bar{\nu} \right] \\ &\quad + \left[\delta + 2\delta^2(2 + \bar{\nu}) + \delta^3(1 + 3\bar{\nu}) \right]. \end{aligned} \quad (343b)$$

Let us now analyze the functions $f_1(\lambda, \theta, \delta)$ and $f_2(\lambda, \theta, \delta)$ in details. We note that the pre-factors outside the square bracket of $f_1(\lambda, \theta, \delta)$ and $f_2(\lambda, \theta, \delta)$ are always positive. Moreover, $p(\lambda)$ and $q(\lambda)$ are again clearly positive in the region $\lambda \in [\lambda_-, \lambda_+]$. In particular, they take the minimum values at λ_{\pm} , given by $p(\lambda_{\pm}) = 2 + \alpha_1$ and $q(\lambda_{\pm}) = 1 + \alpha_2 = 2 - \alpha_3$, where $\alpha_1 = (1 + \delta)(\delta + \sqrt{1 + \delta^2} - 1) \geq 0$, $1 \geq \alpha_2 = \sqrt{1 + \delta^2} - \delta > 0$, and $1 > \alpha_3 = (1 + \delta) - \sqrt{1 + \delta^2} \geq 0$. Therefore, $f_1(\lambda_+, \theta, \delta) > 0$ as $\lambda_+ > 0$. On the other hand, at $\lambda = \lambda_-$ we get

$$\begin{aligned} p(\lambda_-) + 2\theta\lambda_- q(\lambda_-) &= (2 + \alpha_1) + 2\theta\lambda_-(2 - \alpha_3) \\ &= \alpha_1 + (-2\alpha_3\theta\lambda_-) + 2(1 + 2\theta\lambda_-). \end{aligned}$$

The first two summands in the last line of the above expression is clearly positive (note that $\lambda_- < 0$). Moreover, it can be shown that

$$1 + 2\theta\lambda_- = \sqrt{1 + \theta}[\sqrt{1 + \theta} - \sqrt{\theta}] > 0. \quad (344)$$

This also implies that

$$1 + 2\theta\lambda > 0 \quad \text{for } \lambda \in [\lambda_-, \lambda_+]. \quad (345)$$

Therefore, $f_1(\lambda_-, \theta, \delta) > 0$, which implies that $f_1(\lambda, \theta, \delta)$ stays positive in the region $\lambda \in [\lambda_-, \lambda_+]$.

Similarly, we can analyze the second term $f_2(\lambda, \theta, \delta)$. Clearly, $r(\lambda)$ is always positive in the region $\lambda \in [\lambda_-, \lambda_+]$. On the other hand, the first line in the expression of $s(\lambda)$ given by Eq. (343b) is negative whereas the second line is positive; $s(\lambda)$ can take both positive and negative

values in the $(\theta, \delta, \lambda)$ space. Writing Eq. (343b) as $s(\lambda) = -b_1 + b_2$ with both $b_1 > 0$ and $b_2 > 0$, we get

$$r(\lambda) + 2\theta\lambda s(\lambda) = [r(\lambda) - b_2] + (1 + 2\theta\lambda)b_2 + (-2b_1\theta\lambda).$$

By explicitly expanding $r(\lambda)$, it can be seen that all the terms appearing in b_2 completely cancel with some of the terms of $r(\lambda)$. Therefore, $r(\lambda) - b_2 > 0$ for $\lambda \in [\lambda_-, \lambda_+]$. Similarly, according to Eq. (345), the second summand is positive. Finally, the last summand is clearly positive for $\lambda < 0$. Therefore, $f_2(\lambda, \theta, \delta) > 0$ for $\lambda_- \leq \lambda \leq 0$.

At $\lambda = \lambda_+$, we find that $r(\lambda_+) + 2\theta\lambda_+s(\lambda_+)$ changes sign in the parameter space of (θ, δ) . The phase boundary that separates the two regions where this function stays positive and negative respectively is given by

$$f_2(\lambda_+, \theta, \delta) = 0, \quad (346)$$

which is shown in the phase diagram Fig. 13.

4.7 PROBABILITY DISTRIBUTION FUNCTION

The PDF $P(W_\tau)$ is related to the moment generating function $Z(\lambda, \tau)$ as

$$P(W_\tau) = \frac{1}{2\pi i} \int_{-i\infty}^{+i\infty} Z(\lambda, \tau) e^{\lambda W_\tau} d\lambda, \quad (347)$$

where the integration is done in the complex λ plane. Inserting the large τ form of $Z(\lambda, \tau)$ given by Eq. (303), we obtain

$$P(W_\tau = w\tau/\tau_\gamma) \approx \frac{1}{2\pi i} \int_{-i\infty}^{+i\infty} g(\lambda) e^{(\tau/\tau_\gamma) f_w(\lambda)} d\lambda, \quad (348)$$

where

$$f_w(\lambda) = \frac{1}{2}[1 - \bar{v}(\lambda)] + \lambda w. \quad (349)$$

In the large τ limit, we can use the saddle point approximation, in which one chooses the contour of integration along the steepest descent path through the saddle point λ^* . The saddle point can be obtained solving the equation,

$$f'_w(\lambda^*) = 0, \quad (350)$$

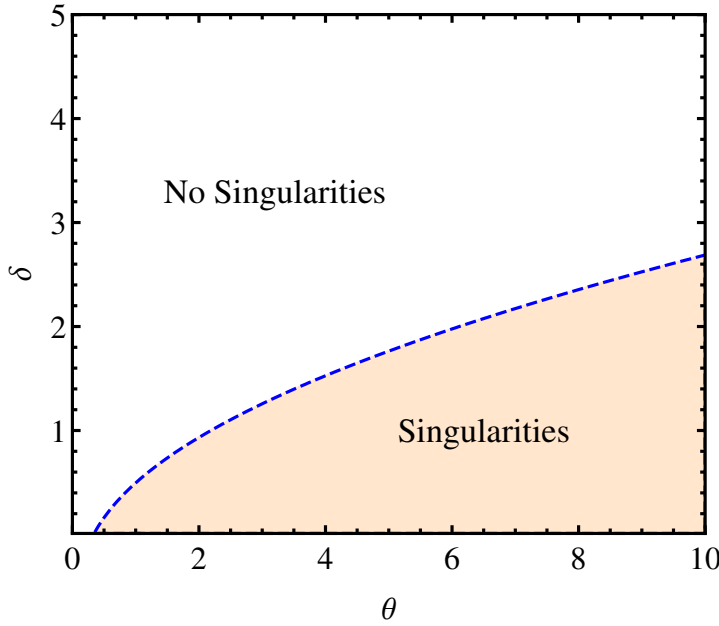


Figure 13: This plot depicts the analytic properties of $g(\lambda)$. In the shaded region of the (θ, δ) plane, $g(\lambda)$ possesses a singularity, where $f_2(\lambda_+, \theta, \delta) < 0$. On the other hand, in the unshaded region $g(\lambda)$ does not have any singularities, where $f_2(\lambda_+, \theta, \delta) > 0$. These two domains are separated by the boundary given by the equation $f_2(\lambda_+, \theta, \delta) = 0$.

or equivalently,

$$\bar{v}'(\lambda^*) = 2w . \tag{351}$$

The above equation yields

$$\theta(1 - 2\lambda^*) = wv(\lambda^*)\sqrt{1 + \delta^2 + 2\delta v(\lambda^*)} . \tag{352}$$

Since θ, δ and $v(\lambda)$ are always positive, it is clear that $\text{sign}(1 - 2\lambda^*) = \text{sign}(w)$.

The above equation can be simplified to the cubic form

$$v^3(\lambda^*) + av^2(\lambda^*) - b = 0 , \tag{353}$$

where

$$a = \frac{\theta + (1 + \delta^2)w^2}{2\delta w^2} , \tag{354a}$$

$$b = \frac{\theta + \theta^2}{2\delta w^2} . \tag{354b}$$

We observe that one of the roots of the cubic equation for $\nu(\lambda^*)$ is real while the other two are complex. Equation (352) suggests the root to be real, and it is given by

$$\nu(\lambda^*) = -\frac{\alpha}{3} \left[1 - (1 + 2k + 3\sqrt{3lk})^{-1/3} - (1 + 2k + 3\sqrt{3lk})^{1/3} \right], \quad (355a)$$

where $l = b/\alpha^3$ and $k = (27/4)l - 1$. Note that $l > 0$. Therefore, $\nu(\lambda^*)$ is evidently real for $k > 0$. On the other hand, when $k < 0$, it can be simplified to the evidently real form

$$\nu(\lambda^*) = -\frac{\alpha}{3} [1 - 2 \cos(\phi/3)], \quad (355b)$$

where $\phi = \tan^{-1} [3\sqrt{3|k|}/(1+2k)] \in [0, \pi]$.

In the limit $w \rightarrow \pm\infty$, from Eq. (354) we have, $\alpha \rightarrow (1 + \delta^2)/(2\delta)$ and $b \rightarrow 0$. Therefore, $l \rightarrow 0$ and $k \rightarrow -1$, giving $\phi \rightarrow \pi$. This yields, $\nu(\lambda^*) \rightarrow 0$. On the other hand, for $w \rightarrow 0$, we have, $\alpha \sim \theta/(2\delta w^2)$. Using this we find that $\nu(\lambda^*) \rightarrow \sqrt{1 + \theta}$. It is also evident as Eq. (352) gives $\lambda^* = 1/2$ for $w = 0$, and then, from Eq. (339c) we get $\nu(1/2) = \sqrt{1 + \theta}$.

Now using Eq. (352), the saddle point $\lambda^*(w)$ can be expressed in terms of $\nu(\lambda^*)$. Therefore, the function $f_w(\lambda)$ at the saddle-point λ^* , can be expressed in terms of $\nu(\lambda^*)$, and is given by

$$\begin{aligned} h_s(w) &:= f_w(\lambda^*) \\ &= \frac{1}{2} \left[\frac{1}{\delta} + 1 + w \right] - \frac{1}{2} \left[\frac{1}{\delta} + \frac{w^2}{\theta} \nu(\lambda^*) \right] \sqrt{1 + \delta^2 + 2\delta\nu(\lambda^*)}. \end{aligned} \quad (356)$$

To find the region in which λ^* lies, it is useful to express $\nu(\lambda)$ in the form

$$\nu(\lambda) = \sqrt{4\theta(\lambda_+ - \lambda)(\lambda - \lambda_-)}, \quad (357)$$

where

$$\lambda_{\pm} = \frac{1}{2} \left[1 \pm \sqrt{1 + \theta^{-1}} \right]. \quad (358)$$

Clearly, $\nu(\lambda)$ has two branch points on the real- λ line at λ_{\pm} . Moreover, it is real and positive in the (real) interval $\lambda \in (\lambda_-, \lambda_+)$. Since, $\lambda_+ -$

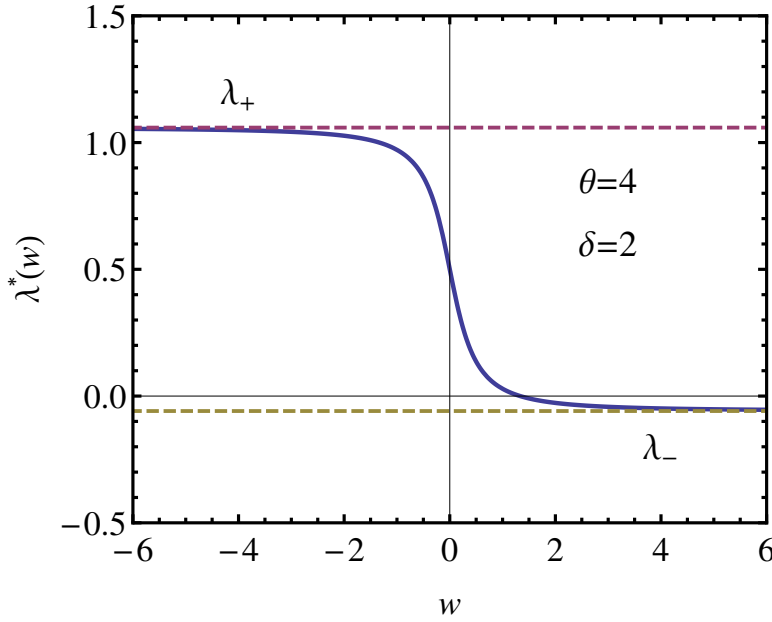


Figure 14: The behavior of λ^* is shown (solid line) as a function of w , for a set of parameters $\theta = 4$, $\delta = 2$, which merges to λ_{\pm} (dashed lines) as $w \rightarrow \mp\infty$.

$\lambda_- = \sqrt{1 + \theta^{-1}}$, as $\lambda \rightarrow \lambda_{\pm}$, we have $\nu(\lambda) \rightarrow 2[\theta(1 + \theta)]^{1/4}|\lambda - \lambda_{\pm}|^{1/2}$.

Therefore, from Eq. (352) we get

$$w \rightarrow \mp \frac{[\theta(1 + \theta)]^{1/4}}{2\sqrt{1 + \delta^2}}|\lambda^* - \lambda_{\pm}|^{-1/2}, \quad \text{as } \lambda^* \rightarrow \lambda_{\pm}. \quad (359)$$

In other words, $\lambda^*(w)$ merges to λ_{\pm} as one takes the limit $w \rightarrow \mp\infty$. This also agrees with the observation that $\nu(\lambda^*) \rightarrow 0$ as $|w| \rightarrow \infty$. For any finite w the saddle point $\lambda^* \in (\lambda_-, \lambda_+)$. In Fig. 14 we plot the saddle point λ^* as a function of w using Eq. (352).

Now, if $g(\lambda)$ is analytic in the range $\lambda \in (0, \lambda^*)$, we can deform the contour along the path of the steepest descent through the saddle point, and obtain $P(W_{\tau})$ using the usual saddle point method. However, more sophistication is needed when $g(\lambda)$ contains singularities. Therefore it is essential to analyze $g(\lambda)$ for possible singularities.

We first recall $g(\lambda)$ from Eq. (340) and Eq. (341),

$$g(\lambda) = [f_1(\lambda, \theta, \delta)]^{-1/2} [f_2(\lambda, \theta, \delta)]^{-1/2}. \quad (360)$$

Following Sec. 4.5, we also recall that $f_1(\lambda, \theta, \delta)$ does not change its sign and always stays positive in the region $[\lambda_-, \lambda_+]$. This is not the

case for $f_2(\lambda, \theta, \delta)$. While $f_2(\lambda, \theta, \delta) > 0$ for $\lambda_- \leq \lambda \leq 0$, in some region in the (θ, δ) space, $f_2(\lambda_+, \theta, \delta) < 0$. Therefore, in that (θ, δ) region, $f_2(\lambda, \theta, \delta)$ must have a zero at some intermediate $\lambda = \lambda_0 > 0$, which gives rise to a branch-point singularity in $g(\lambda)$. Figure 13 shows parameter region in which $g(\lambda)$ possesses a singularity. The phase boundary between the region which $g(\lambda)$ has a singularity and the singularity-free region is given by the equation $f_2(\lambda_+, \theta, \delta) = 0$. In the limit $\delta \rightarrow 0$ we get $\theta \rightarrow 1/3$.

4.7.1 Case of no singularities

In the singularity free region (Fig. 13), the asymptotic PDF of the work done is obtained using the standard saddle point method, which gives

$$P(W_\tau = w\tau/\tau_\gamma) \approx \frac{g(\lambda^*) e^{\frac{\tau}{\tau_\gamma} h_s(w)}}{\sqrt{2\pi \frac{\tau}{\tau_\gamma} f''_w(\lambda^*)}}, \quad (361)$$

where $h_s(w)$ is given by Eq. (356) and

$$f''_w(\lambda^*) = -\frac{\tilde{v}''(\lambda^*)}{2} = \frac{2}{v(\lambda^*)} \frac{\theta + w^2[1 + \delta^2 + 3\delta v(\lambda^*)]}{[1 + \delta^2 + 2\delta v(\lambda^*)]^{1/2}}, \quad (362)$$

which is expressed in terms of w and $v(\lambda^*)$ given by Eq. (355). Fig. 15 shows a very good agreement between the analytic result given by Eq. (361) and numerical simulations.

4.7.2 Case of a singularity

For a given value of δ and θ , the location of the branch point λ_0 is fixed between the origin and λ_+ . On the other hand, the saddle point λ^* increases monotonically along the real- λ line from λ_- to λ_+ as w decreases from $+\infty$ to $-\infty$. For sufficiently large w , the saddle point lies in the interval (λ_-, λ_0) and therefore, the contour of integration can be deformed into the steepest descent path, which passes through

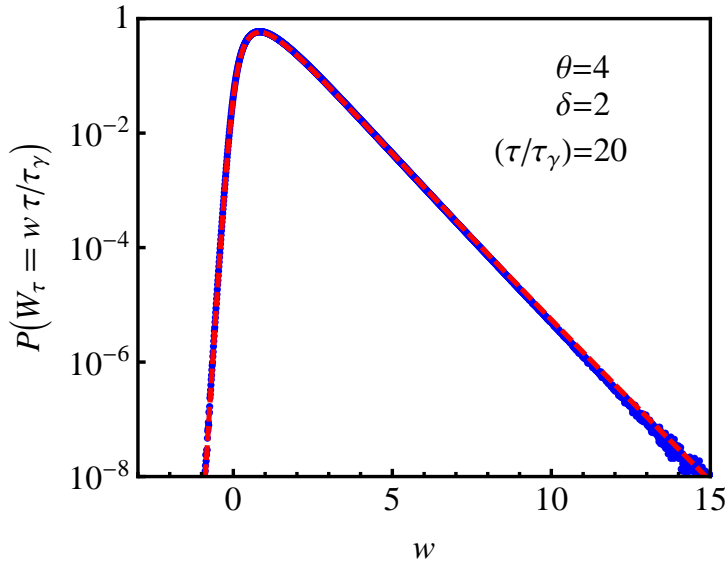


Figure 15: The (red) dashed line plots the analytical result of $P(W_\tau)$ against the scaled variable $w = W_\tau/(\tau/\tau_\gamma)$, while the (blue) points are numerical simulation results.

the saddle point, without touching λ_0 . However, as w decreases, the saddle point hits the branch point at some specific value $w = w^*$ given by

$$\lambda^*(w^*) = \lambda_0 . \tag{363}$$

For $w < w^*$, the steepest descent contour wraps around the branch cut between λ_0 and λ^* . We here present the results for both regimes $w < w^*$ and $w > w^*$ respectively, applying the method developed in [103].

4.7.2.1 $w > w^*$

For $w > w^*$, the contour is deformed through the saddle point without touching the singularity and we obtain

$$P(W_\tau = w\tau/\tau_\gamma) \approx \frac{g(\lambda^*)e^{\frac{\tau}{\tau_\gamma}h_s(w)}}{\sqrt{2\pi\frac{\tau}{\tau_\gamma}f''_w(\lambda^*)}} R_1 \left(\sqrt{\frac{\tau}{\tau_\gamma} [h_0(w) - h_s(w)]} \right), \tag{364}$$

where $f''_w(\lambda^*)$ is given by Eq. (362) and the function $R_1(z)$ is given by

$$R_1(z) := \frac{z}{\sqrt{\pi}} e^{z^2/2} K_{1/4}(z^2/2), \quad (365)$$

with $K_{1/4}(z)$ being the modified Bessel function of the second kind.

4.7.2.2 $w < w^*$

For $w < w^*$, the contribution comes from both the branch point and the saddle point i.e.

$$P(W_\tau) \approx P_B(W_\tau) + P_S(W_\tau), \quad (366)$$

where the branch point contribution is

$$P_B(W_\tau = w\tau/\tau_\gamma) \approx \frac{\tilde{g}(\lambda_0) e^{\frac{\tau}{\tau_\gamma} h_0(w)}}{\sqrt{\pi \frac{\tau}{\tau_\gamma} |f'_w(\lambda_0)|}} R_2\left(\sqrt{\frac{\tau}{\tau_\gamma} [h_0(w) - h_s(w)]}\right), \quad (367)$$

where

$$h_0(w) := f_w(\lambda_0) = \frac{1}{2}[1 - \bar{v}(\lambda_0)] + \lambda_0 w, \quad (368)$$

$$f'_w(\lambda_0) = -\frac{\bar{v}'(\lambda_0)}{2} + w, \quad (369)$$

$$\tilde{g}(\lambda_0) = \lim_{\lambda \rightarrow \lambda_0} |\sqrt{\lambda - \lambda_0} g(\lambda)|, \quad (370)$$

and

$$R_2(z) = \sqrt{\frac{2z}{\pi}} \int_0^z \frac{1}{\sqrt{u}} e^{-2zu+u^2} du. \quad (371)$$

The contribution coming from the saddle point is given by

$$P_S(W_\tau = w\tau/\tau_\gamma) \approx \frac{|g(\lambda^*)| e^{\frac{\tau}{\tau_\gamma} h_s(w)}}{\sqrt{2\pi \frac{\tau}{\tau_\gamma} |f''_w(\lambda^*)|}} R_4\left(\sqrt{\frac{\tau}{\tau_\gamma} [h_0(w) - h_s(w)]}\right), \quad (372)$$

where the function $R_4(z)$ is given by

$$R_4(z) = \sqrt{\frac{\pi}{2}} z e^{z^2/2} \left[I_{-1/4}(z^2/2) + I_{1/4}(z^2/2) \right] - \frac{4z}{\pi} {}_2F_2(1/2, 1; 3/4, 5/4; z^2), \quad (373)$$

and $I_{\pm 1/4}(z)$ are modified Bessel functions of the first kind and ${}_2F_2(a_1, a_2; b_1, b_2; z)$ is the generalized hypergeometric function. We again find a very good agreement between the analytical results and numerical simulations Fig. 16.

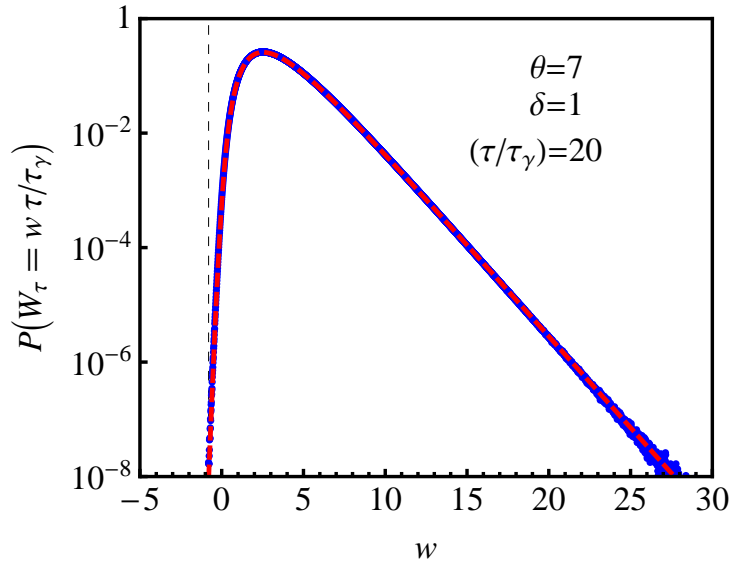


Figure 16: The (red) dashed line plots the analytical result for $P(W_\tau)$, while the (blue) points are numerical simulation results. The vertical dashed line marks the position of the singularity $w^* = -0.801661\dots$ for the values of $\theta = 7$, $\delta = 1$.

4.8 THE CASE OF A BROWNIAN PARTICLE CONNECTED TO TWO THERMOSTATS

We now move to analyze the $\delta = 0$ case, which becomes a special case of the problem of a single Brownian particle connected with two heat baths at different temperatures. This model was introduced by introduced by Derrida and Brunet [111] and later studied by Visco [69] and Imparato [70] in great details. However, these authors computed the current profile and the incomplete LDFs in this problem. Here, we obtain the full statistics.

We first note that, $g(\lambda)$ takes a simple form in the limit $\delta \rightarrow 0$, given by,

$$g(\lambda) = \frac{\sqrt{2\nu}}{\sqrt{\nu+1+2\lambda\theta}} \frac{\sqrt{2}}{\sqrt{\nu+1-2\lambda\theta}}. \quad (374)$$

It is easy to show [100, 71] that $g(\lambda)$ is completely analytic for $\theta \leq 1/3$, and the PDF is obtained using the saddle point method as,

$$P(W_\tau = w\tau/\tau_\gamma) \approx \frac{g(\lambda^*) e^{\frac{\tau}{\tau_\gamma} h_s(w)}}{\sqrt{2\pi \frac{\tau}{\tau_\gamma} f''_w(\lambda^*)}}, \quad (375)$$

where the second derivative of $f_w(\lambda)$ along the real- λ axis at λ^* is given by [100, 71],

$$f''_w(\lambda^*) = \frac{2(w^2 + \theta)^{3/2}}{\sqrt{\theta(1 + \theta)}}, \quad (376)$$

and

$$h_s(w) := f_w(\lambda^*) = \frac{1}{2} \left[1 + w - \sqrt{w^2 + \theta} \sqrt{1 + \frac{1}{\theta}} \right]. \quad (377)$$

On the other hand, if $\theta > 1/3$, it is easy to show that $g(\lambda)$ picks up a branch point singularity at $\lambda = \lambda_0 = 2/(1 + \theta)$, which corresponds to [100, 71],

$$w^* = \frac{\theta(\theta - 3)}{3\theta - 1}. \quad (378)$$

Then one needs to perform a contour integration avoiding the branch cut as mentioned in the last section. For $w > w^*$, using the same prescription [103], we find the PDF as

$$P(W_\tau = w\tau/\tau_\gamma) \approx \frac{g(\lambda^*) e^{\frac{\tau}{\tau_\gamma} h_s(w)}}{\sqrt{2\pi \frac{\tau}{\tau_\gamma} f''_w(\lambda^*)}} \mathbf{R}_1 \left(\sqrt{\frac{\tau}{\tau_\gamma} [h_0(w) - h_s(w)]} \right), \quad (379)$$

where

$$h_0(w) := f_w(\lambda_0) = \frac{1 - \theta}{1 + \theta} + \frac{2w}{1 + \theta}. \quad (380)$$

For $w < w^*$, the contribution to the PDF comes both from the saddle and the branch point.

$$P(W_\tau) \approx P_B(W_\tau) + P_S(W_\tau), \quad (381)$$

where the branch point contribution is

$$P_B(W_\tau = w\tau/\tau_\gamma) \approx \frac{\tilde{g}(\lambda_0) e^{\frac{\tau}{\tau_\gamma} h_0(w)}}{\sqrt{\pi \frac{\tau}{\tau_\gamma} |f'_w(\lambda_0)|}} \mathbf{R}_2 \left(\sqrt{\frac{\tau}{\tau_\gamma} [h_0(w) - h_s(w)]} \right), \quad (382)$$

where

$$\begin{aligned}\tilde{g}(\lambda_0) &= \frac{3\theta - 1}{2\theta\sqrt{2(1+\theta)}}, \\ f'_w(\lambda_0) &= w - w^*,\end{aligned}\quad (383)$$

and the function $R_2(z)$ is given by Eq. (407). The contribution coming from the saddle point is given by

$$P_S(W_\tau = w\tau/\tau_\gamma) \approx \frac{|g(\lambda^*)|e^{\frac{\tau}{\tau_\gamma}h_s(w)}}{\sqrt{2\pi\frac{\tau}{\tau_\gamma}|f''_w(\lambda^*)|}} R_4\left(\sqrt{\frac{\tau}{\tau_\gamma}[h_0(w) - h_s(w)]}\right),\quad (384)$$

where the function $R_4(z)$ is given by Eq. (373). Figure 17 compares the analytical results with the numerical simulations.

4.9 LARGE DEVIATION FUNCTION AND THE FLUCTUATION THEOREMS

The LDF, associated with the PDF, is defined as

$$h(w) = \lim_{(\tau/\tau_\gamma) \rightarrow \infty} \frac{1}{(\tau/\tau_\gamma)} \ln P(W_\tau = w\tau/\tau_\gamma). \quad (385)$$

Due to the large deviation form of the PDF, $P(W_\tau = w\tau/\tau_\gamma) \sim e^{(\tau/\tau_\gamma)h(w)}$, the FT given by Eq. (151), is equivalent to the following symmetry relation of the LDF:

$$h(w) - h(-w) = w. \quad (386)$$

Now, in the parameter region where $g(\lambda)$ is analytic [see Fig. 13], the LDF is given by $h(w) = h_s(w)$. In this case, it is clear from Eq. (356) that the above symmetry relation (386) holds, as $v(\lambda^*)$ is an even function in w .

On the other hand, in the parameter region where $g(\lambda)$ has a singularity, the LDF is given by

$$h(w) = \begin{cases} h_s(w) & \text{for } w > w^*, \\ h_0(w) & \text{for } w < w^*. \end{cases} \quad (387)$$

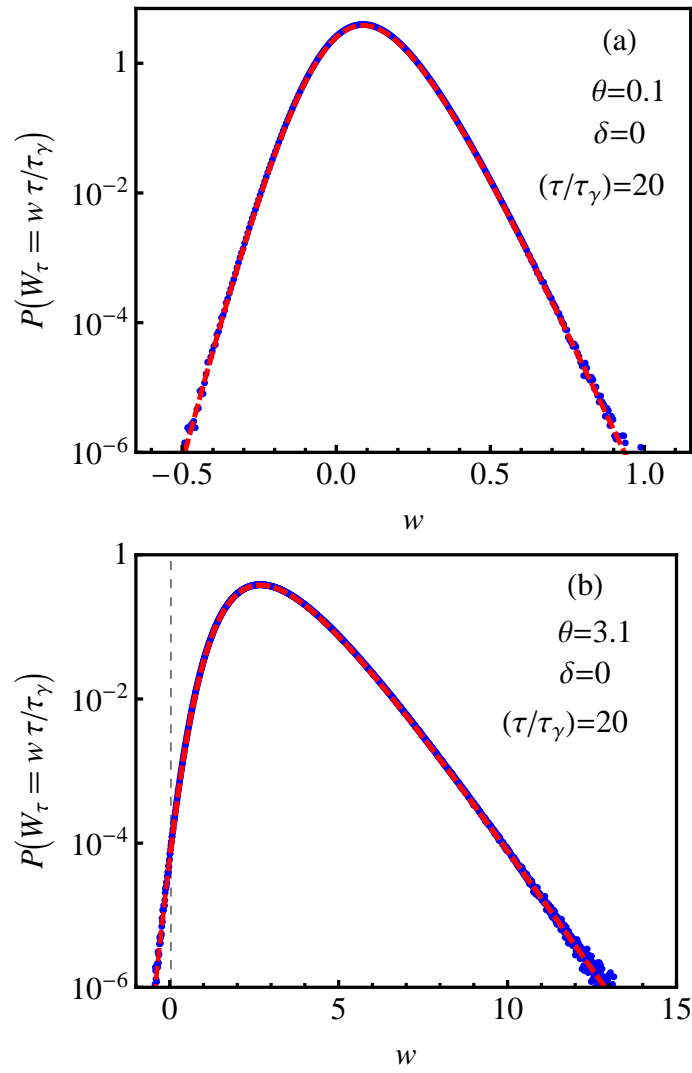


Figure 17: The (red) dashed lines plot analytical results for $P(W_\tau)$, while the (blue) points are numerical simulation results, for the $\delta = 0$ case. The vertical dashed line in (b) marks the position of the singularity which is $w^* = 0.037\dots$ in this case.

Therefore, it is evident that if $w^* < 0$, the symmetry relation (386) holds only in the specific range $w^* < w < -w^*$. Otherwise, it fails to satisfy. Nevertheless, even for $w > w^*$, one still gets a linear relation $h(w) - h(-w) = 2\lambda_0 w$, in the range $w \in (-w^*, w^*)$.

4.10 SUMMARY

In this chapter, we have discussed an underdamped Brownian particle driven by an external correlated stochastic force, modelled by an Ornstein-Uhlenbeck process. We have studied the probability density function of the work done W_τ on the particle by the external random force, in a given time τ . The behavior can be characterized, as before, in terms of two dimensionless parameters, namely, (i) θ , that gives the relative strength between the external random force and the thermal noise, and (ii) δ , that characterizes the ratio between the viscous relaxation time and the correlation time of the external force. In the large τ limit, we obtain the moment generating function (MGF) and then analyze the sub-dominant prefactor. We then compute the PDF by carefully inverting the MGF considering the analytic and singular properties of the prefactor. The entire analytical results have been supported by numerical simulations. We find that in the limit $\delta \rightarrow 0$, our model becomes a special case of a problem of a single Brownian particle coupled to two distinct reservoirs, first proposed by Derrida and Brunet and later studied by Visco. We have computed the full distribution function of the heat flowing from one end to the other which is of very importance in the context of heat transport. Further, we have looked at the validity of the FT for these observables, in terms of the symmetry properties of the large deviation function. We have found that in the (θ, δ) region where $g(\lambda)$ is analytic, the FT is satisfied. On the other hand, in the non-analytic region, the symmetry of the large deviation function breaks down. In particular, the PDF picks up an exponential tail characterized by the singularity and this leads to the violation of the steady state fluctuation theorems.

Along with this work, the issue of a detailed description of the heat flow within two reservoirs connected to a system modelled as a Brownian particle, which was lacking, is now resolved. Perhaps it does not depict the real situation completely, it is of particular impor-

tance since a few exact results are achievable and also few predictions made earlier by the linear response theory can be reverified. Furthermore, we are able to give the full distribution functions for these observables from which any average quantity, specifically the average current, can be computed and verified through experiments. Finally, we provide a nontrivial example where one can compute a whole set of large deviation functions exactly.

ASYMPTOTIC EXPANSIONS OF THE INTEGRALS AROUND THE BRANCH POINT

A.1 STEEPEST DESCENT METHOD WITH A BRANCH POINT

Let us consider the integral

$$I = \frac{1}{2\pi i} \int_{-i\infty}^{i\infty} g_1(\lambda) \frac{e^{\tau f_w(\lambda)}}{\sqrt{\lambda_a - \lambda}} d\lambda, \quad (388)$$

where $\lambda_a > 0$. The position of the saddle point λ^* depends on the value of w , and depending on whether $w > w_a^*$ or $w < w_a^*$ we have $\lambda^* < \lambda_a$ or $\lambda^* > \lambda_a$ respectively. In the following, we consider the two cases one by one.

A.1.1 *The branch point is not between the origin and the saddle point:*

$$\lambda_a \notin (0, \lambda^*)$$

In this case, since λ_a lies outside the interval $(0, \lambda^*)$, one can deform the contour of integration in Eq. (388) into the steepest descent path through λ^* without hitting λ_a (see Fig. 18). Along the steepest descent contour we define

$$f_w(\lambda) - f_w(\lambda^*) = -u^2. \quad (389)$$

Therefore, λ_a is mapped to a branch point at $u = -ib$ with

$$b = \sqrt{f_w(\lambda_a) - f_w(\lambda^*)} \quad (390)$$

and Eq. (388) becomes

$$I = \frac{e^{\tau f_w(\lambda^*)}}{2\pi i} \int_{-\infty}^{\infty} q_1(u) \frac{e^{-\tau u^2}}{\sqrt{b - iu}} du \quad (391)$$

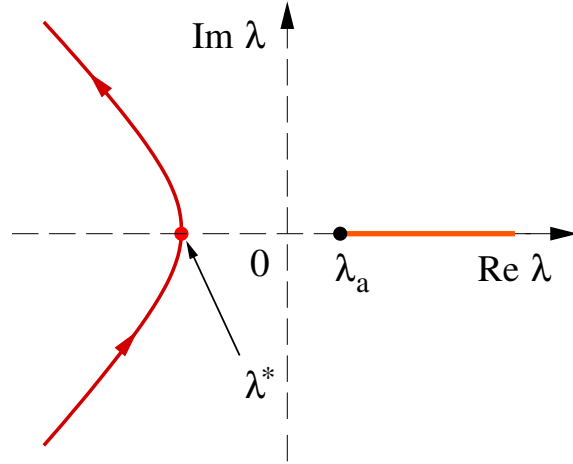


Figure 18: (Color online) Schematic steepest descent contour (in red) for the case when the branch point λ_a is not between the origin and the saddle point λ^* . Here, it is shown for $\lambda^* < 0$, however, one can also have $\lambda^* \in (0, \lambda_a)$. The direction towards which the contour bends, depends on the value of w . Here, it is shown for $w < 0$. For $w > 0$ the contour bends towards the positive $\text{Re}(\lambda)$ axis, whereas for $w = 0$, the steepest descent contour is parallel to the $\text{Im}(\lambda)$ axis. The thick solid (orange) line along the $\text{Re}(\lambda)$ axis from λ_a represents the branch cut.

with

$$q_1(u) = g_1(\lambda) \frac{\sqrt{b - iu}}{\sqrt{\lambda_a - \lambda}} \frac{d\lambda}{du}. \quad (392)$$

Now, making a change of variable $\sqrt{\tau}u \rightarrow u$ and taking the large- τ limit we get

$$I \approx \frac{e^{\tau f_w(\lambda^*)}}{2\pi i} q_1(0) \tau^{-1/4} \int_{-\infty}^{\infty} \frac{e^{-u^2}}{\sqrt{b\sqrt{\tau} - iu}} du, \quad (393)$$

where

$$q_1(0) = g_1(\lambda^*) \frac{\sqrt{b}}{\sqrt{\lambda_a - \lambda^*}} \frac{d\lambda}{du} \Big|_{\lambda \rightarrow \lambda^*}. \quad (394)$$

Using $-u^2 = \frac{1}{2}f''(\lambda^*)(\lambda - \lambda^*)^2 + \dots$ as $\lambda \rightarrow \lambda^*$, it can be found that

$$\frac{d\lambda}{du} \Big|_{\lambda \rightarrow \lambda^*} = \frac{i\sqrt{2}}{\sqrt{f''(\lambda^*)}}. \quad (395)$$

Therefore, we get

$$I \approx \frac{g_1(\lambda^*)}{\sqrt{\lambda_a - \lambda^*}} \frac{e^{\tau f_w(\lambda^*)}}{\sqrt{2\pi\tau f''_w(\lambda^*)}} R_1(\sqrt{\tau}b), \quad (396)$$

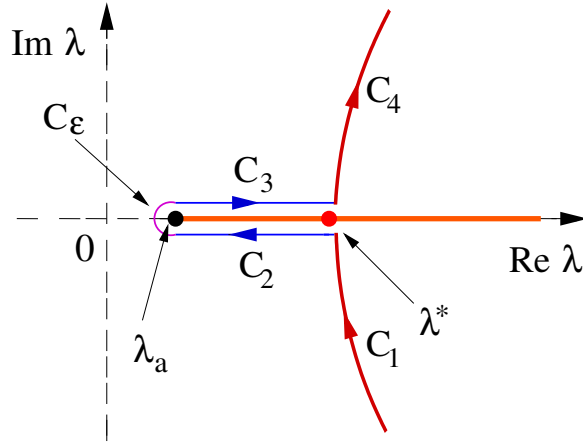


Figure 19: (Color online) Schematic steepest descent contour for the case when the branch point λ_a is between the origin and the saddle point λ^* . The thick solid (orange) line along the $\text{Re}(\lambda)$ axis from λ_a represents the branch cut. The steepest descent contour goes around the branch cut as shown by C_2 and C_3 (in blue). The contribution coming from the circular contour (in magenta) C_ϵ around the branch point becomes zero in the limit of the radius $\epsilon \rightarrow 0$. The direction towards which the contours C_1 and C_4 (shown in red) bend, depends on the value of w . Here, it is shown for $w > 0$. For $w < 0$ the C_1 and C_4 bend towards the negative $\text{Re}(\lambda)$ axis, whereas for $w = 0$, they are parallel to the $\text{Im}(\lambda)$ axis.

where

$$R_1(z) = \sqrt{\frac{z}{\pi}} \int_{-\infty}^{\infty} \frac{e^{-u^2}}{\sqrt{z - iu}} du. \tag{397}$$

We perform this integral in the Mathematica to get Eq. (121).

A.1.2 *The branch point is between the origin and the saddle point: $\lambda_a \in$*

$$(0, \lambda^*)$$

In this case, since λ_a lies in the interval $(0, \lambda^*)$, the deformed contour through λ^* wraps around the branch cut. The contour of integration $C = C_1 + C_2 + C_3 + C_4 + C_\epsilon$ is shown in Fig. 19. The contour C_ϵ

represents the circular contour of radius ϵ going around the branch point, and its contribution becomes zero in the limit $\epsilon \rightarrow 0$. The integral in Eq. (388) can be written as $I = P_B + P_S$, where $P_B(w, \tau)$ is the contribution coming from the integrations along the contours C_2 and C_3 , whereas P_S is the saddle point contribution coming from the integrations along the contours C_1 and C_4 . In the following we evaluate P_B and P_S .

A.1.2.1 Branch cut contribution

We consider,

$$P_B = \frac{1}{2\pi i} \int_{C_2+C_3} g_1(\lambda) \frac{e^{\tau f_w(\lambda)}}{\sqrt{\lambda_a - \lambda}} d\lambda. \quad (398)$$

We note that $\sqrt{\lambda_a - \lambda}$ changes when one goes from C_2 to C_3 . More precisely, $\lambda_a - \lambda = |\lambda_a - \lambda|e^{i\phi}$, where $\phi = +\pi$ on C_2 and $\phi = -\pi$ on C_3 (as $\phi = 0$ for $\lambda < \lambda_a$ on the real- λ line). Therefore, $\sqrt{\lambda_a - \lambda} = +i|\lambda_a - \lambda|^{1/2}$ on C_2 and $\sqrt{\lambda_a - \lambda} = -i|\lambda_a - \lambda|^{1/2}$ on C_3 , using which from Eq. (398) we get

$$P_B = \frac{1}{\pi} \int_{\lambda_a}^{\lambda^*} g_1(\lambda) \frac{e^{\tau f_w(\lambda)}}{|\lambda - \lambda_a|^{1/2}} d\lambda. \quad (399)$$

Since $f_w(\lambda)$ is real, $f_w(\lambda_a) > f_w(\lambda) > f_w(\lambda^*)$ for $\lambda_a < \lambda < \lambda^*$, and $f_w(\lambda)$ is minimum at λ^* along the real λ line, we set

$$f_w(\lambda) - f_w(\lambda_a) = -2bu + u^2. \quad (400)$$

The branch point λ_a is mapped to $u = 0$. Using $f'_w(\lambda^*) = 0$, we find that the saddle point is mapped to $u = b$, and b can be found by putting $\lambda = \lambda^*$ and $u = b$ in the above equation, which gives Eq. (390). With the above mapping from λ to u , Eq. (398) becomes

$$P_B = \frac{e^{\tau f_w(\lambda_a)}}{\pi} \int_0^b q_2(u) \frac{e^{-\tau(2bu - u^2)}}{\sqrt{u}} du, \quad (401)$$

where

$$q_2(u) = g_1(\lambda) \frac{\sqrt{u}}{|\lambda - \lambda_a|^{1/2}} \frac{d\lambda}{du}. \quad (402)$$

From Eq. (400), we get

$$\frac{d\lambda}{du} = \frac{2(u-b)}{f'_w(\lambda)}, \quad (403)$$

which is finite and nonzero everywhere between $u = 0$ and $u = b$.

Near $u = 0$ we get

$$\left. \frac{d\lambda}{du} \right|_{u=0} = \frac{2b}{-f'_w(\lambda_a)}. \quad (404)$$

On the other hand, near $u = b$, by applying L'Hospital rule to Eq. (403) we get

$$\left. \frac{d\lambda}{du} \right|_{u=b} = \frac{\sqrt{2}}{\sqrt{f''_w(\lambda^*)}}. \quad (405)$$

Now, making a change of variable $\sqrt{\tau}u \rightarrow u$ in Eq. (401) and then taking the large- τ limit we get

$$P_B \approx \frac{e^{\tau f_w(\lambda_a)} q_2(0)}{\pi \tau^{1/4}} R_2(\sqrt{\tau}b), \quad (406)$$

where

$$R_2(z) = \int_0^z \frac{1}{\sqrt{u}} e^{-2zu+u^2} du. \quad (407)$$

The asymptotic forms of $R_2(z)$ can be easily determined from the above integral, which gives $R_2(z) \sim \sqrt{\pi}/\sqrt{2z}$ as $z \rightarrow \infty$.

It can be shown that

$$\frac{\sqrt{u}}{|\lambda - \lambda_a|^{1/2}} \frac{d\lambda}{du} \xrightarrow[u \rightarrow 0]{\lambda \rightarrow \lambda_a} \left[\left. \frac{d\lambda}{du} \right|_{u=0} \right]^{1/2}. \quad (408)$$

Therefore,

$$q_2(0) = g_1(\lambda_a) \left[\left. \frac{d\lambda}{du} \right|_{u=0} \right]^{1/2}. \quad (409)$$

A.1.2.2 Saddle point contribution

We consider,

$$P_S = \frac{1}{2\pi i} \int_{C_1+C_4} g_1(\lambda) \frac{e^{\tau f_w(\lambda)}}{\sqrt{\lambda_a - \lambda}} d\lambda. \quad (410)$$

We make a transform from λ to u as defined by Eq. (389). In this case, the branch point λ_a is mapped to a branch point at $u = ib$ where b is given by Eq. (390), and Eq. (410) becomes

$$P_S = \frac{e^{\tau f_w(\lambda^*)}}{2\pi i} \int_{-\infty}^{\infty} q_3(u) \frac{e^{-\tau u^2}}{\sqrt{b + iu}} du \quad (411)$$

with

$$q_3(u) = g_1(\lambda) \frac{\sqrt{b + iu}}{\sqrt{\lambda_a - \lambda}} \frac{d\lambda}{du}. \quad (412)$$

We found in the preceding sub-subsection that $\sqrt{\lambda_a - \lambda^*} = \pm i|\lambda_a - \lambda^*|^{1/2}$ below (+) and above (−) the branch cut respectively. Therefore, $q_3(u)$ approaches two different limits as $u \rightarrow 0$ from above (0^+) and below (0^-) respectively:

$$q_3(0^\pm) = \mp \frac{g_1(\lambda^*)\sqrt{b}}{|\lambda_a - \lambda^*|^{1/2}} \frac{\sqrt{2}}{\sqrt{f''(\lambda^*)}}, \quad (413)$$

where we have used Eq. (395) for the Jacobian. Thus, upon changing $\sqrt{\tau}u \rightarrow u$ and taking the large- τ limit yields

$$P_S \approx \frac{g_1(\lambda^*)}{|\lambda_a - \lambda^*|^{1/2}} \frac{e^{\tau f_w(\lambda^*)}}{\sqrt{2\pi\tau f''(\lambda^*)}} R_4(\sqrt{\tau}b), \quad (414)$$

where

$$\begin{aligned} R_4(z) &= \sqrt{\frac{z}{\pi}} \left[\int_0^\infty \frac{e^{-u^2}}{\sqrt{z + iu}} du - \int_{-\infty}^0 \frac{e^{-u^2}}{\sqrt{z + iu}} du \right] i \\ &= \sqrt{\frac{z}{\pi}} \int_0^\infty du e^{-u^2} \left[\frac{1}{\sqrt{z + iu}} - \frac{1}{\sqrt{z - iu}} \right] i. \end{aligned} \quad (415)$$

We evaluate this integral in Mathematica to get Eq. (373), where the generalized hypergeometric function has the series expansion

$${}_2F_2(a_1, a_2; b_1, b_2; z) = \sum_{n=0}^{\infty} \frac{(a_1)_n (a_2)_n}{(b_1)_n (b_2)_n} \frac{z^n}{n!} \quad (416)$$

with $(a)_n = a(a+1)(a+2)\cdots(a+n-1)$, $(a)_0 = 1$ being the the Pochhammer symbol.

The large z behavior of $R_4(z)$ can be found by expanding the term inside the square bracket in Eq. (415) in powers of $1/z$ and integrating term by term. This gives $R_4(z) \simeq 1/(2\sqrt{\pi}z)$ for large z .

On the other hand, $R_4(z) \simeq \Gamma(1/4)\sqrt{z/2\pi}$ for small z . Using this together with $\lim_{\lambda^* \rightarrow \lambda_a} \sqrt{b/|\lambda_a - \lambda^*|}^{1/2} = [f''(\lambda^*)/2]^{1/4}$ in Eq. (414) we get

$$P_S \approx \frac{\Gamma(1/4) g_1(\lambda^*) e^{\tau f_w(\lambda^*)}}{2\pi [2\tau f_w''(\lambda^*)]^{1/4}} \quad \text{as } \lambda^* \rightarrow \lambda_a. \quad (417)$$

BIBLIOGRAPHY

- [1] Attard Phil. *Thermodynamics and statistical mechanics: equilibrium by entropy maximisation*. Academic Press, 2002.
- [2] De Groot Sybren Ruurds and Mazur Peter. *Non-equilibrium thermodynamics*. Courier Dover Publications, 2013.
- [3] Callen Herbert B. *Thermodynamic and an introduction to thermostatistics*. John Wiley & Sons, 2006.
- [4] Zemansky Mark Waldo. *Heat and thermodynamics*. McGraw-Hill, 1957.
- [5] Landau Lev Davidovich and Lifshitz Evgenii Mikhailovich. *Course of theoretical physics: Vol. 5 (Statistical Physics) and Vol. 9 (Statistical Physics-Part 2: Theory of the Condensed State)*. Elsevier, 1980.
- [6] Huang Kerson. *Introduction to statistical physics*. CRC Press, 2001.
- [7] Plischke Michael and Bergersen Michael. *Equilibrium statistical physics*. World Scientific, 2006.
- [8] Reif Frederick. *Fundamentals of statistical and thermal physics*. Waveland Press, 2009.
- [9] Reichl LE. *A modern course in statistical physics*. 1998. *Edward Arnold, London*, 1986.
- [10] Hill Terrell L. *Statistical mechanics: principles and selected applications*. Courier Dover Publications, 2013.
- [11] Peliti Luca. *Statistical mechanics in a nutshell*. Princeton University Press, 2011.

- [12] Chandler David. Introduction to modern statistical mechanics. *Introduction to Modern Statistical Mechanics, by David Chandler, pp. 288. Foreword by David Chandler. Oxford University Press, Sep 1987. ISBN-10: 0195042778. ISBN-13: 9780195042771, 1, 1987.*
- [13] Van Kampen Nicolaas Godfried. *Stochastic processes in physics and chemistry, volume 1.* Elsevier, 1992.
- [14] Risken Hannes. *Fokker-Planck Equation.* Springer, 1984.
- [15] Gardiner CW. *Stochastic methods.* Springer-Verlag, Berlin–Heidelberg–New York–Tokyo, 1985.
- [16] Balakrishnan Venkataraman. *Elements of Nonequilibrium Statistical Mechanics.* Ane Books, 2008.
- [17] Zwanzig RW. *Nonequilibrium statistical mechanics.* Oxford Univ. Press, 2001.
- [18] Pottier Noëlle. *Nonequilibrium statistical physics.* Oxford Univ. Press, 2010.
- [19] Chou T., Mallick K., and Zia R K P. *Rep. Prog. Phys., 74(11):116601, 2011.*
- [20] Garnier N and Ciliberto S. *Phys. Rev. E, 71(6):060101 (R), 2005.*
- [21] Kubo R. *Reports on Progress in Physics, 29(1):255, 1966.*
- [22] Green Melville S. *The Journal of Chemical Physics, 22(3):398–413, 1954.*
- [23] Kubo R. *Journal of the Physical Society of Japan, 12(6):570–586, 1957.*
- [24] Marconi UMB, Puglisi A, Rondoni L, and Vulpiani A. *Physics Reports, 461(4-6):111–195, 2008.*
- [25] Wax Nelson. *Selected papers on noise and stochastic processes.* Courier Dover Publications, 2003.

- [26] Rudnick Joseph Alan and Gaspari George David. *Elements of the random walk: an introduction for advanced students and researchers*. Cambridge University Press, 2004.
- [27] Weiss G. *Aspects and Applications of the Random Walk (Random Materials & Processes S.)*. North-Holland, 2005.
- [28] Mazo Robert M. *Brownian motion*. Oxford Univ. Press, 2008.
- [29] Sekimoto K. *Berlin:Springer*, 799, 2010.
- [30] Ciliberto S, Joubaud S, and Petrosyan A. *J. Stat. Mech.*, 2010(12):P12003, 2010.
- [31] Ritort F. *J. Phys.: Condens. Matter*, 18(32):R531, 2006.
- [32] Alemany A., Ribezzi M., and Ritort F. *AIP Conference Proceedings*, 1332(1):96–110, 2011.
- [33] Seifert U. *Reports on Progress in Physics*, 75(12):126001, 2012.
- [34] Jarzynski C. *Annu. Rev. Condens. Matter Phys.*, 2(1):329, 2011.
- [35] Van den Broeck C and Esposito M. *Physica A: Statistical Mechanics and its Applications*, 418(0):6 – 16, 2015. Proceedings of the 13th International Summer School on Fundamental Problems in Statistical Physics.
- [36] Evans D J and Searles D J. *Adv. Phys.*, 51(7):1529, 2002.
- [37] Gallavotti G. *Statistical Mechanics: A Short Treatise*, 1999.
- [38] Sevick EM, Prabhakar R, Williams SR, and Searles DJ. *Annu. Rev. Phys. Chem.*, 59(1):603, 2008.
- [39] Jarzynski C. *The European Physical Journal B-Condensed Matter and Complex Systems*, 64(3):331–340, 2008.
- [40] Evans D J and Searles D J. *Phys. Rev. E*, 50(2):1645, 1994.
- [41] Evans Denis J., Cohen E. G. D., and Morriss G. P. *Phys. Rev. Lett.*, 71:2401–2404, 1993.

- [42] Mazonka O and Jarzynski C. *arxiv*, (09912121), 1999.
- [43] van Zon R and Cohen E G D. *Phys. Rev. E*, 67(4):046102, 2003.
- [44] van Zon R and Cohen E G D. *Phys. Rev. Lett.*, 91(11):110601, 2003.
- [45] van Zon R and Cohen E G D. *Phys. Rev. E*, 69(5):056121, 2004.
- [46] Jarzynski C. *Phys. Rev. Lett.*, 78:2690–2693, 1997.
- [47] Jarzynski C. *Phys. Rev. E*, 56:5018–5035, 1997.
- [48] Jarzynski C. *Progress of Theoretical Physics Supplement*, 165:1–17, 2006.
- [49] Liphardt J, Dumont S, Smith S B, Tinoco Jr I, and Bustamante C. *Science*, 296(5574):1832, 2002.
- [50] Collin D, Ritort F, Jarzynski C, Smith S B, Tinoco I, and Bustamante C. *Nature*, 437(7056):231, 2005.
- [51] Saha A and Jayannavar A M. *Phys. Rev. E*, 77(2):022105, 2008.
- [52] Jayannavar A M and Sahoo M. *Phys. Rev. E*, 75(3):032102, 2007.
- [53] Jimenez-Aquino J I, Velasco R M, and Uribe F J. *Phys. Rev. E*, 79(6):061109, 2009.
- [54] Jimenez-Aquino J I, Uribe F J, and Velasco R M. *J. Phys. A: Math. Theor.*, 43(25):255001, 2010.
- [55] Jimenez-Aquino J I. *Phys. Rev. E*, 82(5):051118, 2010.
- [56] Jimenez-Aquino J I. *J. Phys. A: Math. Theor.*, 44(29):295002, 2011.
- [57] Crooks Gavin E. *Phys. Rev. E*, 60:2721–2726, 1999.
- [58] Crooks Gavin E. *Phys. Rev. E*, 60:2721–2726, 1999.
- [59] Seifert U. *Phys. Rev. Lett.*, 95:040602, 2005.
- [60] Lahiri S Saha A and Jayannavar A M. *Phys. Rev. E*, 80(1):011117, 2009.

- [61] Gallavotti G. and Cohen E. G. D. *Phys. Rev. Lett.*, 74:2694–2697, 1995.
- [62] Lebowitz J L and Spohn H. *J. Stat. Phys.*, 95(1/2):333, 1999.
- [63] Kurchan J. *J. Phys. A: Math. Gen.*, 31(16):3719, 1998.
- [64] Maes C. *Seminare Poincare*, 2:29, 2003.
- [65] Maes C and Netocny K. *J. Stat. Phys.*, 110(1/2):269, 2003.
- [66] Farago J. *J. Stat. Phys.*, 107(3/4):781, 2002.
- [67] Imperato A and Peliti L. *C. R. Physique*, 8(5-6):556, 2007.
- [68] Baiesi Marco, Jacobs Tim, Maes Christian, and Skantzos Nikos
S. Phys. Rev. E, 74:021111, 2006.
- [69] Visco P. *J. Stat. Mech.*, 2006(06):P06006, 2006.
- [70] Fogedby H C and Imperato A. *J. Stat. Mech.*, 2011(05):P05015, 2011.
- [71] Sabhapandit S. *Phys. Rev. E*, 85(2):021108, 2012.
- [72] Saito K and Dhar A. *Phys. Rev. E*, 83(4):041121, 2011.
- [73] Kundu A, Sabhapandit S, and Dhar A. *J. Stat. Mech.*, 2011(03):P03007, 2011.
- [74] Fogedby H C and Imperato A. *J. Stat. Mech.*, 2012(04), 2012.
- [75] Saito K and Dhar A. *Phys. Rev. Lett.*, 104(4):040601, 2010.
- [76] Taniguchi T and Cohen E G D. *J. Stat. Phys.*, 126(1):1, 2007.
- [77] Taniguchi T and Cohen E G D. *J. Stat. Phys.*, 130(1):1, 2008.
- [78] Taniguchi T and Cohen E G D. *J. Stat. Phys.*, 130(4):633, 2008.
- [79] Cohen E G D. *J. Stat. Mech.*, 2008(07):P07014, 2008.
- [80] Hatano T and Sasa SI. *Phys. Rev. Lett.*, 86:3463–3466, 2001.

- [81] Sasa SI. *Journal of Statistical Mechanics: Theory and Experiment*, 2014(1):P01004, 2014.
- [82] Wang G M, Sevick E M, Mittag E, Searles D J, and Evans D J. *Phys. Rev. Lett.*, 89(5):050601, 2002.
- [83] Wang G M, Reid J C, Carberry D M, and Williams D R M. *Phys. Rev. E*, 71(4):046142, 2005.
- [84] Trepagnier E H, Jarzynski C, Ritort F, Crooks G E, Bustamante C J, and Liphardt J. *Proc. Natl Acad. Sci. USA*, 101(42):15038, 2004.
- [85] van Zon R, Ciliberto S, and Cohen E G D. *Phys. Rev. Lett.*, 92(13):130601, 2004.
- [86] Ciliberto S, Imperato A., Naert A., and Tanase M. *Phys. Rev. Lett.*, 110(18).
- [87] Carberry D M, Reid J C, Wang G M, Sevick E M, Searles D J, and Evans D J. *Phys. Rev. Lett.*, 92(14):140601, 2004.
- [88] Khan M and Sood A K. *Europhys. Lett.*, 94(6):60003, 2011.
- [89] Blickle V, Speck T, Helden L, Seifert U, and Bechinger C. *Phys. Rev. Lett.*, 96(7):070603, 2006.
- [90] Douarche F, Ciliberto S, Petrosyan A, and Rabbiosi I. *Europhys. Lett.*, 70(5):593, 2005.
- [91] Douarche F, Ciliberto S, and Petrosyan A. *J. Stat. Mech.*, 2005(09):P09011, 2005.
- [92] Douarche F, Joubaud S, Garnier N B, Petrosyan A, and Ciliberto S. *Phys. Rev. Lett.*, 97(14):140603, 2006.
- [93] Speck T, Blickle V, Bechinger C, and Seifert U. *Europhys. Lett.*, 79(3):30002, 2007.
- [94] Touchette H. *Physics Reports*, 478(1-3):1 – 69, 2009.

- [95] Derrida B. *Journal of Statistical Mechanics: Theory and Experiment*, 2007(07):P07023, 2007.
- [96] Harris R J and Schutz G M. *Journal of Statistical Mechanics: Theory and Experiment*, 2007(07):P07020, 2007.
- [97] Kurchan J. *Physica A: Statistical Mechanics and its Applications*, 418(0):170–188, 2015.
- [98] Mallick K. *Physica A: Statistical Mechanics and its Applications*, 418(0):17 – 48, 2015. Proceedings of the 13th International Summer School on Fundamental Problems in Statistical Physics.
- [99] Gomez-Solano J R, Bellon L, Petrosyan A, and Ciliberto S. *Europhys. Lett.*, 89(6):60003, 2010.
- [100] Sabhapandit S. *Europhys. Lett.*, 96(2):20005, 2011.
- [101] Verley G, Van den Broeck C, and Esposito M. *Phys. Rev. E*, 88:032137, 2013.
- [102] Verley G, Van den Broeck C, and Esposito M. *New Journal of Physics*, 16(9):095001, 2014.
- [103] Pal A and Sabhapandit S. *Phys. Rev. E*, 87:022138, 2013.
- [104] Pal A and Sabhapandit S. *Phys. Rev. E*, 90:052116, 2014.
- [105] Touchette H. *Private Communication*.
- [106] Imperato A, Peliti L, Pesce G, Rusciano G, and Sasso A. *Phys. Rev. E*, 76(5):050101, 2007.
- [107] Sekimoto K. *Prog. Theor. Phys. Supp.*, 130:17, 1998.
- [108] Noh JD and Park JM. *Phys. Rev. Lett.*, 108(24):240603, 2012.
- [109] Kwon C, Noh JD, and Park H. *Phys. Rev. E*, 88:062102, 2013.
- [110] Kim K, Kwon C, and Park H. *Phys. Rev. E*, 90:032117, 2014.
- [111] Derrida B and Brunet E. *Les Ulis: EDP Sciences*, 2005.
- [112] Baek Y and Kafri Y. *J. Stat. Mech.*, 2015(8):P08026, 2015.